A HYBRID OPTIMIZATION SCHEME FOR HELICOPTERS WITH COMPOSITE ROTOR BLADES

A Thesis
Presented to
The Academic Faculty

by

Jieun Ku

In Partial Fulfillment
of the Requirements for the Degree
Doctor of Philosophy in
Aerospace Engineering

School of Aerospace Engineering
Georgia Institute of Technology
August 2007

A HYBRID OPTIMIZATION SCHEME FOR HELICOPTERS WITH COMPOSITE ROTOR BLADES

Approved by:

Professor Dewey H. Hodges
School of Aerospace Engineering
Georgia Institute of Technology

Professor Vitali V. Volovoi
School of Aerospace Engineering
Georgia Institute of Technology

Professor Daniel P. Schrage
School of Aerospace Engineering
Georgia Institute of Technology

Professor Kip P. Nygren
Civil & Mechanical Engineering
United States Military Academy

Professor Olivier A. Bauchau
School of Aerospace Engineering
Georgia Institute of Technology

Date Approved: 18 May 2007

To my loving Family,

and my grandmother Jungrye Lee (1921-1997)

PREFACE

"Live as if you were to die tomorrow. Learn as if you were to live forever.".

Gandhi (1869 – 1948)

"Honesty is the first chapter of the book of wisdom."

Thomas Jefferson (1743 – 1826)

"Ignorance, the root and the stem of every evil."

Plato (428/427 BC – 348/347 BC)

ACKNOWLEDGEMENTS

First, I would like to show my sincere gratitude to Profs. Daniel P. Schrage and Dewey H. Hodges for their support and encouragement.

Prof. Schrage opened up the new world of helicopter to me in my early years at Georgia Tech and allowed me to experience many other aspects of the helicopters. For those years, he is the one who helped my blinded eyes to open to a new field, and I am truly thankful for that.

In later years of my Ph.D. program, Prof. Hodges is the one who led me through my academic career. I learned much more than I could learn at other places in those years. What I learned from him was not only academics but also fairness and attitude towards life. His patience and advice not only as a teacher but also as a person guided me through difficult times and helped me to make it to this point. I thank to both professors with a few words that can never show how much I appreciate their efforts. What I learned from them as a person will teach me through my life.

Another professor I have great thank to is Professor Vitali V. Volovoi. His brilliant ideas and knowledge in many areas guided me the right direction and amazed me for many times. He expanded my view.

Also, I thank to Profs. Olivier A. Bauchau and Kip P. Nygren for being my committee members and sharing their knowledge and wisdom. These words are inadequate to express my deep respect for these professors.

For my family, I want to express my love. My mother, Moonae Son, my father, Hanchul Ku and my sister Eunjin Ku, were the best family anybody ever could ask for. For teaching me the value of honesty and respecting others at an early age, for loving me and supporting me, for telling me to hold my head up but not to become arrogant and always proud of myself, I am truly blessed; I become better person everyday because of them. As the graduation date has gotten close, I am reminded of my grandmother who passed away in

Dec. 1999. She enriched my childhood, made me understand that love is endless and always told me how proud she was of me. And I know that she is proud of me finishing my Ph.D. as I promised her. I once again thank my family for filling up my life with such beautiful memories, and part of my heart is always with them. Also, I want to say thanks to my husband, Keith R. Pervine, for being a supportive and loving husband. I respect him and am proud of him for his courage to serve the country during Operation Iraqi Freedom.

During my years at Georgia Tech, I had many great colleagues. Among many, I would like to send my special regards and thanks to Seong Sik Ahn for his endless desire for knowledge and supportive discussions. I wish many success in his incoming years.

Finally, I thank to God for allowing me to have loving family, great professors and encouraging colleagues and being the backbone of our lives.

"Yea though I walk through the valley of death, I will fear no evil: for Thou art with me; Thy rod and Thy staff they comfort me."
(Psalm 23:4)

TABLE OF CONTENTS

DEDICATION iii

PREFACE iv

ACKNOWLEDGEMENTS v

LIST OF TABLES x

LIST OF FIGURES xi

SUMMARY xiii

I INTRODUCTION 1

1.1 Problems in Rotorcraft Optimization 1

1.2 Problems in Methodology Selection 2

1.3 Motivation 2

1.4 Organization of the work 3

II EARLY STUDIES 5

2.1 Overview 5

2.2 General Concepts in Optimization 5

2.3 Fundamentals of Rotorcraft Optimization 6

2.4 Single Discipline/Criterion Optimization 6

2.4.1 Vibratory Hub load/Vibration Reduction with Frequency Placement 7

2.4.2 Weight Reduction 8

2.4.3 Performance Optimization 9

2.4.4 Aeroelastic Optimization 9

2.4.5 Aeromechanical Stability 10

2.4.6 Structural Optimization with Composite Rotor Blade 12

2.5 Multi-Criteria/Multi-Objective Methodology 13

2.5.1 Multi-objective Optimization 13

2.5.2 Sequential Multi-Criteria Optimization 14

2.5.3 Integrated Optimization 14

2.6 Non-Gradient Methods 16

2.6.1 Description of Genetic Algorithm 17

2.6.2 Research Related to the Genetic Algorithm 20
2.6.3 Enhanced Genetic Algorithm 20
III INTEGRATING GLOBAL AND LOCAL OPTIMIZATION 26
3.1 Overview 26
3.2 Construction of Global Level 26
3.2.1 Description of methodology 26
3.2.2 Implementation 29
3.2.3 Results 30
3.2.4 Description of previous local level optimization 31
3.2.5 Conclusions for Constructing multi-level Optimization 32
3.3 Coupled Aspects of Global and Local Optimization 32
3.3.1 Description of methodology 32
3.3.2 Implementation 38
3.3.3 Results 39
IV PRELIMINARY STUDIES OF GGTH BLADE OPTIMIZATION 43
4.1 Overview 43
4.2 Description of Generic Georgia Tech Helicopter (GGTH) 43
4.3 Design Space Exploration 46
4.3.1 Global Level 46
4.3.2 Local Level 50
4.4 Design of Experiments (DOE) 50
4.5 Verification of Meta-Models 56
4.5.1 Response Surface Methodology(RSM) 56
4.5.2 Kriging Model 58
4.5.3 Comparison of RSM and Kriging Model 59
V IMPLEMENTATION – GGTH BLADE OPTIMIZATION 65
5.1 Overview 65
5.2 Methodology 65
5.3 Baseline Model 71
5.3.1 EA Rotor System 71

5.3.2 Analysis Models 71
5.4 Surrogate Models 73
5.5 Optimization 76
5.5.1 Global level 76
5.5.2 Local level 78
5.6 Results 79
5.6.1 Global Level 79
5.6.2 Local Level 80
5.6.3 Verification 81
VI CONCLUSIONS AND RECOMMENDATIONS 93
6.1 Conclusions 93
6.2 Recommendations 95
APPENDIX A DESCRIPTION OF TOOLS 97

LIST OF TABLES

1 Global level design values 28

2 Global level design parameters 30

3 Result of global level design variables 30

4 Initial and Final Values of Design Variable for Global Level 40

5 Initial and Final Values of Gradient-Based Optimization for each Candidates from GA 40

6 Range of Natural Frequencies of EA Rotor System 46

7 Advantage and Disadvantage of DOE [1] 55

8 Number of Experiments for three-level factorial 56

9 Correlation Functions of DACE [2] 59

10 Recommendations for surrogate model choice and use [3] 61

11 Design Parameters 73

12 Design of Experiment(DOE) Parameters 74

13 Statistical Information of RSM Models 75

14 Design Parameters 77

15 Upper and Lower Bound of Design Variables 78

16 Initial and Final Values of Gradient-Based Optimization for each Candidates from GA 80

17 Final Values of Local Level Optimization 80

LIST OF FIGURES

1 Schematic Flow Chart of Global Level Optimization for multi-level Methodology . . . 27

2 Baseline Rotor System in Global Optimization . . . 29

3 Simple DYMORE Model for Global Analysis . . . 30

4 Convergence History of Global Level Optimization of multi-level Methodology 31

5 Schematic Flow Chart of Coupled Methodology . . . 33

6 Example of using GA to Find Promising Regions . . . 35

7 History of Best Fitness with Different Population Size . . . 37

8 DYMORE Model for Global Analysis . . . 38

9 History of Global Level Convergence . . . 39

10 Population Variation of Objective Function with Generation . . . 41

11 Convergence History of Candidate 11 . . . 42

12 Convergence History of Global Level Optimization with Candidate 11 . . . 42

13 Proposed Georgia Tech Evolving Rotorcraft Preliminary Design Methodology [4] . . . 44

14 Schematic of Rotor System of GGTH . . . 45

15 DOE and Design Space of 1st Natural Frequency . . . 47

16 DOE and Design Space of 2nd Natural Frequency . . . 47

17 DOE and Design Space of 3rd Natural Frequency . . . 47

18 DOE and Design Space of 4th Natural Frequency . . . 48

19 DOE and Design Space of 5th Natural Frequency . . . 48

20 DOE and Design Space of 6th Natural Frequency . . . 48

21 DOE and Design Space of 7th Natural Frequency . . . 49

22 DOE and Design Space of 8th Natural Frequency . . . 49

23 Design space of Flapwise Bending Stiffness with [45°/-45°] lay-up . . . 50

24 Design space of Lead-Lag Bending Stiffness with [45°/-45°] lay-up . . . 51

25 Design space of Torsional Bending Stiffness with [45°/-45°] lay-up . . . 51

26 Design space of Sectional Mass [slug] with [45°/-45°] lay-up . . . 52

27 Design space of Flapwise Bending Stiffness with Flexure Dimension of h = 0.04 ft, t = 0.02 ft . . . 52

28 Design space of Lead-Lag Bending Stiffness with Flexure Dimension of h = 0.04 ft, t = 0.02 ft 53
29 Design space of Torsional Bending Stiffness with Flexure Dimension of h = 0.04 ft, t = 0.02 ft 53
30 Sampling of DOE 54
31 Approximated Form of RSM 57
32 Exact Function vs Predicted Samples 62
33 Predicted Response 63
34 Error of Predicted Function from Exact Function 64
35 Automative procedure of VABS 67
36 Final Methodology 69
37 Structural Design and Optimization Process in IPPD 70
38 Rotor System Analysis Model 71
39 Main Effects of Design Variables for Cross-sectional Model II 82
40 Main Effects of Design Variables for Cross-sectional Model III 83
41 Predicted Linear RSM Model 84
42 Predicted Quadratic RSM Model 84
43 Flow chart of methodology 85
44 Cross-Section of the Blade 85
45 Cross-Section of the Blade 86
46 Cross-Section of the Blade 86
47 Convergence History of Global Level Optimization – Case I 87
48 Convergence History of Global Level Optimization – Case II 88
49 Local Level Phase 1 Optimization – Global Level Case I 89
50 Local Level Phase 1 Optimization – Global Level Case II 90
51 Local Level Phase 2 Optimization – Global Level Case II 91
52 Final Configuration of Cross-Section Model 91
53 Fan Plot of Rotor Blade with Final Optimum Values 92
54 VABS elements and corresponding integration schemes[5] 98
55 VABS Lay-up Convention[5] 98

SUMMARY

Rotorcraft optimization is a challenging problem due to its conflicting requirements among many disciplines and highly coupled design variables that affect the overall design, which therefore have to be considered concurrently. Also, the design process for a composite rotor blade is often ambiguous because of its design space. Furthermore, analytical tools that are being used do not produce acceptable results compared with flight test when it comes to aerodynamics and aeroelasticity unless realistic models are used, which of course leads to excessive computer time per iteration.

To comply these requirements, computationally efficient yet realistic tools for rotorcraft analysis, such as VABS and DYMORE that decompose a three-dimensional rotor blade analysis into a two-dimensional cross-sectional analysis and a one-dimensional beam analysis. Also, to eliminate the human interaction between iterations, a previously VABS-ANSYS macro was modified and automated. The automated tool shortened the computer time needed to generate the VABS input file for each analysis from hours to seconds. MATLAB was used as the wrapping tool to integrate VABS, DYMORE and the VABS-ANSYS macro into the methodology. This methodology uses the so-called Genetic Algorithm and gradient-based methods as optimization schemes. The baseline model is the rotor system of Generic Georgia Tech Helicopter (GGTH), which is a three-bladed, soft-in-plane, bearingless rotor system. The resulting multi-level methodology is a two-level optimization, global and local. The global-level optimizer is constructed with frequency placement and autorotation index constraints, with cross-sectional stiffnesses and mass per unit length as design variables. The local-level optimizer uses ply angles and size parameters of the structure inside the blade as design variables and tries to achieve stiffness and mass requirements to satisfy the global-level constraints. Previous studies showed that when stiffnesses are used as design variables in optimization, these values act as if they are independent and produce

infeasible design requirements that cannot be achieved by local-level optimization. To force design variables at the global level to stay within the feasible design space of the local level, a surrogate model was adapted into the methodology. For the surrogate model, different "design of experiments" (DOE) methods were tested to find that DOE method which is most suitable from the aspect of computational efficiency. The response surface method (RSM) and Kriging were tested for the optimization problem. To construct RSM models, ModelCenter was used, and for Kriging the DACE (Design and Analysis of Computer Experiments) toolbox in MATLAB was used.

The results show that using the surrogate model speeds up the optimization process. Also, the Kriging model shows superior performance over RSM models. As a result, the global-level optimizer produces requirements that the local optimizer can achieve.

CHAPTER I

INTRODUCTION

Rotorcraft optimization is a challenging problem. Not only does the problem itself have conflicting requirements from different disciplines, but also the methodology has to be chosen in a very careful manner. Also, the optimization of a rotor system is inherently multidisciplinary and, especially for blades made of composite materials, often ambiguous because of its design space. Regardless of these difficulties, analytical tools that are being used do not produce acceptable results compared with flight test when it comes to aerodynamics and aeroelasticity. This can be overcome by using more sophisticated models, which unfortunately leads frequently to excessive computer time per iteration. The problems related to rotorcraft optimization and the cautions involved in selecting methodology are discussed in following two sections, respectively.

1.1 Problems in Rotorcraft Optimization

Rotorcraft optimization has many disciplines that need to be considered concurrently. In other words, a manual approach that needs human intervention during the iteration process cannot achieve the optimal design efficiently within given time and resource. Also, design variables have strong couplings that affect more than one discipline, much of the time without clear indication. Furthermore, this problem must address many conflicting objective functions, such as (a) frequency placement to reduce vibration does not guarantee a reduced vibratory hub load, (b) elastic couplings do not always lead to aeromechanical and dynamic stability occurring at the same time, (c) using a tuning mass to avoid resonance will generate a weight penalty, and (d) optimized performance, aerodynamics and acoustics can limit the design space of structural optimization significantly. Regardless of these difficulties, analysis tools that are being used do not produce acceptable results compared to experimental data, especially for aerodynamics and aeroelasticity. This can be overcome by using more sophisticated models, which unfortunately leads frequently to excessive computer time per

iteration.

1.2 Problems in Methodology Selection

The two main concepts of optimization methodology are gradient-based and non-gradient-based. Gradient-based methods are advantageous when the design space is unimodal, when the proper step size for the calculation of the objective function gradient can be optimized or provided in a timely manner, and when design variables are only continuous. In contrast to gradient-based methods, non-gradient-based methods such as the genetic algorithm (GA) can handle any type of design variables (e.g. integer, decimal or binary), any type of design space (e.g. convex or nonconvex). Also, this method does not require the calculation of the gradient. However, the GA has its disadvantages, such that resolution affects the length of string and population size that can cause significant increase in computation time. There are advanced versions of the GA that have adopted other methodologies to overcome these limitations, such as the response surface method, neural networks, and immune systems. There was also other research done to modify the original GA and make it suitable for different types of design problem, such as the K-S function, constraint handling aspects, and multicriteria or large design problems. Furthermore, there have been other attempts to combine the gradient-based method with the GA to take only superior characteristics of each methods. However, no universal methodology, as such, exists. Therefore, the basic information of design problem must be identified in advance then, design method can be selected that can sometimes lead to repeated trial and error.

1.3 Motivation

There now exist computationally efficient tools for rotorcraft analysis, such as VABS [6, 7, 8, 9] and DYMORE [10, 11]. VABS is based on the notion that a three-dimensional (3-D) rotor blade analysis can be split into one-dimensional (1-D) beam analysis and a two-dimensional (2-D) cross-sectional analysis. VABS provides the cross-sectional stiffnesses for realistic cross-sections in a relatively short time; and DYMORE can analyze a flexible multi-body system such as a rotorcraft, using the blade properties calculated by VABS. This splitting does not result in poor results as would be expected for an over-simplified model.

Moreover, it requires orders of magnitude less computational effort than that demanded by a full 3-D analysis of a realistic rotor blade. Using the hybrid method with an advanced GA benefits in dealing with any type of design variables and design space that does not requires high computation time to explore the design space in the optimization. Also, this GA will provide the several promising regions with local minima, increasing the chances of finding the global minimum. Since the method uses an integrated scheme, the methodology is capable of capturing the couplings among disciplines. Aeromechanical stability is, for example, strongly influenced by elastic couplings. However, in spite of the massive amount of published research focusing on this effect, it is quite difficult to identify exactly what this influence is. Here this influence will be identified through parametric study and the optimization process. Finally, it is pointed out that work combining dynamical optimization with aeromechanical optimization is scarce.

The present work is motivated by the above findings and attempts to find an optimization methodology that is capable of being adopted into any stage of the design process, interactive with any tools, and which can be further integrated with other disciplines such as trajectory optimization, performance optimization, and controls. Also, to identify the role of aeroelastic couplings and suitable optimization conditions such as design variables and constraints, parametric studies will be performed in conjunction with sensitivity analysis. The hybrid method with an advanced GA will be used for exploration of the design space, to attempt to find promising regions based on the objective function. An efficient cross-sectional analysis tool such as VABS and the flexible multi-body dynamics analysis tool DYMORE can assure the relatively accurate and efficient analysis for the process, and using MATLAB as the wrapper provides a capability that makes the methodology flexible and adaptable.

1.4 Organization of the work

This thesis consists of four main parts. The first part reviews the literature related to rotorcraft blade optimization. The second part focuses on constructing a global level optimization, integrating this global level optimization with a local level optimization structure

that has been previously constructed, and shows the coupled aspects at both levels of the optimization. The third part consists of preliminary design studies based on the methodology. Finally, the implementation of the Elastic Articulation (EA) rotor of the GTGH (Georgia Tech Generic Helicopter) will be shown with consideration of aeromechanical stability.

CHAPTER II

EARLY STUDIES

2.1 Overview

This chapter describes the general concepts in rotorcraft optimization and related literature. The literature survey is presented in four categories: the historical perspective, a single-discipline method, a multidisciplinary (integrated) method, and non-gradient methods. After previous research related to rotorcraft optimization is examined, the motivation for this work is stated along with the organization of this thesis.

2.2 General Concepts in Optimization

The optimization of rotorcraft starts from the general concept of a numerical optimization problem that consists of an objective function and constraints, both of which depend on design variables. The general form of the equations is

$$\begin{aligned} \text{Minimize:} \quad & F(\mathbf{X}) \\ \text{Subject to:} \quad & \mathbf{G}_j(\mathbf{X}) \leq 0 \quad j = 1, 2, \ldots, J \\ & \mathbf{H}_k(\mathbf{X}) = 0 \quad k = 1, 2, \ldots, K \end{aligned} \tag{1}$$

where $\mathbf{X} = (x_1, x_2, ...x_n)$ are independent design variables, and $F(\mathbf{X})$ is the objective function. The functions $\mathbf{G}_j(\mathbf{X})$ and $\mathbf{H}_k(\mathbf{X})$ are inequality and equality constraints functions, respectively. This simple numerical formulation was recognized by Schmit [12] for its applicability to the engineering design problem in 1960. Based on this finding, Stepniewski et al. suggested the application to helicopters in 1970 [13]. However, the formulation was not widely adopted by the rotorcraft industry until the early 1980's due to the complexity of the rotorcraft optimization problem itself, even when a simple formulation used. Design of rotorcraft requires that several disciplines must be considered at the same time: aerodynamics, performance, dynamics, strength, aerelasticity, and acoustics. Also, there are other considerations that need to be accounted for, such as life-cycle cost, manufacturing, mission

profiles, and maintainability. These aspects, which are frequently coupled with conflicting objectives, need to be optimized throughout the design process to have a truly optimal design. Furthermore, the design space is rarely convex, the number of design variables is not manageable with manual approaches, and analysis tools often give results that differ from test results. In 1985, Miura [14] concluded that the best way to use optimization methods for helicopter problems is to use the best technology available at the time.

2.3 Fundamentals of Rotorcraft Optimization

The benefits of using optimization methodology start from eliminating man-in-the-loop iterations, not overlooking a potentially superior design that may not be recognized otherwise, and integrating multidisciplinary criteria in the early design process. However, identifying which design parameters have significant effects on the overall design or objective function must be carried out beforehand. This section points out research that is recognized as part of the cornerstone for rotorcraft optimization.

Vibration causes many problems in rotorcraft, such as reducing fatigue life, dynamical instability, and discomfort of crews and passengers. Vibration has long been the salient issue in rotorcraft design; it is not an overstatement to say that successful rotorcraft design depends on how well vibration is treated. Pursuant to this, Blackwell [15] explored the sensitivity of vibration to blade design with parametric studies. He used the number of blades, the blade spanwise mass distributions, chordwise offset of sectional mass center to aerodynamic center, blade bending stiffness, blade built-in twist, tip sweep, and camber to show how these parameters affect helicopter vibration. The research was mainly focused on comparing analytical parameter sensitivities with tests and other analytical results, but it also helped to define design variables that have significant effects on vibration. From his conclusions it was shown that blade built-in twist does not have a large impact on vibration reduction.

2.4 Single Discipline/Criterion Optimization

As previously stated, there are multiple disciplines to be considered in rotorcraft optimization, such as performance, dynamics, aeromechanics, structures, and acoustics. Also, there

can be multiple objectives that need to be achieved in any single discipline. This section reviews previous research that was focused on a single discipline or a single criterion. This research is categorized based on its objective.

2.4.1 Vibratory Hub load/Vibration Reduction with Frequency Placement

The main source of vibration in rotorcraft is the main rotor. As a rational approach to the problem, an optimization deals mainly with the rotor system. To this end, there are two approaches that can be considered. The first approach aims at reducing the vibratory hub load. Since the vibratory hub load propagates through the fuselage and causes problems stated earlier, there were investigations focused on this aspect. The second approach tries to place the natural frequencies of rotor within the range that does not coincide with with 1/rev and $n \pm 1$/rev at operational speed.

Pritchard et al. [16] used tuning masses to reduce the vibratory hub loads by systematically placing tuning masses along the blade span without adding a large mass penalty. The mass and spanwise position of the tuning masses were the design variables. The blade natural frequencies were limited by additional behavior constraints. Objective function and behavior constraints were expanded in a linear Taylor series.

Anusonti-Inthra and Gandhi [17] demonstrated that optimal multicyclic variation of blade root flap and lag stiffness can produce simultaneous reductions in vibratory hub loads. The baseline was a four-bladed BO-105 type hingeless rotor helicopter. They used both gradient- and non-gradient-based optimization schemes, and both of them were successful in reducing hub vibration. Furthermore, they showed that the required stiffness variations could be reduced by introducing a penalty on the input in the objective function used for minimization. Multi-cyclic flap and lag stiffness variations were seen to be effective in reducing hub vibration even when the fundamental rotor properties were changed.

Peters et al. [18] used rotor blade frequency placements for vibration reduction by using CONMIN [19]. This research attempted to find a mass and stiffness distribution for given desired frequencies and achieved 26% weight reduction. Taylor [20] presented a theoretical

approach that used certain blade mode shapes instead of its natural frequencies as constraints. This study showed reductions in vertical hub vibration as well as blade fatigue loading. It demonstrated that desensitizing certain blade modes to aerodynamic loading can result in a large vibration reduction.

Yuan and Friedmann [21] also proposed a structural optimization study of a composite rotor blade with swept tip for vibration reduction. A structural optimization study was conducted by combining the aeroelastic analyses developed in the study with an optimization package (DOT) to minimize the vibratory hub loads in forward flight, subject to frequency and aeroelastic stability constraints. Frequency placement and hover aeroelastic stability constraints were placed on the design. The objective function and constraints were expanded in a linear Taylor series expansion, and semi-analytical sensitivities were used. The hingeless blade was modeled by beam finite elements with a single finite element to model the swept tip. Composite blade cross-sectional properties were calculated by a separate linear, two-dimensional cross-sectional analysis. Numerical results showed that the flap-torsion coupling associated with tip sweep can induce aeroelastic instability due to frequency coalescence. This instability can be removed by appropriate ply orientation of composite materials. Optimization results show remarkable reductions in vibration levels. The tip sweep was the most dominant design variable for the cases considered. This study showed the presence of local minima in the design procedure.

2.4.2 Weight Reduction

Chattopadhyay and Walsh [22] described a procedure for minimum weight design of helicopter rotor blades with constraints on multiple coupled flap-lag natural frequencies, autorotational inertia and centrifugal stress. The design variables used were the box beam cross-sectional dimensions, the magnitudes of nonstructural segment weights and the blade taper ratio. They used a linear approximation technique involving Taylor series expansion to the reduce analysis time. Studies were performed to assess the effects on the optimum blades design of constraints on higher frequencies and stress. The results of the study indicated that there is an increase in the blade weight and a significant change in the design

variable distributions with an increase in the number of frequency constraints.

2.4.3 Performance Optimization

Walsh [23] performed aerodynamic performance optimization of by using the point of taper initiation, root chord, taper ratio, and maximum twist as design variables. The objective function was to minimize power required in hover. The constraints used are (a) required power less than the available power, (b) section drag divergence Mach number, (c) maximum section lift coefficient, (d) trim condition for the rotor, and (e) a lower limit on the blade tip chord. Sensitivity analyses were carried out by forward finite differences. The optimization procedure obtained the optimal design, but it was closer to blade stall than the baseline design. The importance for the design process of including the wake for performance optimization was shown.

2.4.4 Aeroelastic Optimization

During the late 1980's and early 1990's there was a spurt of activity in the aeroelastic analysis of composite helicopter rotors. A series of aeroelastic optimization studies was carried out by Chopra and his coworkers throughout 1990's. The early studies discussed showed the potential of optimization methods in reducing vibration and blade weight and improving performance and aeroelastic stability. Smith and Chopra [24] addressed this issue by extending the earlier models to include certain nonclassical effects. They also investigated aeroelastic stability, hub loads, and aeromechanical stability in forward flight.

Chandra and Chopra [25] presented a free-vibration analysis of a rotating, structurally-coupled composite I-beam. A linear analysis based on Vlasov theory was developed to obtain coupled flap-lag-torsion equations of motion for a composite I-beam with constrained warping and transverse shear effects. Results showed that: (a) the constrained warping influences the natural frequencies by increasing the effective torsional stiffness; (b) bending-torsion coupling creates coupled flap-torsional modes that result in the increase of natural frequencies; and (c) rotor angular speed increases the natural frequencies. For the beams considered in this study, the lag mode was least influenced by rotor angular speed.

Bir and Chopra [26] presented an improved aeroelastic formulation for advanced geometry blades involving variable sweep, droop, pretwist, and planform. The blade was modeled as a series of arbitrarily oriented elastic segments, each of which consisted of one or more beam finite elements with fuselage dynamic interaction. Results indicated that tip droop has a larger stabilizing effect than sweep; anhedral has a destabilizing effect, especially on the second blade lag mode; and sweepback has a destabilizing effect for higher value of thrust. The vibratory components of the flap and lag response were hardly affected by sweep. However, the blade torsional vibratory loads were significantly increased due to sweep.

Ganguli and Chopra [27] performed aeroelastic and sensitivity analyses of the rotor based on a finite element to perform optimization studies for a four-bladed, soft in-plane composite rotor consisting of a two-cell thin-walled beam. The design variables used were the ply angles of the laminated walls of the composite beam. The objective function was to minimize the 4/rev hub loads, with blade frequencies and aeroelastic stability in forward flight as constraints. Optimum design solutions show a reduction in the objective function of about 20% due to elastic stiffnesses and an additional 13% due to composite couplings.

2.4.5 Aeromechanical Stability

Aeromechanical instability in helicopters occurs because of coupling between the rotor and fuselage motion. Ground and air resonance are aeromechanical problems that are caused by the interaction of rotor blade lead-lag motion with certain motions of the helicopter. In ground resonance, the lead-lag motion of the blades reacts with the motion of the hub parallel to the plane of rotation, which further excites the lag motion. Ground resonance instability can be very violent and lead to catastrophic failure. Air resonance occurs mostly in hingeless rotors. The large hub moments that occur when the rotor tilts can give rise to body motion even when the helicopter is in flight, which can couple with blade lead-lag motion and lead to air resonance. Therefore, ensuring adequate aeromechanical stability margins is vital in the design of helicopters with soft-inplane rotors [28]. Over the years, helicopters have been equipped with auxiliary lead-lag dampers to alleviate aeromechanical instability.

However, associated with the use of lead-lag dampers are increased complexity, weight, cost, drag, and maintenance requirements. Additionally, modern day elastomeric dampers are susceptible to fatigue. The elimination of lead-lag dampers, resulting in the development of a damperless rotor, would further simplify the hub, and reduce weight, aerodynamic drag, and maintenance costs. However, the design of a damperless, yet aeromechanically stable, configuration is truly a challenge, and while several concepts have shown promise, there has been no generally accepted solution for eliminating lag dampers [29]. One concept for improving rotor-body aeromechanical stability characteristics is through the use of aeroelastic coupling. Aeroelastic coupling creates changes in the blade pitch as a result of blade flap and lag displacements, as well as coupling between flap and lead-lag motion. The effects of pitch-lag, pitch-flap, and flap-lag couplings on aeromechanical stability have been examined by many researchers.

Bousman [30] performed a test for the hover case to examine the effects of structural flap-lag and pitch-lag coupling on isolated rotor blade lead-lag stability. Flap-lag coupling was introduced by inclining the principal axes of the blade structure up to 60 degrees. Pitch-lag coupling was obtained either alone or in combination with flap-lag coupling through the use of skewed flexural hinges. The principal results showed that both structural flap-lag and pitch-lag coupling when used separately are beneficial for blade stability. Moreover, when the couplings are combined, the lead-lag damping is significantly greater than it would be if the individual contributions were superimposed. Pitch-flap coupling was shown to have only a minor effect on blade lead-lag damping.

Gandhi and Hathaway [31] used optimization methods to alleviate the ground resonance problem of soft in-plane rotors using aeroelastic-coupling parameters. The objective was to use aeroelastic couplings to obtain a helicopter that does not need auxiliary lag dampers. They used a rotor fuselage model with six degrees of freedom, which were cyclic flap (two degrees of freedom), cyclic lag (two degrees of freedom), fuselage roll and pitch. For optimization, the pitch-flap coupling and pitch-lag coupling were used as design variables. They concluded that the most beneficial couplings were negative pitch-lag coupling, positive pitch-flap coupling, flap flexibility outboard of pitch bearing, and lag flexibility inboard

of pitch. Hathaway and Gandhi [32] continued their study, basically adding blade flap and lag stiffnesses as design variables to a previous study [31]. They were motivated by the fact that values of aeroelastic couplings that are generally stabilizing for ground resonance may lead to rotor frequencies that are unacceptable from a handling qualities perspective. Constraints were imposed to prevent excessive changes in the rotor frequencies. Numerical results for a soft in-plane helicopter rotor showed that aeroelastic couplings and blade stiffness properties, along with landing-gear stiffness and damping properties, could be used to design a helicopter rotor without lag dampers. Also, a concurrent approach to optimization where the pitch-flap and pitch-lag couplings are simultaneously considered as design variables was superior to the sequential approach where the blade stiffness and frequency targets were set before any attempt to incorporate aeroelastic couplings.

2.4.6 Structural Optimization with Composite Rotor Blade

Composite materials have shown their superiority over metals for many applications for decades. Composite materials can improve fatigue strength, damage tolerance, corrosion resistance, stiffness-weight ratio, and life-cycle costs. Also, when a rotor blade is manufactured with composite materials, the stiffnesses of a cross-section can be manipulated by changing the lay-up angles and number of plies. Such a capability is referred to as "tailorability." Tailoring is the process of adapting the mass and stiffness characteristics of a composite structure in an effort to improve one or more structural responses. Design methodologies that do not take advantage of composites may overlook potential advances in blade technology. Additional improvements can be achieved in areas such as weight, frequency placement, and ballistic tolerance provided the blade is designed through use of a methodology capable of exploiting the versatility of composite materials. Also, there is variety of selection in composite materials based on its objective. Corresponding to these advantageous characteristics of composite materials, there has been a wide range of research carried out since the 1980's, especially in reducing weight and manipulating aeroelastic couplings.

2.5 Multi-Criteria/Multi-Objective Methodology

After thorough research making use of a single discipline or objective, combining multiple criteria into one process was started. In this section, three distinguishable definitions are used: multi-objective optimization, sequential optimization, and integrated optimization. Multi-objective optimization uses a weighted sum of objective functions as one to achieve conflicting and/or coupled requirements. Such optimization may but does not necessarily involve more than one discipline. Sequential optimization links more than one discipline, dividing them into groups. Once the grouping is done based on the objective function, optimization proceeds with the first group. Once it reaches an optimum, a second optimization starts, adding constraints or more design variables. This continues until the optimization procedure goes through however many groups are defined. This method does not have an iterative process between phases. The third is the integrated method, distinguished by iterative processes and concurrent changes in overall design. Previous studies related with each topic follows.

2.5.1 Multi-objective Optimization

Davis and Weller [33], considered an automated design optimization analysis using relaively simplistic analytical models to reduce the computer time. Modal-based optimization criteria were defined and adopted to calculate a coupled-mode eigenvalue analysis. Problems considered were maximization of bearingless rotor structural damping, blade natural frequency placement, minimization of hub shears, and minimization of modal vibration indices. They showed that parameter scaling by normalization provided significant improvement in optimizer performance, that frequency placement criteria alone may lead to increased vibratory response, and that minimizing modal vibration indices was the most effective criteria considered for reducing rotor vibratory loads. Because of the existence of local minima, the authors suggested the use of several starting points with a gradient-based method.

2.5.2 Sequential Multi-Criteria Optimization

Nixon [34] developed structural design methodology based on two sequential procedures. The first performs an optimization that satisfies aerodynamic, performance, strength, and autorotation constraints for static load cases. Then, the blade is tuned to avoid resonances at the operating rotor angular speed. Titanium single-spar, composite single-spar, and composite multi-spar concepts were examined. The author emphasized the importance of applying optimization to an already fairly good design. He stated that a poor design can restrict the movement of design variables towards a good design. To avoid this, he imposed frequency constraints after a minimum weight static design was achieved. The results demonstrated that the composite configurations show a weight reduction compared to the metallic one.

2.5.3 Integrated Optimization

Barwey and Peters [35] addressed the first significant step in the integrated optimization method by combining structural optimization with dynamics. They also used a blade with realistic cross-sections instead of a box-beam configuration. The rotor system was a soft-in-plane hingeless rotor. The composite blade sections were analyzed using a 2-D finite element code. The results indicate extreme sensitivity of the optimization process to the way frequency constraints were formulated as well as to the starting design. The study showed the effectiveness of simpler and more numerous versus complicated and less numerous frequency constraints when trying to achieve the same goal.

Chattopadhyay et al. [36] used an integrated aerodynamic load/dynamic optimization procedure to minimize blade weight a nd 4/rev vertical hub shears in forward flight. The "Global Criteria Approach" (GCA) was used to form ulate a multi-objective optimization, and results were compared with those obtained by using formulations based on a single objective function. Constraints were imposed on natural frequencies, autorotational inertia, and centrifugal stress. The program CAMRAD [37] was used for blade aerodynamic and dynamic analyses, and CONMIN [19] was used for optimization. The vertical airload distributions on the blade, before and after optimization, were compared. The total power

required by the rotor to produce the same amount of thrust per area is also calculated before and after optimization. Results of this study indicated that integrated optimization can significantly reduce blade weight and vertical hub shears as well as oscillatory vertical blade airload distributions and the total power required. They found that the GCA for formulating the multi-objective function optimization was very effective. The approach yielded a design in which the blade weight and vertical hub shears were significantly reduced relative to the baseline design. Inspection of the vertical airload distributions for the initial and optimum designs indicated that optimization significantly reduced the amplitude of these loads due to reduced thrust requirement. However, the optimum rotors maintained slightly higher values of the vertical force per unit area, indicating a more effective use of the area. The authors used both single and multi-objective functions based on the GCA. Constraints were imposed on blade frequency, autorotation, and stress due to centrifugal force. Design variables included flap and lead-lag stiffness, taper ratio, and root chord. First-order Taylor series approximations were developed for objective functions and constraints. Results showed that the combined minimization of vertical hub shear and weight led to a reduction in vertical hub shears and blade weight. The optimum design also had a lower power requirement, although power was not included in the objective function.

Chattopadhyay and Chiu [38] extended [36] by including additional design variables such as spanwise distributions of blade bending stiffnesses, torsional stiffness, nonstructural mass, chord, radius of gyration and blade taper ratio, and adding constraints on 3/rev radial shear, 3/rev flapping and torsional moments, 4/rev lagging moment, blade natural frequencies, weight, autorotational inertia, centrifugal stress and rotor thrust. Furthermore, they enhanced the objective function for 4/rev vertical and 3/rev inplane shears by including more components of the vibratory hub loads. The results showed that the move limit used in the approximate analysis affects the optimum results obtained. The move limit used here acts same as step size but has 2-D directionality.

Walsh et al. [39] combined performance and dynamics analyses with a general purpose optimizer. The optimization procedure minimized a linear combination of power required and vibratory hub shear. The procedure was demonstrated for two cases. The designs

from the integrated procedure were compared with sequential procedure results that were optimized for performance first and then for dynamics. The results showed the superiority of integrated methods to the sequential method. After integration of aerodynamics and dynamics, Walsh et al. [40, 41] added structural optimization into the integrated method using multilevel decomposition. The upper level objective function was a linear combination of performance and dynamic measures. The lower level optimization was focused on producing the stiffnesses required by the upper level. The authors found that using a lower level optimizer to find the initial stiffnesses for upper level leads to a better solution.

Kim and Sarigul-Klijn [42, 43] developed a multidisciplinary optimization method that strives for minimum weight and vibration, and maximum material strength of a rotor blade with a constraint to avoid flutter. The blade was modeled as an articulated, flexible blade with a thin-walled, multi-celled cross-section. The structural dynamic and aeroelastic analysis of the rotor blade were performed using the Rayleigh-Ritz method. They decomposed the optimization into two levels to handle the design process more efficiently. Throughout the optimization procedure, many local optima were found due to the high nonlinearities of both constraints and objective functions. A different set of starting points had to be used to achieve improved results since the methodology was gradient-based.

2.6 Non-Gradient Methods

During the last two decades of active research in rotorcraft optimization with gradient based methods, many researchers encountered limitations of such methods. The calculation of gradients is a major problem because the finite difference derivatives can be inaccurate unless a proper step size is used, and a feasible design must exist to be used as a starting point. Also, analytical derivatives require extensive changes in analysis programs. Furthermore, due to the characteristics of design variables in rotorcraft optimization, not all design variables can be treated as continuous [44]. Finally, most design spaces in rotorcraft optimization problem are nonconvex, so that local minima exist. To overcome these difficulties that gradient-based methods have to reach the global minimum, the use of gradient-free methods such as the Genetic Algorithm (GA) has been growing. Hajela [45, 46]reviewed

extensively its status and the potential of non-gradient based methods. Among the many different non-gradient base methods, the GA appeared to be the best candidate due to its maturity level and the possibility of incorporating into it other optimization schemes such as neural networks, fuzzy logic, and immune system. Therefore, the focus in this section will be on using the GA in conjunction with several other methods that can be incorporated into the GA.

2.6.1 Description of Genetic Algorithm

The GA is motivated by adaptation and natural selection in biological populations, where genetic information stored in chromosomes as strings and population evolves over generations to adapt favorably to a static or changing environment. In Holland's [47] original work, the GA was characterized by bit strings of possible solutions to a given problem, and by transformations used to vary and improve these coded solutions. The algorithm is based on the survival of fittest, where members of the population that are deemed most fit are selected for reproduction and given the opportunity to strengthen the chromosomal makeup of the progeny generation. This approach is facilitated by defining a fitness function or a measure indicating the goodness of a member of the population in a given generation. Goldberg [48] deals with the GA in an extensive and detailed manner.

For the GA, the design variables can be in either integer or decimal form. However, the most convenient way to handle a design variable is to convert it into a binary equivalent that maps into a fixed length string of 0 and 1. These number are called strings that constitute a population of designs with corresponding fitness value calculated through the objective function. Once a chromosome-like representation of a design variable is randomly generated, the GA simulates the genetic process through three principal steps: selection, crossover, and mutation.

Selection: The selection process is one that biases the search toward producing more fit members in the population and eliminating the less fit ones. One simplistic approach to selecting members from an initial population to participate in the reproduction is to assign

each member a probability of selection on the basis of its fitness. The fitness is a measurement to indicate the performance of a particular genetic makeup to the problem. The fitness associated with a chromosome can simply be an objective function value, or a scaled value of the objective function. A greater fitness of a chromosome indicates better/more viable genetic structure which offers better performance in minimizing the problem. A new population pool of the same size as the original is created, but has a higher average fitness value. However, no new designs are created in this process; the less fit ones are simply eliminated and additional copies of the more fit designs are brought into the population. Three different tournament approaches were examined: global fitness tournament, two-branch tournament [49], and Pareto domination tournament [50] with two fitness functions for weight and power required. The *global fitness tournament* is a typical approach to perform multi-objective design that utilizes a single global fitness function. To perform the global function selection, two candidate strings were chosen without replacement, and the one with the better global fitness measure survives which leaves only half of the population at the end. The *two-branch tournament* has same procedure as the global fitness tournament except this allows the replacement for each fitness function. The *Pareto domination tournament* examines two fitness functions simultaneously. This approach selects two strings, and their two fitness function values are compared. Total domination requires that the surviving individual have both a lower power fitness and a lower weight fitness. If neither string in a pair dominates the other, one is randomly selected. This compromises between the aggressive selection resulting from the total domination scheme, and the diversity maintained by the non-dominant random selection.

Crossover: The crossover process allows for an exchange of design characteristics among members of the population pool with the intent of improving the fitness of the next generation. While there is a number of different ways in which the crossover operation can be implemented, a widely practiced approach is the two-point crossover. In this approach, two mating parents are selected at random; the random number generator is invoked to identify two sites on the strings, and the strings of 0 and 1 enclosed between the chosen sites are

swapped between the mating strings. A probability of crossover is defined to determine if crossover should be implemented for the chosen pair of mating strings. An approach for implementing crossover when using real number strings is described in Ref. [51]. There are several types of crossovers, however, the initial concept is Single Point Crossover (SPC). Though this method is simple and straightforward, it has a major weakness: SPC is the duplication of long string segments from parents. The end effect is that the majority of the overall string structure of children will be like the parents. In other words, the population after the SPC will not be improved much. Due to this limitation on varying genetic structure of only a single parameter while the others remain intact, the SPC strategy cannot efficiently combine possible schemas that are beneficial in fewer generations. Additionally, the segments being exchanged always contain the endpoints of the strings [52]. Two common alternatives are two-point crossover and parameterized uniform crossover. With the two-point crossover, two crossover positions are randomly determined, and the genetic materials within these two positions are exchanged. In this manner, the endpoint effect can be eliminated, and the degree of genetic mixing is greater. These advantages manifest the superiority of two-point crossover relative to SPC in the performance of function optimization [53]. Parameterized uniform crossover operates the procedure at the bit level instead of at the string level [54]. The crossover is conducted on each bit in which the exchange occurs at the position with probability p. Values of p varying from 0.5 to 0.8 are typically used [52].

Mutation: Mutation safeguards the genetic search process from a premature loss of valuable genetic information during reproduction and crossover. Mutation operates at the bit level with relative low operation rate by randomly switching a 0 to 1 or vice versa at a selected mutation site on the chosen string.This change occasionally modifies some genetic patterns and creates different variable values. These modifications can be considered as perturbations of variable values which provides chances to explore the subspace of variable value combinations that cannot be obtained from either reproduction or crossover.

2.6.2 Research Related to the Genetic Algorithm

Tarzanin et al. [55] investigated the use of non-gradient methods for selecting a good initial starting design and avoiding local minima. They used the Tech-02 rotor analysis developed at Boeing Helicopters combined with traditional gradient-based optimization. Numerical studies were conducted for a four-bladed rotor with the objective being to increase thrust. The results showed that the optimal blade design achieved the desired thrust while reducing vibration levels and total blade weight. The authors also investigated workstation parallel processing to utilize unused CPU cycles and use several workstations simultaneously to conserve cycle time.

Akula and Ganguli [56] used the GA to solve the inverse problem of creating the rotor blade mass and stiffness properties given the blade's natural frequencies. A finite element model of a rotating beam was used, and the mass and stiffness at each element was used as design variable. The objective function minimized the difference between the frequencies predicted by the model and the desired (or test) frequencies. Constraints were placed on the blade total mass and inertia. It was found that the algorithm could be used to construct a finite element model of the rotor blade from its frequencies given its total mass and inertia. Excellent results were obtained using the first 10 frequencies, but the results became less accurate when only the first 4 frequencies were used.

The GA showed potential in dealing with integer, discrete, and continuous variables and in avoiding getting stuck at local minima. Also, there is no need for calculation of gradients. However, the GA also showed poor performance when continuous variables need high resolution, leading to high computational time and cost.

2.6.3 Enhanced Genetic Algorithm

Even the GA requires high computational cost with high-resolution chromosomes. The GA maintains its advantageous features over gradient-based methods and other non-gradient methods as computation power increases. In fields of computer and system science, GA's have been actively researched and enhanced to deal with limitations.

GA with KS function: Kreisselmeier-Steinhauser (K-S) function is a method that combines several objective and constraint functions into a single envelope function, making it a member of the Sequential Unconstrained Minimization Techniques (SUMT) [57]. One of the significant features of this approach is that it makes use of a single "pull" or "draw-down" factor for the entire problem, rather than separate draw-down or weighting coefficients for each objective and constraint. The general form of K-S function is

$$f_{KS}(\mathbf{x}) = f_{max} + \frac{1}{\rho} \ln \left[\sum_{m=1}^{n_{obj}+n_{con}} \exp^{\rho[f_m(\mathbf{x})-f_{max}]} \right] \tag{2}$$

where the draw-down factor, ρ, serves to "pull" the KS function envelope closer to the edges of the bounded feasible design space. For the GA, it was desired to use $f_{KS}(\mathbf{x})$ as the fitness function. The value of draw-down factor, ρ needs to be selected based on the design problem. Crossley [58] combined the GA with K-S function. He implied the methodology onto truss structure and rotor system design problem [59, 60]. He stated that even the K-S function can be effectively combined with a GA for optimal design tasks that require multiple objective functions with different types of variables. However, due to the intensity of computation cost, it is suitable only for problems that can justify its high cost, such as a rotorcraft optimization problem.

GA in Multi-criteria Design: In a number of MDO design problems, the statement of the optimization problem calls for allocation of resources in a manner that satisfies multiple, and sometimes conflicting criteria. A commonly adopted approach is to treat one of the multiple criteria as the scalar objective function for the problem, and to formulate appropriate design constraints to accommodate the requirements on the other criteria. While the apparent simplicity afforded by this approach is quite attractive,effective arguments can be made against its use. At a philosophical level, one can always contend that there is a natural separation of criteria and constraints in any design problem. Additionally, when one formulates criteria as constraints, the ability to learn about the extent of the feasible set is seriously compromised. In other words, a multiple criterion approach offers a solution in which a tradeoff pattern emerges, indicating how improvement in any one criterion

would adversely affect another. Finally, it is also known that the treatment of criteria as constraints does not yield the same optimal design as when solving the multi-criterion problem. The GA approach has been adopted for this problem in some recent studies. In Ref. [61], the ability of the GA to simultaneously discover multiple relative optima through the sharing function approach [62] was exploited to solve multi-criteria structural design problems. Another adaptation of the GA in multicriterion problems is available in Ref. [63].

GAs in Large-Scale Problems: The GA handles a continuous variable by treating it as a discrete variable with the precision of representation given by the binary string length, which suggests the longer string lengths represent higher precision. However, the resolution of continuous variables cannot be increased indefinitely because considering a fine precision in the representation of a design variable implies a larger number of design alternatives. This requires a proportionately increased population size, and therefore will drastically increase the computation time. To resolve this dilemma, gradually increasing the precision of design variables is suggested. This method starts from relatively small population with low resolution of design variables. Once the promising regions are identified, resolution and population size are increased and optimization is conducted within those regions. This method was suggested by Lin and Hajela [64], who attempted a multistage search with directed crossover. The primary motivation behind the directed crossover strategy is to identify a significant bit position on the string, and to constrain the crossover operation to these bit locations. The process is initiated in the usual manner with random selection of crossover sites on the mating strings, and with no preference allocated to any particular site. After the crossover operation, the fitness change of each mating pair is recorded. Use these fitness changes, a crossover gain is assigned to each bit involved in the crossover. The crossover gains are accumulated over a few generations, and then used to perform two-point or multipoint crossover operations. They provided one alternative way to handle large number of population size effectively, therefore reducing the computation cost. Similar ideas have been studied under the banner of dynamic parameter encoding [65].

Parallel GA: The implementation of GA's in parallel has been the subject of considerable research. The parallel genetic algorithm (PGA) divides the population into a number of sectors, and mating is restricted to members in a particular sector. Minimal migration of members from one sector to another is permitted. Also, as a result of some overlap among the sectors, information flows out to the whole population through a diffusion process. Then, each individual may improve its fitness during its lifetime, e.g., by local hill-climbing. After such local hill-climbing, it mates with an individual in its vicinity, with the offspring being subjected to further hill-climbing. The child may then replace the parent, depending on fitness value. The primary difference between PGA and GA is that the former uses few intelligent and active members in the search as opposed to the latter, which uses more (albeit passive) members to conduct the search. In fact, the power of the PGA stems from a combination of the processing speed of parallel hardware and software speed on the inherent parallelism available in the GA. The usefulness of stochastic search methods in MDO problems is severely limited without the use of global function approximations. Given that these methods are primarily based on the use of function information only, the use of response surface-based approximations is a viable option. The use of these response surfaces, however, requires that the order of the surface be first specified. Neural network-based function approximations have also been extensively explored in this context, and are briefly discussed in Refs. [66, 67].

GAs in Decomposition-Based Design: An alternative approach to adapting the GA search for large scale design problems is based on partitioning the problem into an appropriate number of subproblems. A reasonable approach for partitioning is one in which balanced subsets of design variables are assigned to different subproblems, and where each subproblem would be responsible for meeting the system-level design objectives and for satisfying constraints most critically affected by the design variables of that subproblem. A formal manner of partitioning the problem was presented in Ref. [68]. Crossley [60] demonstrated the successful application of the GA to a multiobjective design problem. He showed that the GA can identify non-dominated individuals in a multiobjective design

space; the number and quality of these designs increase during the execution of the algorithm. Three different tournament approaches, were examined: global fitness tournament, two-branch tournament, and Pareto domination tournament with two fitness functions for weight and power required. These fitness functions are constructed using a penalty function approach. The author concluded that the two-branch is the best approach for this specific problem. Handling constraints in the GA was critical, as was the case for a single objective function. This study used same design variables as Ref. [44]. As expected the GA required a large number of function evaluations, and can provide only low or moderate precision unless lengthy design strings are used, which would further increase the size of the optimization problem. The author suggested to perform an initial search with the GA, select some promising configurations, and then optimize these further using conventional gradient-based methods, which is what is meant by a hybrid method. The GA strategy in each subproblem works with shorter string lengths; and, hence, smaller population sizes are required in each subproblem. The principal challenge in this approach is that the constraint sets identified for a particular subproblem, are not completely independent of the design variables that may have been assigned to another subproblem. One strategy that allows for subproblem coordination is based on the simulation of a biological immune system. In Ref. [69], Lee decomposed optimization into subproblems, with a structure in which the subproblems optimization represents an inner loop, and the system-level optimization an outer loop. The subproblems are identified by a neural network, which determines the relationships between inputs (design variables) and outputs (objective and constraint values) and, therefore, which groups of design variables and objective/constraints are most closely coupled. Lee and Hajela [69] applied the GA for the rotor design problem. The authors divided the optimization problem into a set of subproblems and followed a decomposition-based strategy. The decomposed problems were then solved in parallel. For numerical results, the authors considered a hingeless composite rotor blade. The objective was to design the blade geometry and structure to minimize a weighted sum of the rotor hub shear force and bending moments for a hingeless rotor in forward flight. Constraints were imposed on power required in hover and in forward flight, the figure of merit, lift performance, blade

weight, local buckling stresses in the structural box-beam section, and failure criteria for the composite structure. The design variables were tuning mass, thickness of the blade spar, blade twist, taper, angular speed, and ply layup angle in the vertical web of the wall. Thicknesses of the plies were treated as discrete variables based on keeping an integer number of plies. Numerical results showed the effectiveness of the decomposition-based approach over traditional strategies, with lower computer time requirements.

CHAPTER III

INTEGRATING GLOBAL AND LOCAL OPTIMIZATION

3.1 Overview

In this chapter, the works related to constructing a global level optimization procedure and integrating it with previous work on local level optimization are discussed. First, a short discussion is presented on constructing a global level to develop multi-level optimization, along with a simple example. Then, coupled aspects of global and local level optimization are investigated using the hybrid approach. The example is optimized through a multi-level/multi-phase optimization process. The results from optimization were reexamined by conducting a global level optimization using the final value obtained at the local level as a starting point.

3.2 Construction of Global Level

Multi-level optimization started from the idea to integrate the optimization of blade cross-sectional properties into the general framework of rotorcraft optimization. The methodology leaves cross-sectional optimization procedure developed previously at the local level and constructs a new level that deals with design variables that affect the overall rotorcraft configuration. This new level is called the "global level" which is descriptive of its characteristics.

3.2.1 Description of methodology

At the global level, the optimization process seeks a structural configuration that satisfies global constraints, including constraints from other relevant disciplines. The global level discipline used here concerns rotorcraft dynamics, specifically focusing on efforts to place blade frequencies in regions that obviate resonance. DYMORE [10, 11] was selected as the blade analysis tool because of its ability to interact with VABS [] used in the local (i.e. cross-sectional) level optimization. The multi-level starts with an initial analysis using VABS to

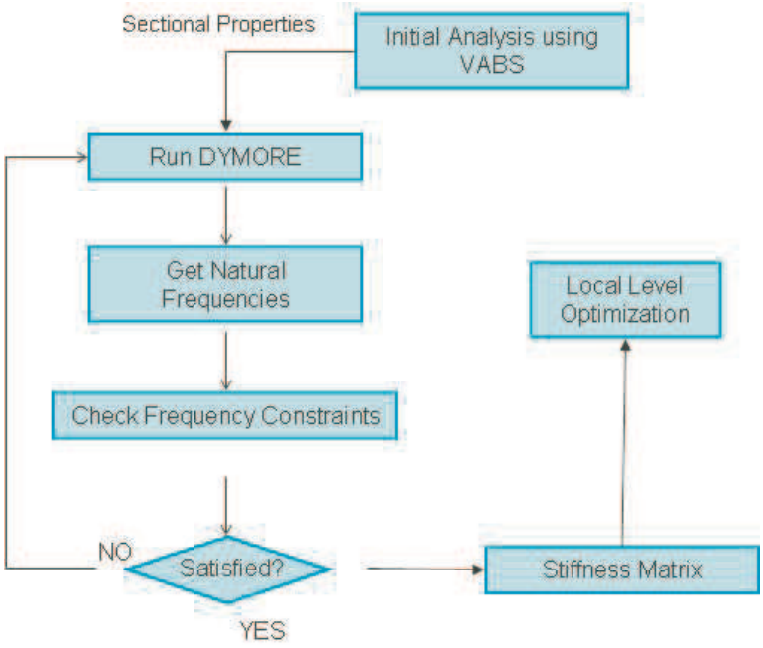

Figure 1: Schematic Flow Chart of Global Level Optimization for multi-level Methodology

provide the initial input values of DYMORE such as the cross-sectional stiffness matrix, mass per unit length, moments of inertia. Once DYMORE runs with these values, the natural frequencies are determined and become constraints for the global level. Throughout the global level optimization, if such a configuration exists, the required cross-sectional stiffnesses can be defined that need to be achieved by local level optimization. A schematic of the global level optimization is provided in Fig. 1.

Global level

1. Design Variables: At the global level, rotor radius, taper, and rotor angular speed are used as design variables. These three variables are determined based on outside considerations, thus providing an interface with other disciplines; however, they also have effects on both stiffness and mass properties as well as vibration characteristics of the designed blade. The initial values of the design variables are provided in Table 1 with their Lower Bound (LB) and Upper Bound (UB) values. During optimization, the upper and lower bounds of the rotor radius were set to be $\pm 15\%$ of initial value, and the taper ratio was between 0.2 and 0.8 of chord. These LB and UB values are

Table 1: Global level design values

Variable	Value	LB	UB	Units
Radius (R)	150	127.5	172.5	in
Angular speed (Ω)	59.2	25	60	rad/s
Taper Ratio (t)	0.5	0.2	0.8	

set to avoid excessive and drastic changes in overall design configuration and maintain the flexibility in structural optimization.

2. Objective Function: The objective function at the global level is to minimize the difference between target weight and the weight per iteration from optimization process. The target weight needs to be determined from either the weight or performance discipline. Therefore, it varies throughout the design process, but the weight from the initial analysis was used for the current optimization. Thus, the optimization problem is posed as:

$$\text{Minimize:} \quad \frac{W_i}{W_t} - 1 \quad i = 1, 2, \ldots, N \tag{3}$$

where W_t is the target weight that the optimization needs to achieve, and W_i is the weight calculated from each step of iteration.

3. Constraints: Total three types of constraints are imposed. The constraints are of the following forms.

$$60 - AI \leq 0 \tag{4}$$

$$\begin{aligned} f_i &\leq 0.95 \times \Omega \\ 1.05 \times \Omega &\leq f_i \\ f_i &\leq 0.95 \times 3 \times \Omega \\ 1.05 \times 3 \times \Omega &\leq f_i \\ f_i &\leq 0.95 \times 4 \times \Omega \\ 1.05 \times 4 \times \Omega &\leq f_i \\ f_i &\leq 0.95 \times 5 \times \Omega \\ 1.05 \times 5 \times \Omega &\leq f_i \end{aligned} \tag{5}$$

$$\Omega \times R \leq 1.05 \times V_{tip} \tag{6}$$

The first constraint used is that the Auto-rotation Index (AI) must be greater than 60. This constraint pertains to the auto-rotational inertia and related factors of safety. This value is known as a safe value for helicopters with a single rotor system [70]. The second constraint is that all frequencies must avoid coincidence with certain integer multiples of the rotor angular speed, namely $N \times \Omega$/rev and $(N \pm 1) \times \Omega$/rev, which for this example is 3, 4 and 5/rev along with the requirement that 1/rev that must be avoided regardless of the number of blades. The bandwidth of the zone to be avoided was set to be $\pm 5\%$ of 3, 4 and 5/rev. Also, considering that rotor radius and angular speed affect the tip speed, another constraint was to bound the tip speed to be within $\pm$ 5% of the initial value.

3.2.2 Implementation

The analysis model defined for global level is shown in Fig. 2. This rotor is a 4-bladed articulated rotor system. Only one blade was modeled using DYMORE and the result is shown in Fig. 3. The design parameters are target weight, tip speed, and angular speed and come from aerodynamic analysis. The parameter values are given in Table 2.

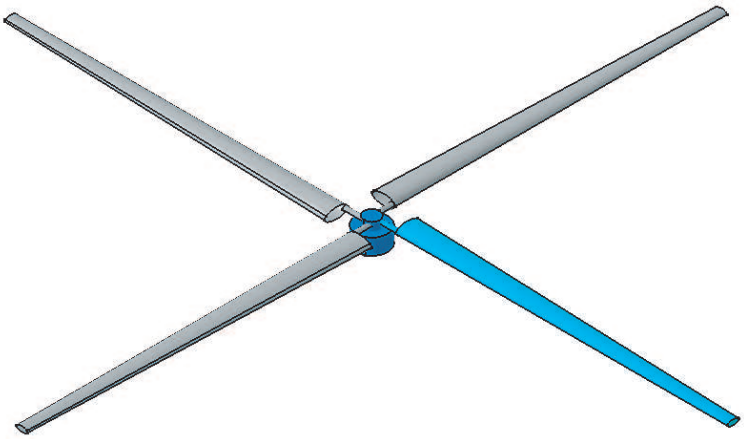

Figure 2: Baseline Rotor System in Global Optimization

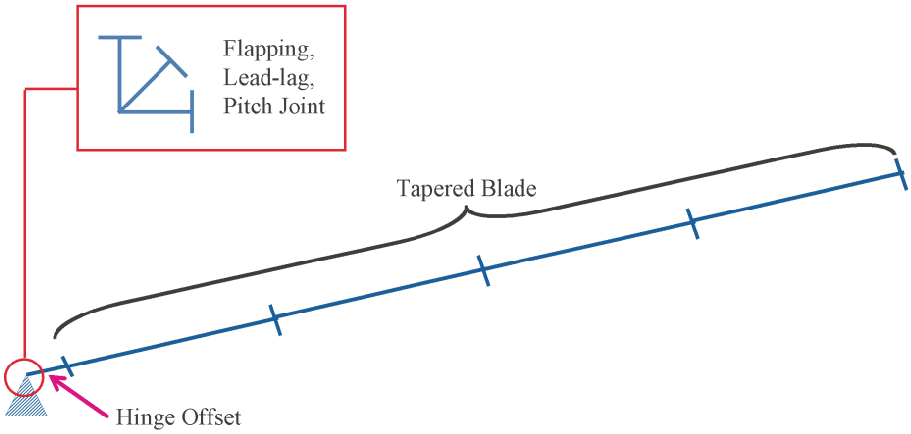

Figure 3: Simple DYMORE Model for Global Analysis

Table 2: Global level design parameters

Parameter	Value	Units
Target Weight (W_t)	104.7	lb
Tip Speed (V_{tip})	740	ft/sec
Number of Blade (N)	4	

3.2.3 Results

The result from global level optimization is shown in Table 3 with initial and final value of design variables. The final value of the radius is 88% of initial value, and the angular speed and taper ratio were determined as 25 rad/sec and 0.32, respectively. Through iteration, the target weight was reduced by 3.7%. Since the final values satisfy the frequency constraints, weight reduction was an additional benefit. The history of convergence for each design variable and objective function is provided in Fig. 4; these results are non-dimensionalized by their initial values.

Variable	Initial Value	Final Value
Radius (R)	150	132.49
Angular Velocity (Ω)	59.2	25
Taper Ratio (t)	0.5	0.32
Target Weight (W_t)	140.7	135.46

Table 3: Result of global level design variables

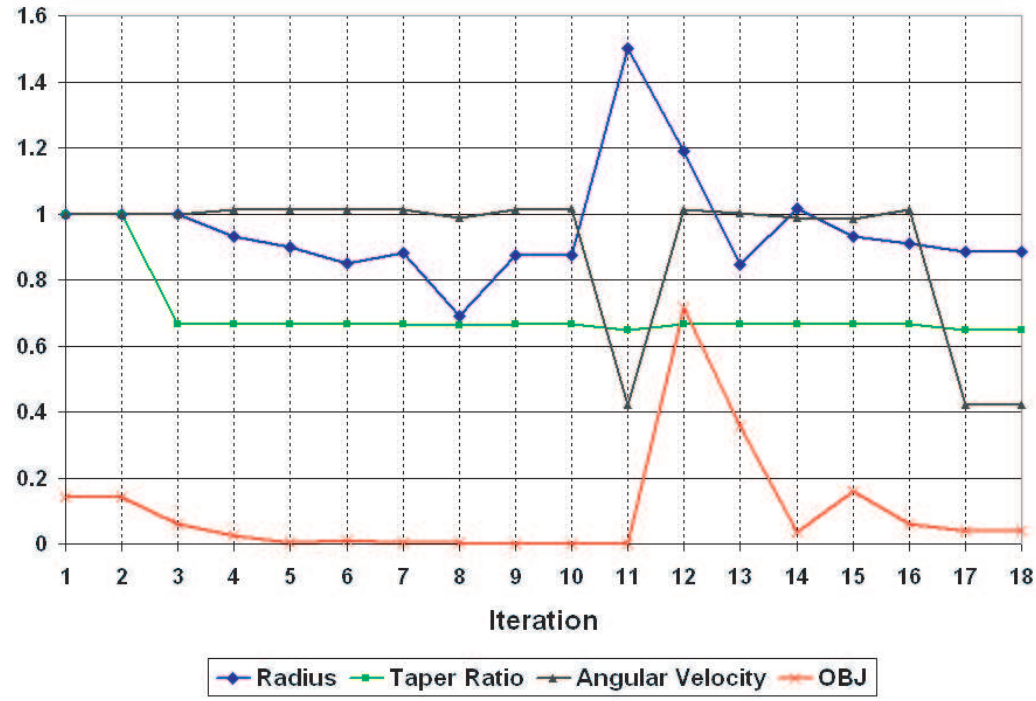

Figure 4: Convergence History of Global Level Optimization of multi-level Methodology

3.2.4 Description of previous local level optimization

A short description of cross-sectional optimization [71, 72] is provided here. The goal of local-level optimization is to find a specific cross-sectional layout that satisfies certain given constraints. The single web, D-spar cross-sectional configuration is considered. The given airfoil shape is VR-7 with chord length 20.2 in. Since the outer contour of the cross-section is determined by aerodynamics, only the variables pertaining to the internal lay-out of the blade are allowed to change, such as thicknesses of the three structural elements, web location and orientation, etc. The leading-edge cap is considered to be made of titanium to provide erosion protection. The objective function was to minimize the distance between shear and aerodynamic centers. The design variables were the fiber orientations, ply thickness of the D-spar, skin, and web, as well as the web location and orientation – a total of 17 design variables and 8 behavior constraints.

3.2.5 Conclusions for Constructing multi-level Optimization

This global level optimization was linked with the local optimization procedure developed previously in Ref. [73]. While this procedure decouples the cross-sectional optimization from the global-level optimization efficiently, there were several significant challenges that needed to be overcome in order to make such decoupling useful: (a) There was no clear indication how global and local level optimizations iterate through design process. (b) The ply angles were set to be varied continuously, which does not occur in real designs. (c) There was no investigation pertaining to nongradient-based optimization methods even though it was evident that many local minima exist, preventing the optimizer from reaching the global minimum. (d) The local optimization showed extreme sensitivity to the starting points, but no suggestions for selecting starting points were made.

3.3 Coupled Aspects of Global and Local Optimization

In this section, the main effort is to make interactive multi-level methodology to couple the global and local optimization processes more efficiently, and to suggest an alternative approach to overcome the presence of local minima in the local level optimization. The analysis tools and the base coding tool are the same as in the previous section. A slightly modified baseline model was used for implementation, and a detailed description of this approach is presented in the following sections.

3.3.1 Description of methodology

The global level optimization pursues the same procedure as previous methodology. However, the local level optimization needed to be modified to ensure the iterativeness between global and local level. Also, instead of using different gradient-based method for two separated phase [73], the GA was adopted in the local level optimization.

As shown in Fig. 5, the global level passes the required stiffness matrix to the local level after the optimization process. The local level uses these values as constraints and objective function values that will be varied based on the initial value of parameters at the global level. Once the local level reaches the optimal values, if there is more than one

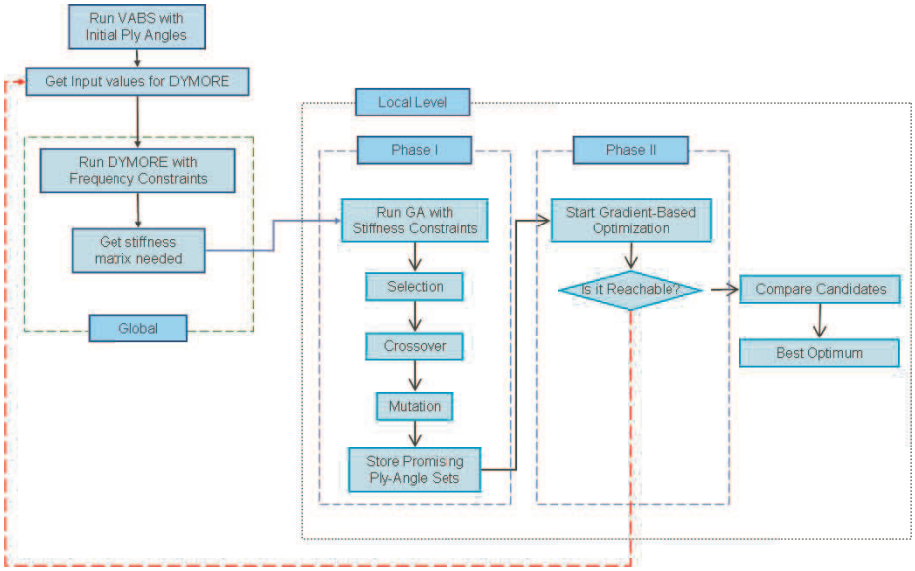

Figure 5: Schematic Flow Chart of Coupled Methodology

configuration, additional criteria must be used to select a better design. Comparing the candidate processes will be based on VABS along with additional criteria such as stress requirements and location of the shear center. However, if the local level cannot reach an optimal value with given requirements, the best of the final candidates will be used as a starting point for global level optimization, and the whole process iterates.

Global level The design variables, objective function and constraints of global level are provided here, respectively.

1. Design Variables: In contrast to the first suggested global optimization, the blade radius and angular speed are fixed. Also, the sectional mass is no longer used as a design variable since there will be no significant mass changes along the blade length. Instead, the weight of the tip mass and tuning mass, the taper ratio and the location of the taper initiation were added into design variables along with axial stiffness, torsional stiffness, and two bending and shear stiffnesses. To prevent significant increase in computation time of analysis in the global level, the model was simplified by locating the tuning mass at the taper initiation point.

2. Objective Function: The objective function for the global level is to minimize the

difference between the target weight and calculated weight that are generated for each iteration. The objective function can be expressed as

$$\text{Minimize:} \quad \left|\frac{W_t - W_i}{W_t}\right| \tag{7}$$

3. Constraints: Three types of constraints were imposed. The first constraint is that the Autorotation Index (AI) must be greater than 60. This value is the minimum required value for the single rotor case [70].

$$60 - AI \leq 0 \tag{8}$$

The second constraint is related with the taper initiation location. The taper is to be started between 30% and 70% of blade length.

$$0.3 \times \text{Radius} \leq f_i \leq 0.7 \times \text{Radius} \tag{9}$$

The last constraints set is to place frequencies in favorable regions. The 1/rev frequency is must be avoided regardless number of blades. Also, other frequencies are not to coincide with N or $N\pm1$/rev to avoid resonances that can lead to catastrophic failure. In this methodology, high frequencies were not considered. Thus,

$$\begin{aligned} f_i &\leq 0.8 \times \Omega \\ 1.2 \times \Omega &\leq f_i \\ f_i &\leq 0.8 \times 3 \times \Omega \\ 1.2 \times 3 \times \Omega &\leq f_i \\ f_i &\leq 0.8 \times 4 \times \Omega \\ 1.2 \times 4 \times \Omega &\leq f_i \\ f_i &\leq 0.8 \times 5 \times \Omega \\ 1.2 \times 5 \times \Omega &\leq f_i \end{aligned} \tag{10}$$

Local level: The local level uses two phases. The phase 1 is an exploratory phase of the optimization that uses GA to find regions containing local minima and possibly the global minimum. In GA, as generation proceeds, each population clusters around any local minima. This phenomenon is defined as "clustering" here. To show the extreme example of

such clustering, a simple example is provided along with the design space in Fig. 10. Sub-figure (a) shows the 3-D design space which clearly indicates the many local minima and (b) is the design space projected onto the surface as 2-D. By using GA, the first generation is randomly scattered on the 2-D design space in (c), and the final generation is clustered around local minima in sub-figure (d). This example shows that using GA to select the starting points of gradient-based method leads to a better chance of finding the global minimum.

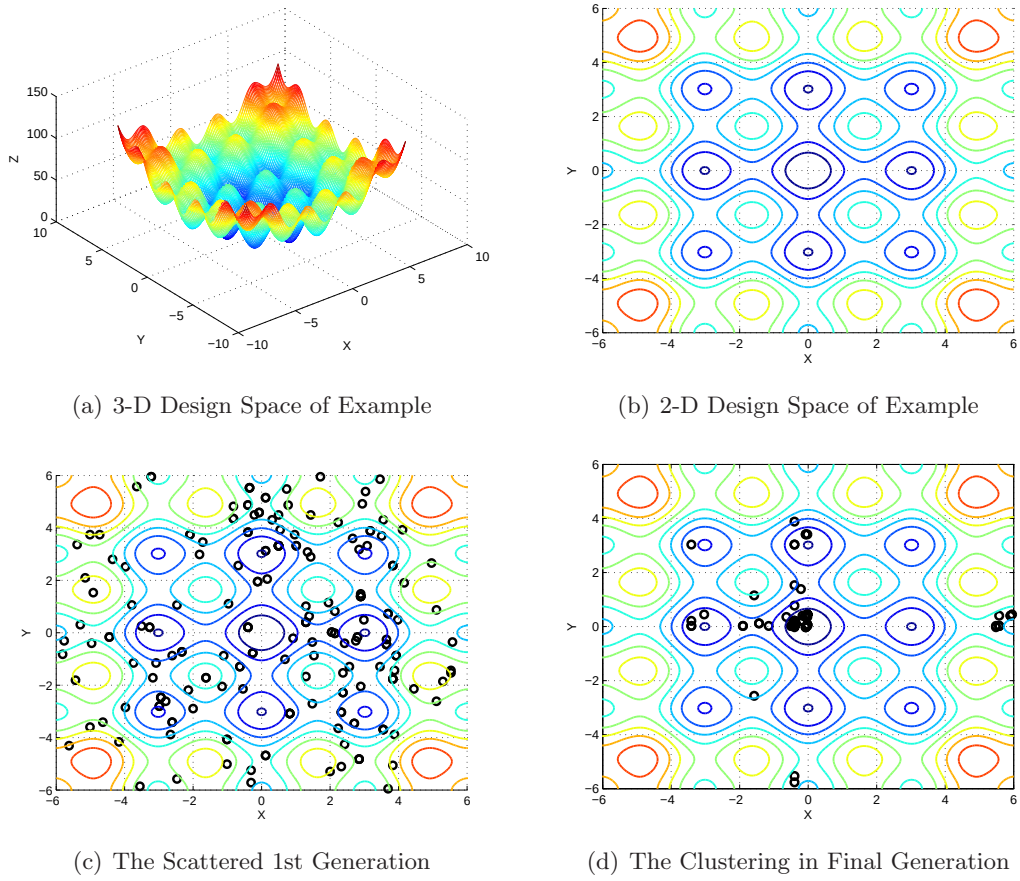

(a) 3-D Design Space of Example

(b) 2-D Design Space of Example

(c) The Scattered 1st Generation

(d) The Clustering in Final Generation

Figure 6: Example of using GA to Find Promising Regions

Starting from same idea, GA was used for local level at phase 1 to explore the design space with limited number of generations. As the iteration goes in GA, the populations will form clusters near any local minima. Once the clusters are formed, promising starts points are identified. The second phase comes in when these cluster are confirmed to contain the global minimum by running same algorithm several times and using only repeated

candidates. The second phase uses a gradient-based method to calculate a more precise ply-angle for optimum lay-ups.

1. Design Variables: At the local level, design variables were selected that can affect the stiffness matrix used in calculating the objective function and constraints. A total of seven design variables was used for this research, which are five ply-angles for the D-spar and one ply-angle each for the skin and web.

2. Objective Function: The objective function of the local level minimizes the difference between the stiffnesses required for the global level, and those are generated by optimization of the lay-up angle. VABS then produces the 6×6 cross-sectional matrix including couplings. However, only the torsional stiffness has a significant effect on global optimization. The objective function is then

$$\text{Minimize:} \quad \frac{|GJ_t - GJ_i|}{GJ_t} \tag{11}$$

3. Constraints:

$$\begin{aligned} 0.95\times \leq \frac{|EA_{req} - EA_i|}{|EA_{req}|} &\leq 1.05 \\ 0.95\times \leq \frac{|EI_{22_{req}} - EI_{22_i}|}{|EI_{22_{req}}|} &\leq 1.05 \\ 0.95\times \leq \frac{|EI_{33_{req}} - EI_{33_i}|}{|EI_{33_{req}}|} &\leq 1.05 \\ 0.95\times \leq \frac{|GJ_{req} - GJ_i|}{|GJ_{req}|} &\leq 1.05 \end{aligned} \tag{12}$$

where EA_{req}, $EI_{22_{req}}$, $EI_{33_{req}}$, GJ_{req} are the stiffnesses associated with axial, flapwise bending, chordwise bending, and torsional deformation, respectively, and are required to satisfy global level constraints; and EA_i, EI_{22_i}, EI_{33_i}, GJ_i are stiffnesses associated with axial, flapwise bending, chordwise bending, and torsional deformation calculated in the local level optimization using VABS, respectively.

Determining Population size based on Number of Design Variables The GA, as used at the local level, is not required to find the final optimum value. Instead, GA plays a role as a filter to find promising starting points for the gradient-based method used in phase 2. Therefore, increasing number of populations and generations at the same time

is not necessary. An effort was made to identify effects of the number of populations and generations along with their relations to overall process.

Two cases were tested for such an attempt. The first case starts with number of population equals to 100 with 10 generations. Each generation stores the best fitness string, and at the end there are 10 candidates. The second case starts with number of population equals to 200 with five generations. However, it stores two best fitness per generation that results same number of candidates at the end. Since this process was conducted to show the trends, only four design variables were used to represent the skin, web, upper and lower side of D-spar. These cases were ran five times each, since the initial population is random based on the characteristics of GA. The history of best fitness based on this investigation is in Fig. 7.

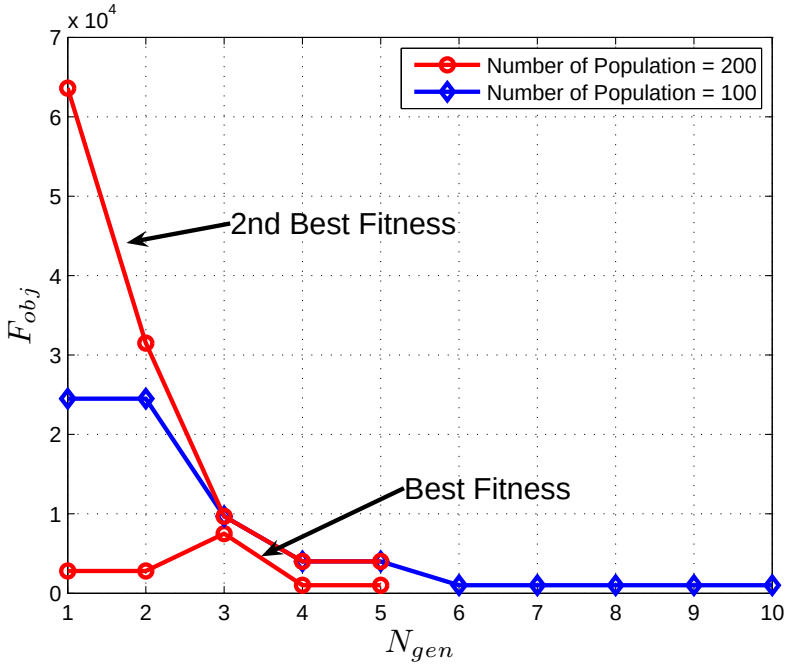

Figure 7: History of Best Fitness with Different Population Size

The best and second best fitnesses are indicated for a population size of 200, and the best fitness is indicated for a population size of 100. Since this investigation is focused on determining the total population within the same computation time, the number of generations is different. The results showed that a larger population size converges to a

better solution in fewer generations. From the results, it was concluded that a population size of 200 is sufficiently efficient to carry out the optimization process when the number of variables is four.

3.3.2 Implementation

Global Level Model The multi-body model was constructed for global level analysis. The blade used here is divided into uniform and tapered section. The tuning mass and tip mass were added to balance the blade weight and improve the dynamic behavior. To simplify the model, the tuning mass is located where the taper is initiated. The model schematic is shown in Fig. 8.

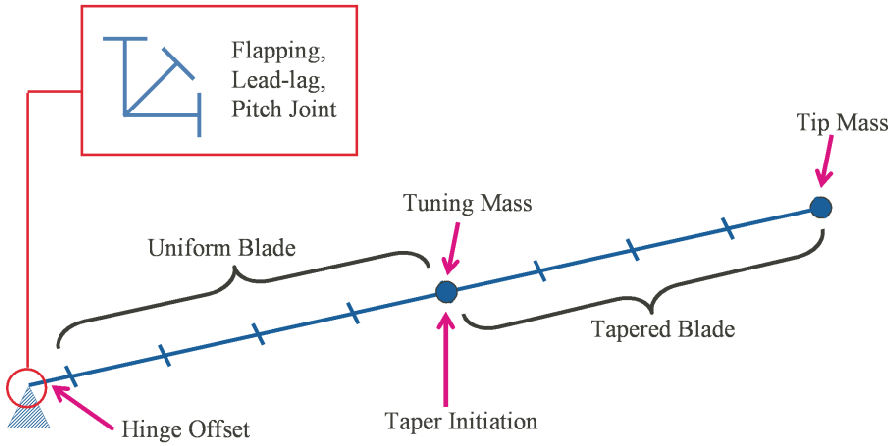

Figure 8: DYMORE Model for Global Analysis

Local Level Model The baseline [73] is modeled using the NASA preliminary design report for a composite blade retrofit for the XV-15 rotor [74]. To reduce the number of design variables, previous cross-sectional model was simplified. Instead of using different ply-angle lay-ups for upper and lower part of the D-spar, same sequence of ply-angles were used. Also, the configuration was fixed to have 90° web and the location of the web was set to be at the quarter chord. The ply-angle and number of lay-ups of skin and web were kept the same. This simplification resulted in seven design variables instead of 17.

3.3.3 Results

The results are provided separately for each level.

Global Level Results The convergence history of global level optimization is shown in Fig. 9. The result was achieved with the initial run of VABS. The initial and final values of design variables are provided in Table 4.

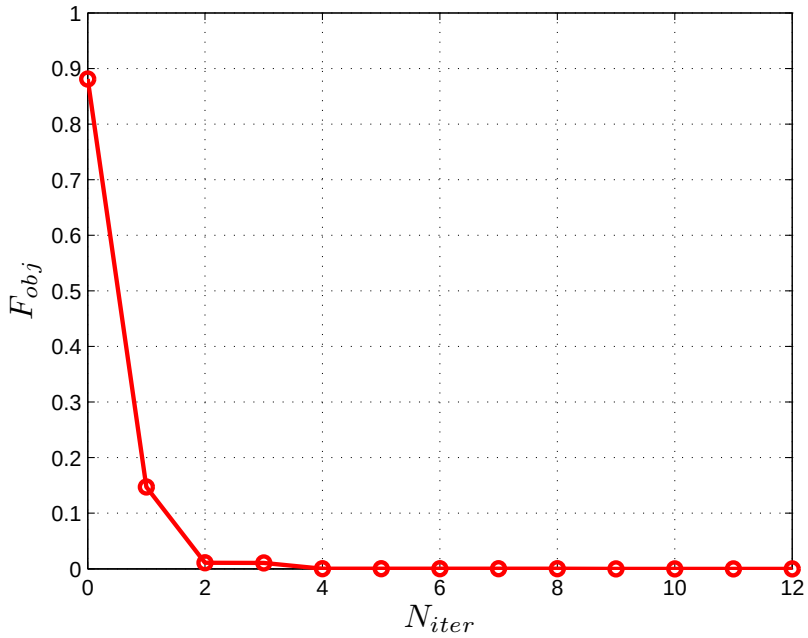

Figure 9: History of Global Level Convergence

Local Level Results With stiffness constraints that are generated at the global level optimization, the local level optimization was performed through two phases. Phase one used a population size of 400 with seven design variables. After five generations, the first generation and the final generation were compared based on the objective function value. The Fig. 10 showed that GA started clustering around local minima after five generations. From the fifth generation, 12 minimum values were selected for phase two. Phase two used "fmincon" in MATLAB as the optimizer. Table 16 is provided to show the initial and final values of objective function and ply-angles for each candidate.

Table 4: Initial and Final Values of Design Variable for Global Level

Variable	**Initial Values**	**Final Values**	**Units**
Location of Taper Initiation	45	45.22668	in.
Taper Ratio	0.6	0.78379	
Weight of Tuning Mass	0.2	63.18105	lb
Weight of Tip Mass	12	74.98101	lb
Axial Stiffness	0.152776	0.152776	$\times 10^9$ lb/ft^2
Chordwise Bending Stiffness	0.120091	0.120091	$\times 10^9$lb/ft^2
Flapping Bending Stiffness	0.269611	0.269611	$\times 10^{10}$lb/ft^2
Torsional Stiffness	0.380418	0.380418	$\times 10^8$lb/ft^2
Shear Stiffness	0.607106	0.607106	$\times 10^7$lb/ft^2
Shear Stiffness	0.134318	0.134318	$\times 10^7$ lb/ft^2

Table 5: Initial and Final Values of Gradient-Based Optimization for each Candidates from GA

	Candidate 1		Candidate 2		Candidate 3		Candidate 4	
	Initial	Final	Initial	Final	Initial	Final	Initial	Final
F_{obj}	0.5407	0.0005	0.9416	0.0081	0.0733	0.0003	1.6566	0.0126
θ_{D_1}	30	31.3950	30	26.7014	30	29.8619	30	31.9554
θ_{D_2}	-45	-43.9453	60	70.6024	45	46.9227	45	30.0390
θ_{D_3}	60	58.9395	0	-4.1863	90	88.0369	-45	-30.0000
θ_{D_4}	45	45.0000	45	45.0000	45	45.0000	45	45.0000
θ_{D_5}	45	45.0000	60	60.0000	45	45.0000	0	0
θ_{skin}	0	-1.0490	60	70.6003	60	61.9571	60	75.0000
θ_{spar}	-45	-45.0000	-45	-45.0000	45	45.0000	0	0
	Candidate 5		Candidate 6		Candidate 7		Candidate 8	
	Initial	Final	Initial	Final	Initial	Final	Initial	Final
F_{obj}	2.6521	0.1617	0.1514	0.0289	3.4817	0.0431	0.5554	0.0195
θ_{D_1}	30	32.9041	30	29.8155	30	9.5393	30	31.3966
θ_{D_2}	-45	-30.0000	-45	-60.0000	60	-60.0000	45	15.0000
θ_{D_3}	45	30.0000	60	-15.0000	0	-60.0000	90	40.3190
θ_{D_4}	45	45.0000	45	-45.0000	45	-45.0000	45	-45.0000
θ_{D_5}	45	45.0000	45	60.0000	60	90.0000	45	90.0000
θ_{skin}	30	15.0000	0	45.0000	60	45.0000	60	-60.0000
θ_{spar}	45	45.0000	-45	45.0000	-45	0	45	-45.0000
	Candidate 9		Candidate 10		Candidate 11		Candidate 12	
	Initial	Final	Initial	Final	Initial	Final	Initial	Final
F_{obj}	3.6718	0.1877	0.4248	0.0431	0.8811	0	0.4027	0.0050
θ_{D_1}	30	6.4603	30	29.4408	30	32.1066	30	29.1458
θ_{D_2}	45	-59.6985	-45	82.0318	0	8.2503	-45	-49.5909
θ_{D_3}	-45	44.9989	45	52.9619	45	38.3761	30	25.1547
θ_{D_4}	45	30.0000	45	45.0000	45	45.0000	60	60.0000
θ_{D_5}	0	-45.0000	45	90.0000	45	45.0000	45	45.0000
θ_{skin}	60	30.0000	30	67.9661	30	23.3707	0	-3.7556
θ_{spar}	0	45.0000	45	45.0000	60	60.0000	-45	-45.0000

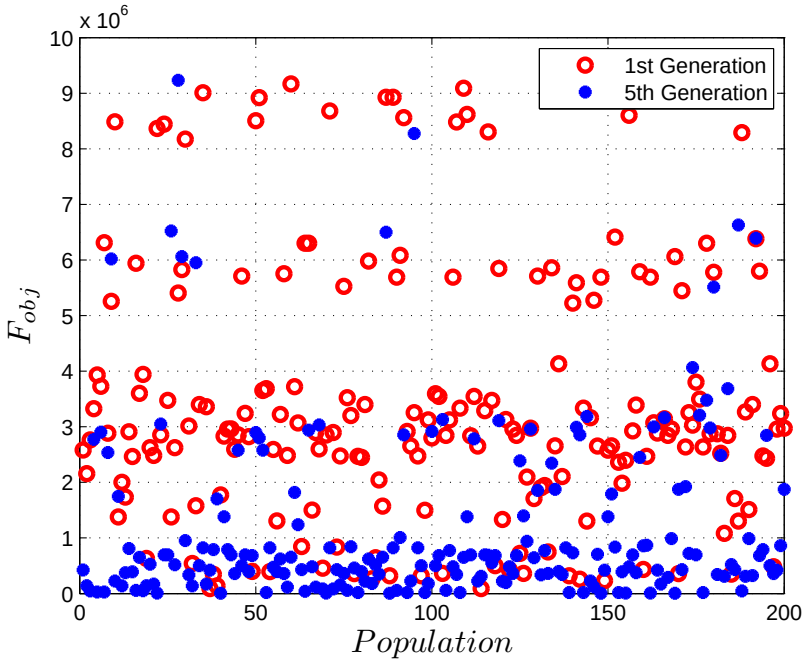

Figure 10: Population Variation of Objective Function with Generation

After phase two, only candidate 11 achieved the minimum value without violating the constraints. The convergence history of candidate 11 is in Fig. 11. To confirm the feasibility of the final design, the global optimization was performed with ply-angles of candidate 11, and the global level optimization achieved the optimum value. This shows that the optimization process found the feasible optimum value without getting stuck at the local minima.

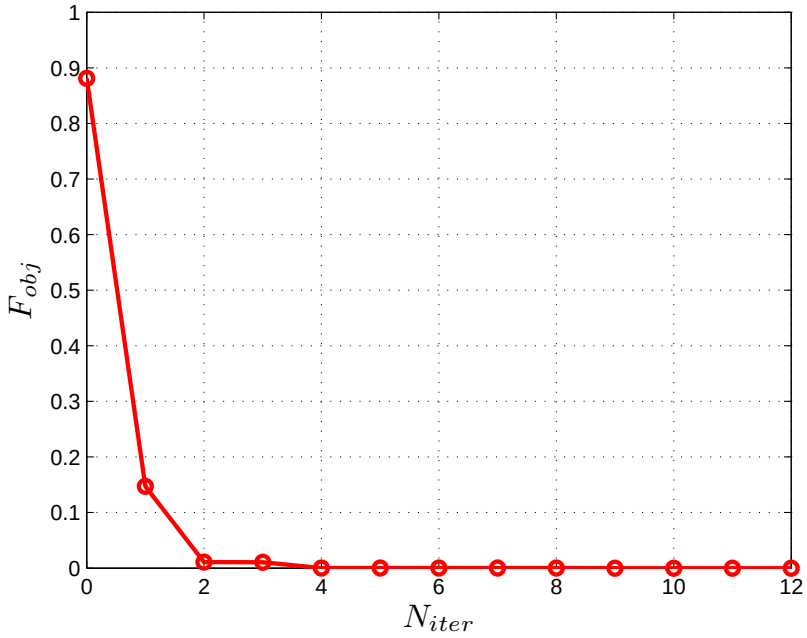

Figure 11: Convergence History of Candidate 11

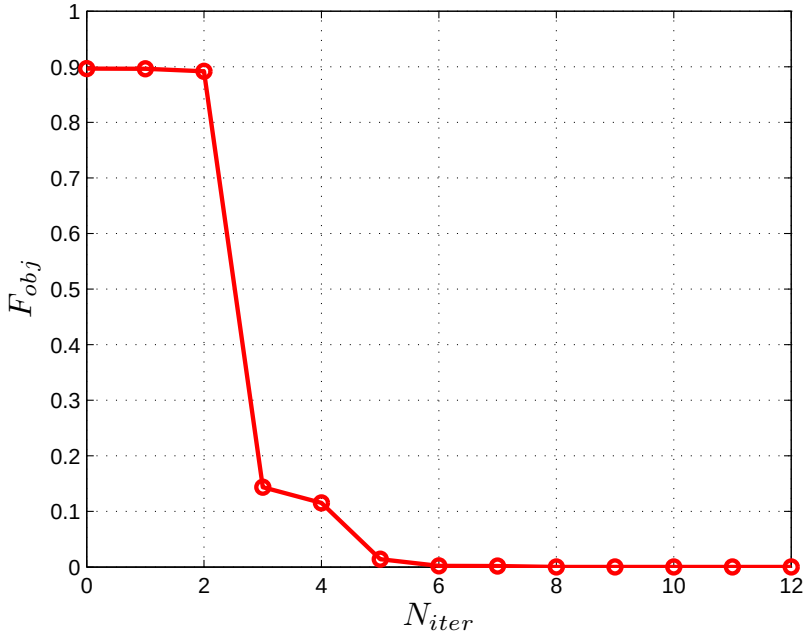

Figure 12: Convergence History of Global Level Optimization with Candidate 11

CHAPTER IV

PRELIMINARY STUDIES OF GGTH BLADE OPTIMIZATION

4.1 Overview

In this chapter, a description of the baseline model implemented in Chapter 5 and preliminary studies about design methodology are provided. In the first section, short history of baseline model is provided with design methodology that is used to develop the baseline model. In the following sections, using the simplified global and local level analysis model, the design space is explored. For design space exploration, Design of Experiments (DOE) was used. After introduction of DOE, surrogate models were described and compared using different DOE methods. The previous methodology that is suggested in Chapter 3 is then finalized based on the findings of this chapter.

4.2 Description of Generic Georgia Tech Helicopter (GGTH)

The baseline model implemented here is the Generic Georgia Tech Helicopter (GGTH) with a three-bladed bearingless rotor system. GGTH was developed to satisfy today's challenging market as a training helicopter. A training helicopter needs to offer superior performance, high handling qualities, and safety at a price competitive with that of other helicopters already in market. The priority of this design effort was focused on the simplification of systems and subsystems for both the vehicle and the process by which it would be built. Therefore, an Integrated Product and Process Development (IPPD) methodology was used to drive the design solution. The IPPD methodology is depicted in Fig. 13.

As work on this system progressed, simplification of the rotor system became its main focus, and thus the so-called Elastic Articulation (EA) rotor system was selected. The first attempt to develop the EA rotor system was made in the early 1960s [75]. The main idea was to eliminate unwanted feeback signals for the gyro control system by matching the in-plane stiffness at the blade root to the flapwise stiffness. This led to the need for a torsionally soft flexure that plays the roles of flap, lead-lag and feathering hinges of the

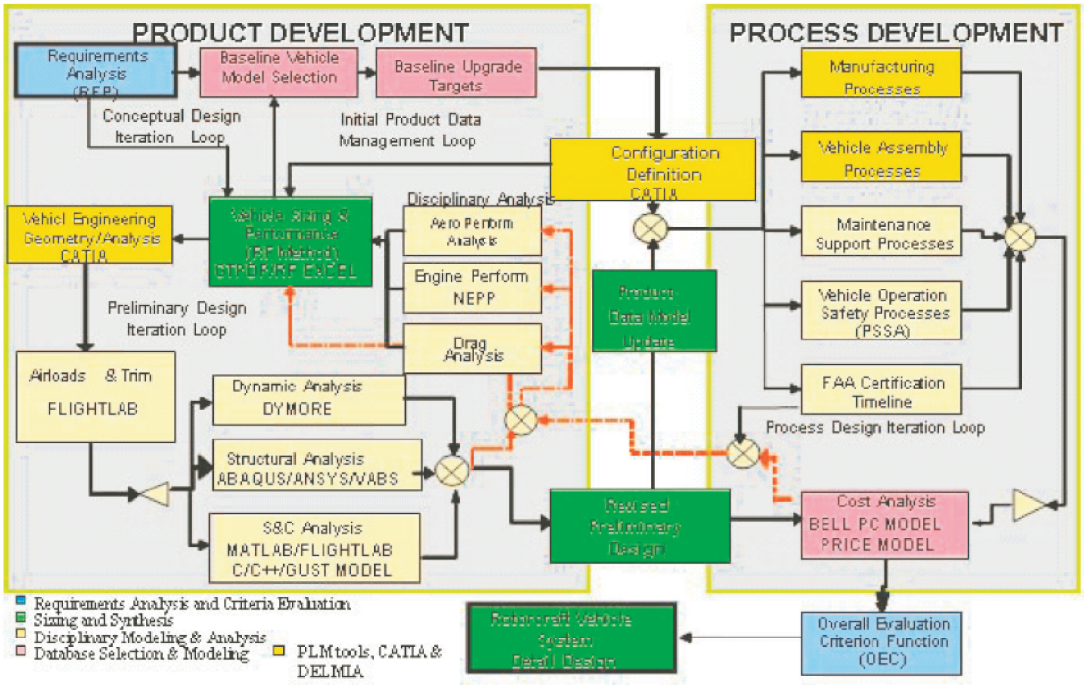

Figure 13: Proposed Georgia Tech Evolving Rotorcraft Preliminary Design Methodology [4]

articulated rotor system. The flexure was designed as stainless steel, and at first a single torque tube was used [76, 75]. Starting from the original idea, the EA rotor system was reintroduced in [75] with composite materials. The EA rotor system proved to have several advantageous aspects compared with other types of rotor systems. The EA rotor system reduces the number of structural parts in the hub, such as all bearings, blade dampers, and droop stops. By locating a torque tube on each side of the flexure, the EA rotor system provides multiple load paths that ensure safety of the system in case any part fails that does not result in the total loss of a blade. Therefore, advantages of the EA rotor system can be summarized as simplicity and safety. The structure of the EA rotor system is depicted in Fig. 14.

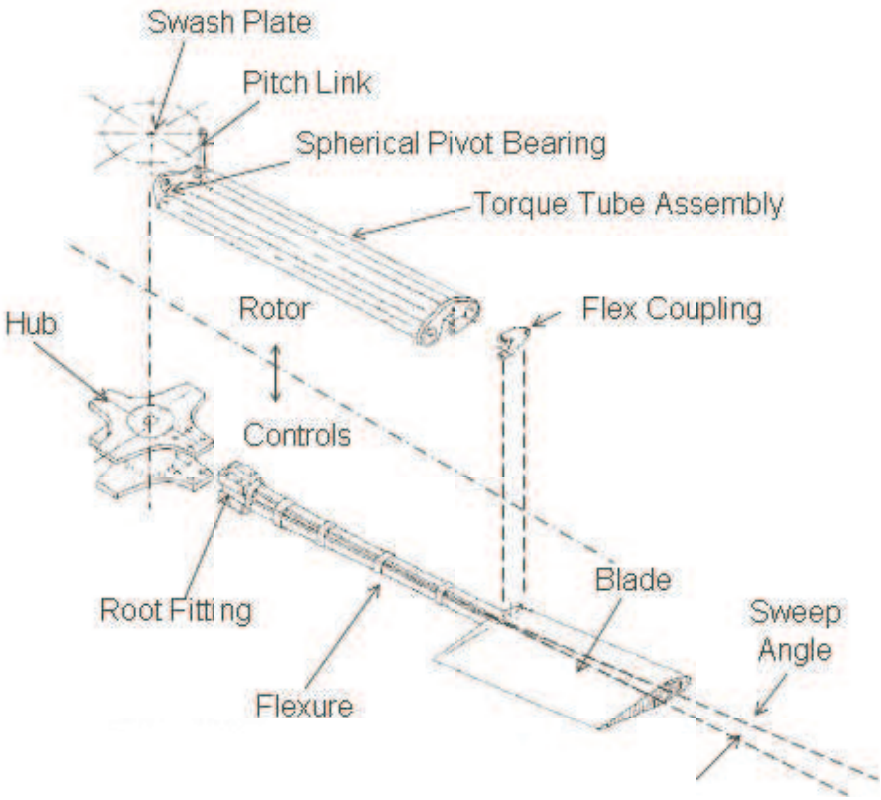

Figure 14: Schematic of Rotor System of GGTH

Table 6: Range of Natural Frequencies of EA Rotor System

	1st Frequency	2nd Frequency	3rd Frequency	4th Frequency
Lower Limit	8.78859	10.4836	32.8518	38.8791
Upper Limit	24.6391	28.5947	60.0747	99.7165
	5th Frequency	6th Frequency	7th Frequency	8th Frequency
Lower Limit	73.2110	87.9414	117.013	178.032
Upper Limit	136.712	157.714	195.612	266.617

4.3 Design Space Exploration

A preliminary design study is performed here. Such studies provide insight in selecting design variables and their bounds, objective functions, constraints and design space to establish the optimization problem in next chapter. As presented in the previous chapter, the methodology will carry two separate levels of optimization, global and local. Therefore, design space exploration was performed at both levels. The analysis model used for DOE here is the baseline model that has four design variables at the local level. A description of the model is found in chapter 5.

4.3.1 Global Level

At the global level, five design parameters were selected that can most strongly affect the dynamic behavior of the rotor system: flapwise bending stiffness, chordwise bending stiffness, torsional stiffness, sectional mass and tip mass. DOE was performed with these parameters using five-level full factorial, and the main effects were investigated. The two most influential parameters were selected to further investigate the design space for each natural frequency for the EA rotor blade. The original design provided the angular speed $\Omega = 41.14$ rad/sec. Since the GGTH has a three-bladed rotor system, and only low frequency regions will be examined to ensure avoidance of 1, 2, 3 and 4/rev resonances, only the first eight natural frequencies needed to be considered. The results are shown in Figs. 15 – 22. Based on DOE and design space exploration, typical ranges of each frequency can be found in Table 6.

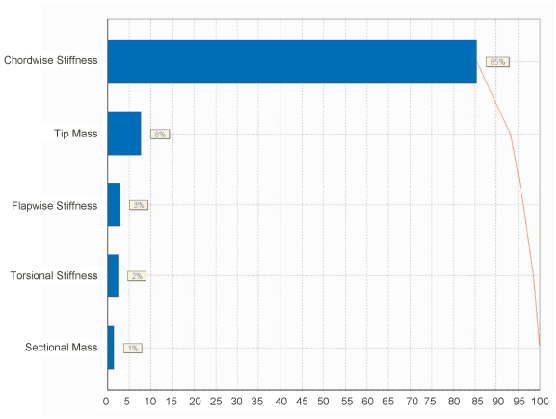

(a) Pareto Plot

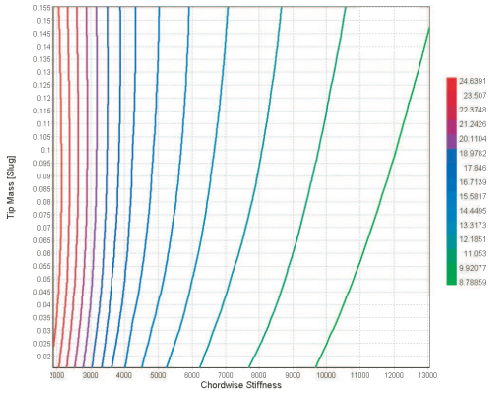

(b) Design Space with 2 Main Effect

Figure 15: DOE and Design Space of 1st Natural Frequency

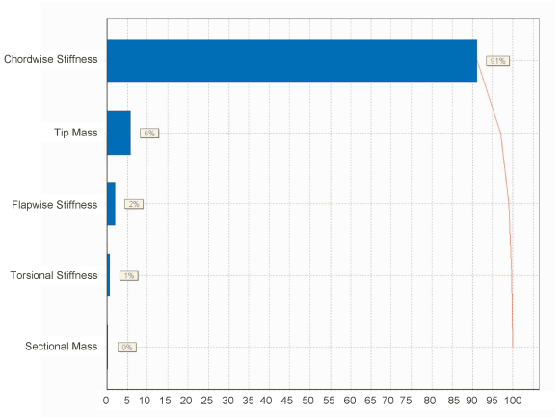

(a) Pareto Plot

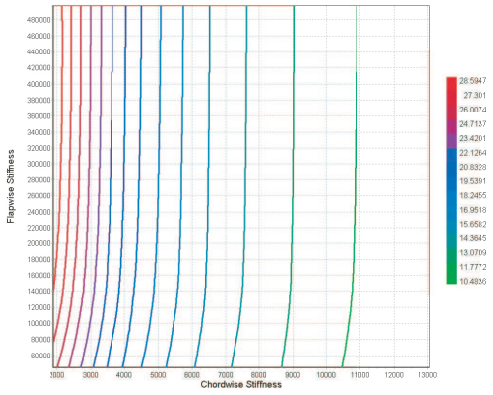

(b) Design Space with 2 Main Effect

Figure 16: DOE and Design Space of 2nd Natural Frequency

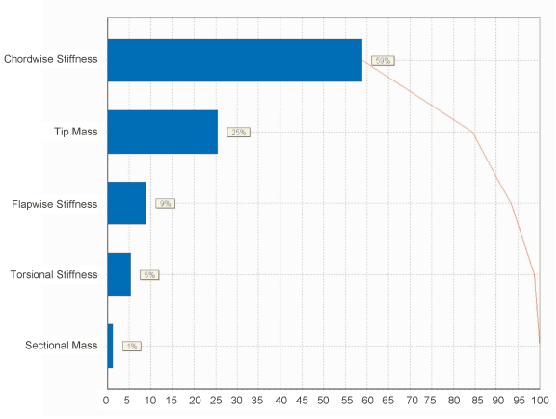

(a) Pareto Plot

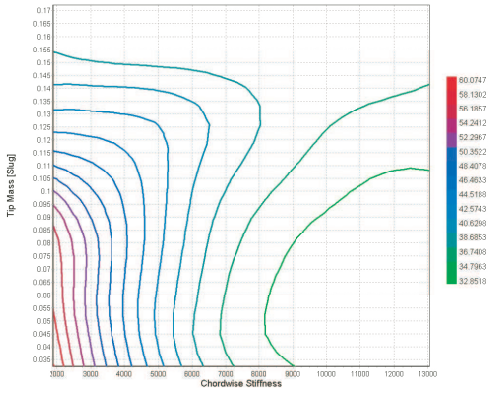

(b) Design Space with 2 Main Effect

Figure 17: DOE and Design Space of 3rd Natural Frequency

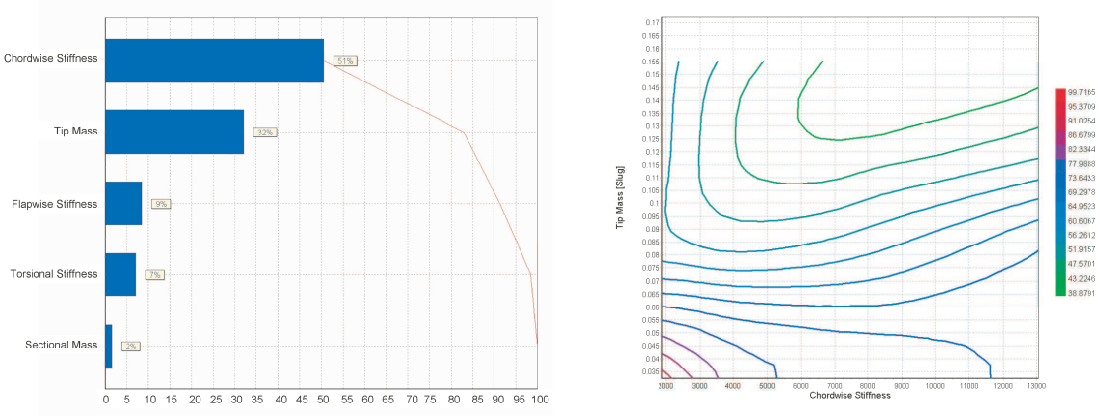

(a) Pareto Plot (b) Design Space with 2 Main Effect

Figure 18: DOE and Design Space of 4th Natural Frequency

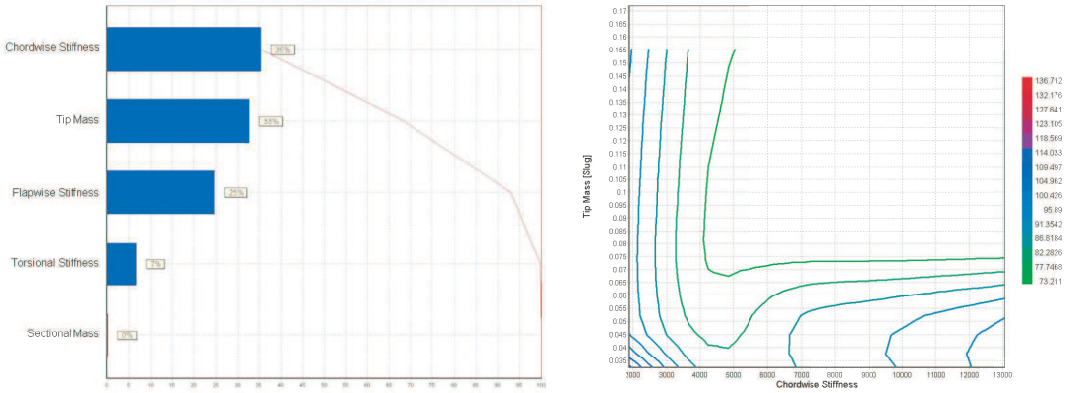

(a) Pareto Plot (b) Design Space with 2 Main Effect

Figure 19: DOE and Design Space of 5th Natural Frequency

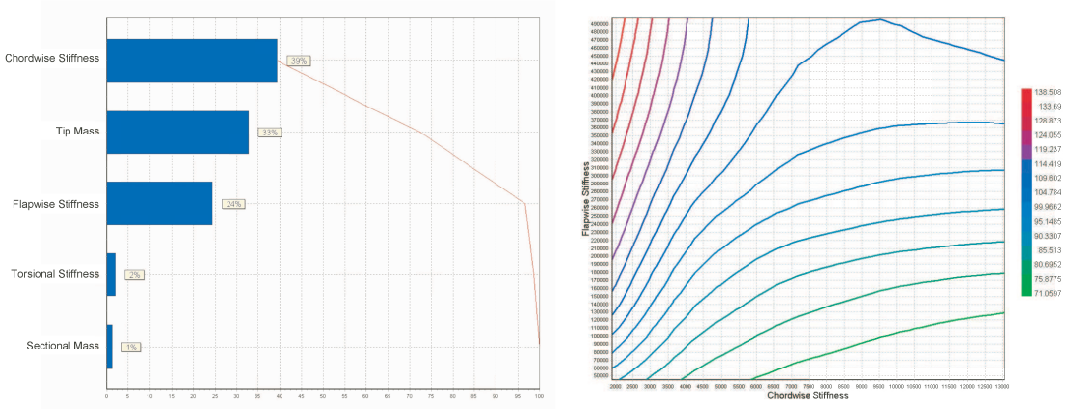

(a) Pareto Plot (b) Design Space with 2 Main Effect

Figure 20: DOE and Design Space of 6th Natural Frequency

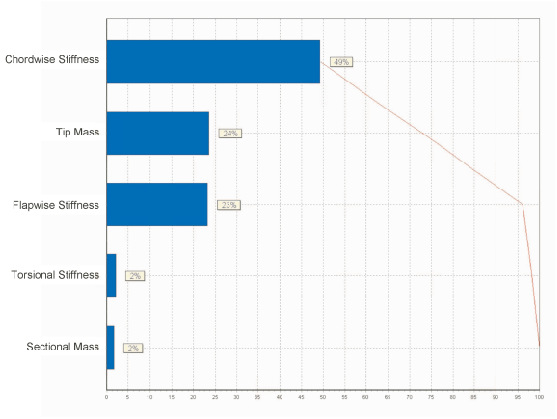

(a) Pareto Plot

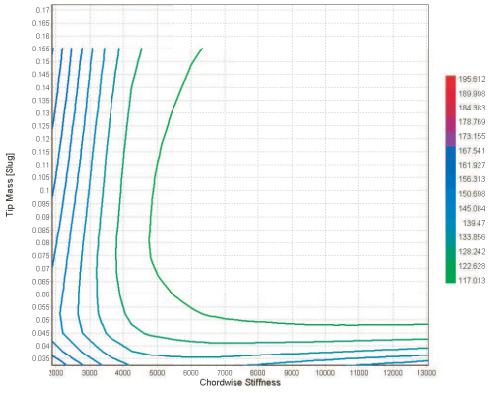

(b) Design Space with 2 Main Effect

Figure 21: DOE and Design Space of 7th Natural Frequency

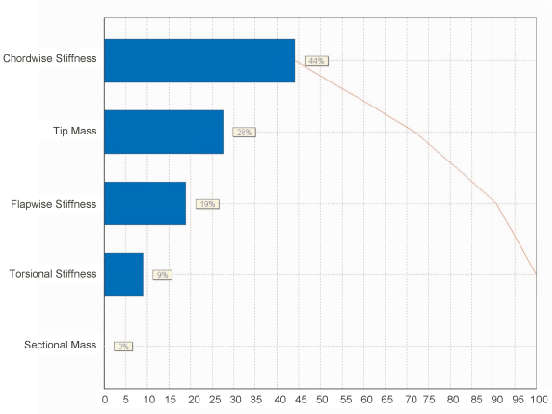

(a) Pareto Plot

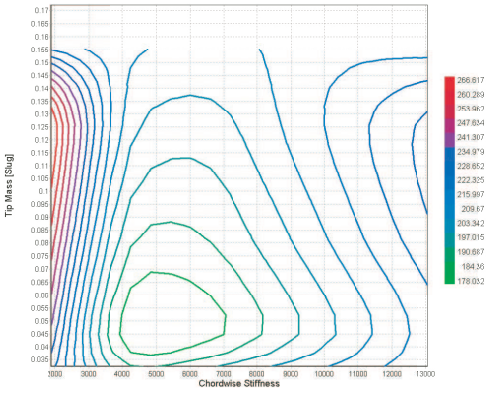

(b) Design Space with 2 Main Effect

Figure 22: DOE and Design Space of 8th Natural Frequency

4.3.2 Local Level

At the local level, the main effects of responses come mainly from size of flexure. Since there will also be changes of stiffnesses based on ply angles, each case was investigated using MATLAB. The first group of the figures (Figs. 23 – 26) have ply angles fixed at [45°/-45°] with the size of the flexure varying. The second group of figures (Figs. 27 – 29) has the flexure size fixed and varying ply angles. As is shown in these figures, the size of flexure affects the design space more drastically and makes it more complicated.

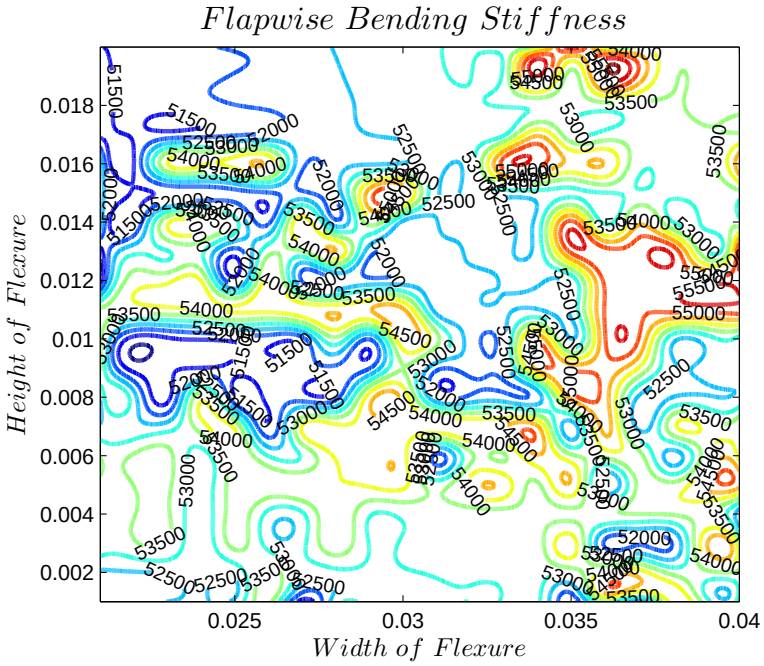

Figure 23: Design space of Flapwise Bending Stiffness with [45°/-45°] lay-up

4.4 Design of Experiments (DOE)

In the finalized methodology in Chapter 5, a surrogate model was incorporated into the original method suggested in Chapter 3. Since DOE needs to be conducted beforehand to construct the surrogate model, the description of DOE and its comparison is provided in this section.

DOE was developed in 1920's. DOE is a series of tests to observe and identify the changes in response based on changes made to input parameters. To maximize the use

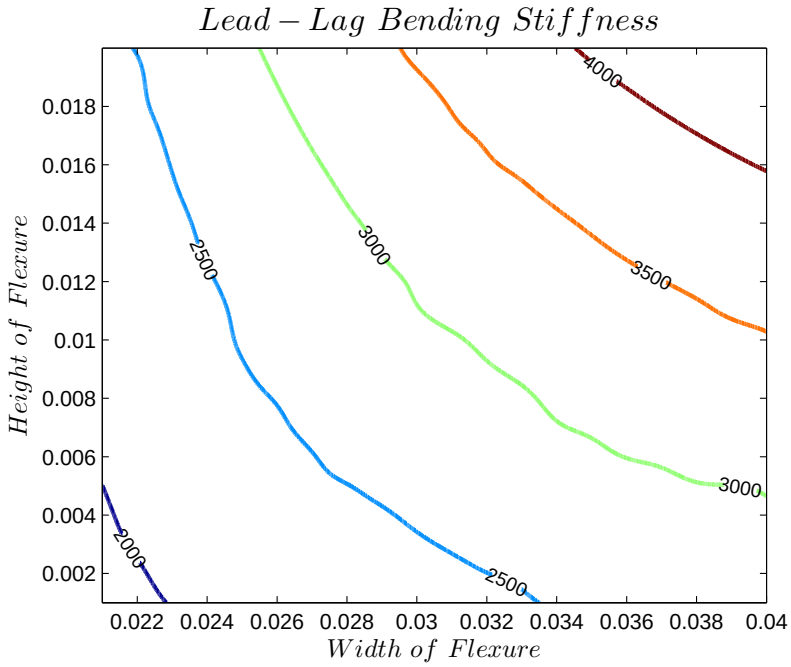

Figure 24: Design space of Lead-Lag Bending Stiffness with [45°/-45°] lay-up

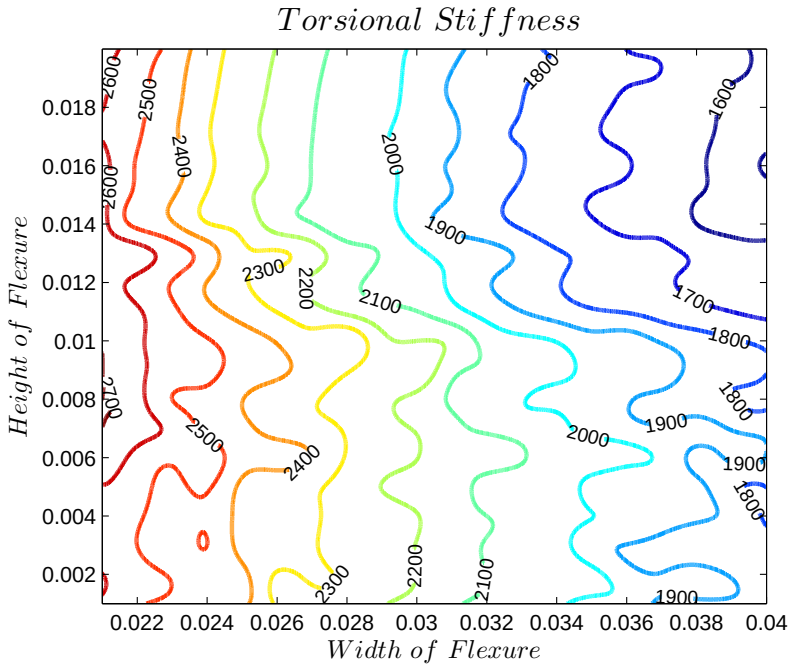

Figure 25: Design space of Torsional Bending Stiffness with [45°/-45°] lay-up

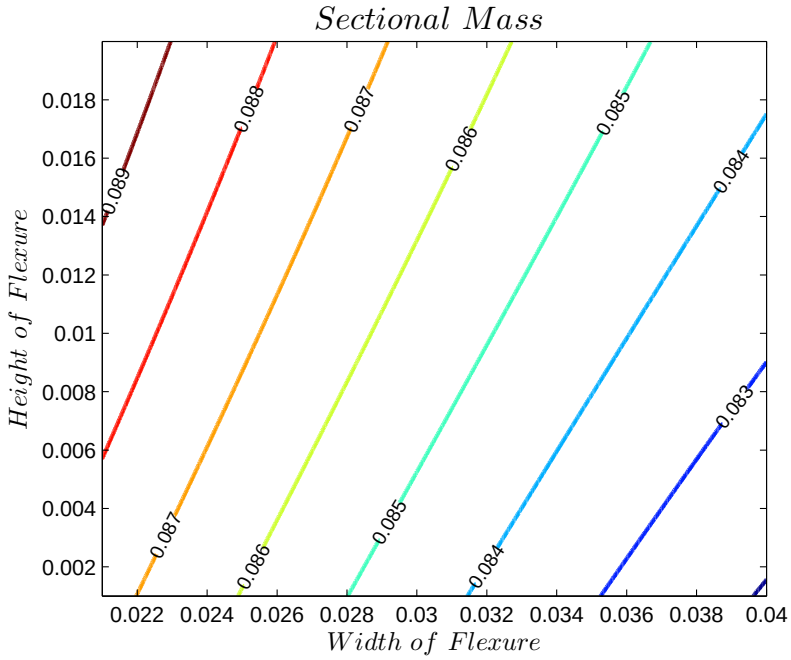

Figure 26: Design space of Sectional Mass [slug] with [45°/-45°] lay-up

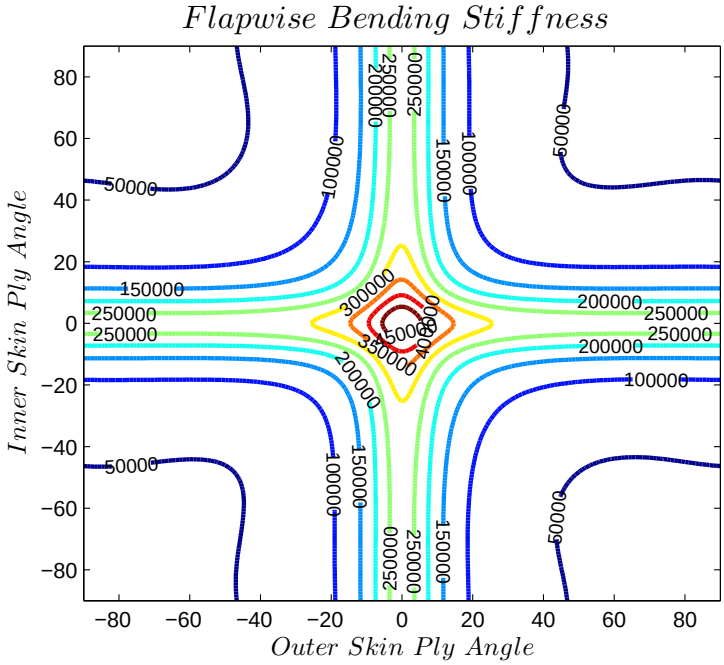

Figure 27: Design space of Flapwise Bending Stiffness with Flexure Dimension of $h = 0.04$ ft, $t = 0.02$ ft

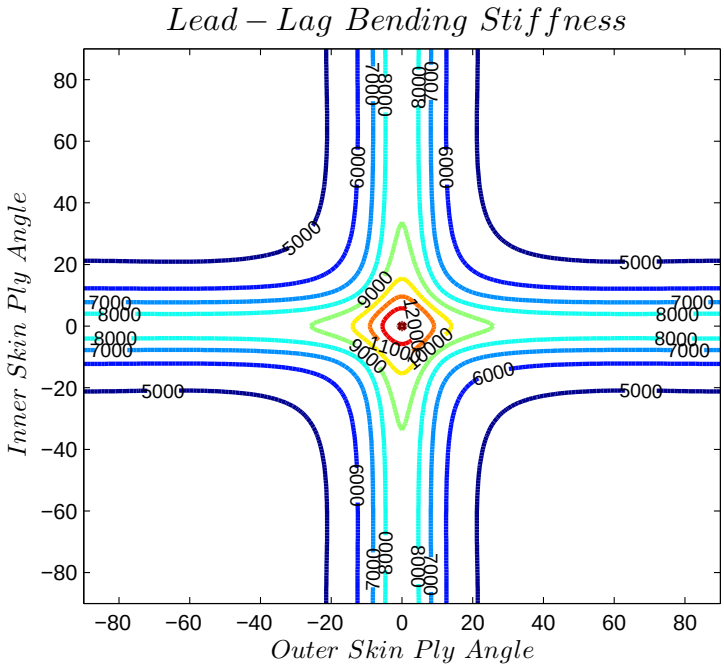

Figure 28: Design space of Lead-Lag Bending Stiffness with Flexure Dimension of $h = 0.04$ ft, $t = 0.02$ ft

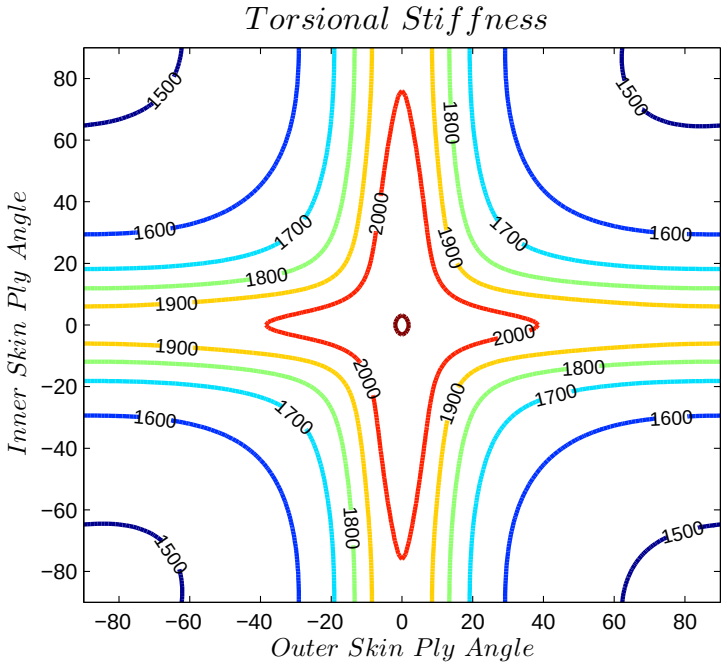

Figure 29: Design space of Torsional Bending Stiffness with Flexure Dimension of $h = 0.04$ ft, $t = 0.02$ ft

of DOE, changes in input parameters need to be purposely selected. Four classic designs of DOE are full factorial, Box-Behnken, Latin Hyper Cube and Central Composite. The typical sampling of each DOE is shown in Fig. 30 [1].

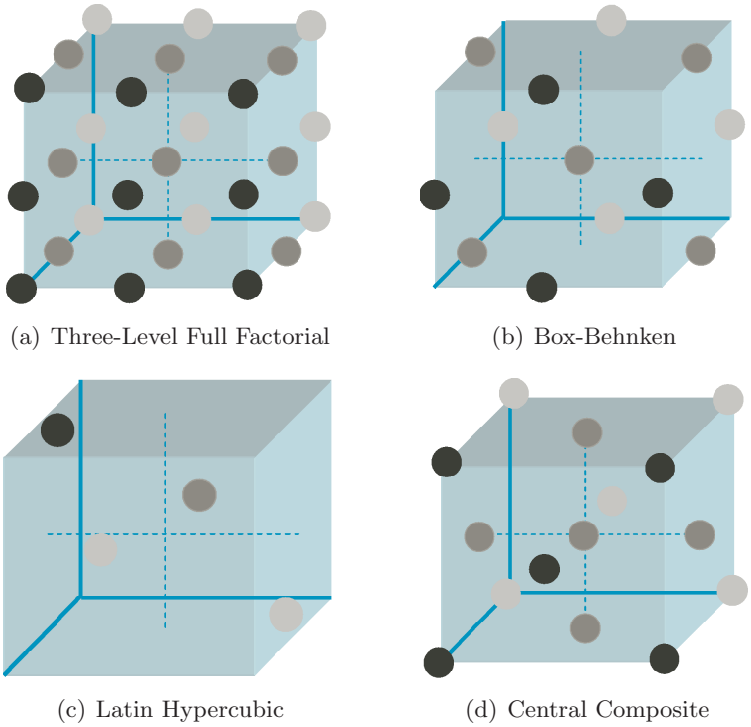

(a) Three-Level Full Factorial (b) Box-Behnken

(c) Latin Hypercubic (d) Central Composite

Figure 30: Sampling of DOE

In order to construct surrogate models, DOE needs to be run with design parameters within given range of those parameters. However, due to characteristics of each DOE concept, selection of suitable DOE for surrogate model is to be decided based on number of variables, time consumption to run DOE, how the design space needs to be explored and so on. Advantages and disadvantages of each DOE concept is provided in Table 7

Full Factorial: The Full Factorial DOE is the most basic sampling method through out the design space. The number of experiments to be run is to be decided based on the level of design parameters. The most common levels to be used are two-level and three-level Full Factorial DOE. The two-level Full Factorial design produces the minimum number of experiments to be run to capture the design space for linear RSM(Response Surface Method) and the three-level Full Factorial DOE is needed for quadratic RSM model. The

Table 7: Advantage and Disadvantage of DOE [1]

Full-Factorial	• Reduces error by considering every point • Excessive number of cases to test
Box-Behnken	• Has better convergence of analysis tools • Extrapolation to extremes of design space is needed • Extrapolation causes error for non-linear design space
Latin Hyper Cube	• Highly accurate on interior • Poor accuracy on edges of design space
Central Composite	• Extremes of the design space considered • Extrapolation is minimized • Large design space can result in many uncovered design space

two-level Full Factorial design can capture the main effects of the design parameters and the three-level Full Factorial design can capture the main effects, quadratic effects and interactions[].

Latin Hyper Cube: McKay et al [77] suggested the strategy for generating random sample points. To ensure portions of the vector space is represented, Latin Hyper Cube divide the interval of each dimension into m non-overlapping intervals that has equal probability of uniform distribution. Samples are to be paired from each dimension that satisfies orthogonality.

Central Composite Design(CCD) and Box-Behnken Design: To capture the interaction and quadratic effects of the design parameters, three-level factorial designs are needed. However, most of times, the three-level factorial design is not feasible due to the number of design parameters that leads to unmanageable numbers of experiments to be run or time consumption of analysis code that leads to unrealistic time span needed. In both cases, two-level factorial design can be used alternatively. The Central Composite Design and Box-Behnken design are most popular DOE that can be sued instead [78].

D-Optimal Design: While four classic DOE are balanced or orthogonal designs, there is a new design called D-Optimal. The D-Optimal design is form of computer-aided designs,

Table 8: Number of Experiments for three-level factorial

	7 variables	15 variables	Equation
Full Factorial	2,187	14,348,907	3^n
Box-Behnken	61	$\cdots$	
Central Composite	143	32,299	$2^n + 2n + 1$
D-Optimal	36	144	$\frac{(n+1)(n+2)}{2}$

* For Box-Behnken design only exists for 3,4,5,6,7,9,10,11,12 and 16 input parameters.
** For Latin Hyper Cube design, number of experiments to be run is decided by user.

and it comes particularly useful when classical designs do not apply. D-optimal designs are optimizations based method. The design starts of a set of candidate and algorithm chooses a optila set of design runts based on the criterion, maximizing $|\mathbf{X}'\mathbf{X}|$. The detailed information can be found in [1]. The minimum number of experiments that needs to be run for each DOE is provided in Table 8.

4.5 Verification of Meta-Models

A meta-model can be categorized as parametric or non-parametric [79]. A parametric meta-model assumes the approximation model to be a specific form while a non-parametric meta-model does not have a specific form for the approximation function, instead predicting the response of the system based on its correlated data. The linear and quadratic approximation of RSM are used as parametric meta-model and Kriging was used as non-parametric meta-model. Each model was created based on different DOE described above and compared to select most efficient DOE method for the optimization problem. The mathematical description and its comparison is in following sections.

4.5.1 Response Surface Methodology(RSM)

Response Surface Methodology (RSM) is developed to approximate the response of DOE for slow running processes. Simple linear and quadratic approximations were used as parametric surrogate models. The mathematical form of linear approximation is

$$\hat{y} = \beta_0 + \sum_{i=1}^{k} \beta_i x_i \tag{13}$$

and a detailed approximation for three design parameters is of the form

$$\hat{y} \quad = \quad \beta_0 + \beta_1 x_1 + \beta_2 x_2 + \beta_3 x_3 \tag{14}$$

Another RSM with quadratic approximation can be expressed as

$$\hat{y} = \beta_0 + \sum_{i=1}^{k} \beta_{ii} x_i^2 + \sum_{i} \sum_{j>i} \beta_{ij} x_i x_j \tag{15}$$

with its detailed form for typical three design parameters given as

$$\begin{aligned} \hat{y} \quad = \quad & \beta_0 + \beta_1 x_1 + \beta_2 x_2 + \beta_3 x_3 \\ & \beta_{12} x_1 x_2 + \beta_{13} x_1 x_3 + \beta_{23} x_2 x_3 \\ & \beta_{11} x_1^2 + \beta_{22} x_2^2 + \beta_{33} x_3^2 \end{aligned} \tag{16}$$

The coefficients of Eq.(13) through Eq.(17) are calculated by using least squares regression as follows:

$$\beta = \left[\mathbf{X}'\mathbf{X}\right]^{-1} \mathbf{X}' y \tag{17}$$

The typical approximation of these functions can be shown as in Fig. 31. From Fig. 31, one can observe that, for linear approximation with full factorial, a two-level DOE will be sufficient to capture the characteristics of the approximated function. However, for a quadratic approximation, at least a three-level DOE is needed to capture the center location of approximated function. If a cubic model is needed, the number of designs that need to be run will increase as the level of DOE increases. Therefore, even for RSM models, the approximation need to be selected based on consideration of a time-consuming process that is required to be run in order for DOE to capture the suitable approximated function.

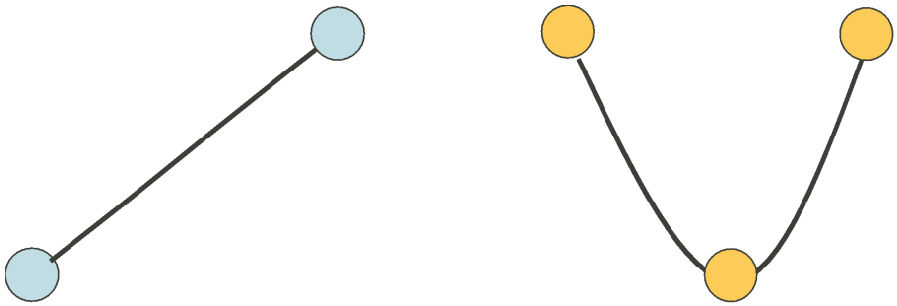

(a) Linear Approximation (b) Quadratic Approximation

Figure 31: Approximated Form of RSM

4.5.2 Kriging Model

Kriging was developed by geologists to predict mineral concentrations over mines [80, 81]. Since Kriging does not have any specific form of approximation function, the method simply predicts the estimated response from a given set of data points and their correlation based on a Gaussian Process that gives flexibility to the surrogate model over a highly non-linear design space. The Kriging approximation is based on a relation of the form

$$y(\mathbf{x}) = f(\mathbf{x}) + Z(\mathbf{x}) \tag{18}$$

where $y(\mathbf{x})$ is the unknown function of interest, $f(\mathbf{x})$ is a known function of $\mathbf{x}$, and $Z(\mathbf{x})$ is a Gaussian Process with mean zero, variance σ^2, and non-zero covariance. The known function $f(\mathbf{x})$ can be a constant, linear or quadratic function. The calculated value for the point at which the response is to be determined is based on the weighted sum of data from nearby points. Kriging starts by calculating the covariance between given data sets. The covariance matrix $Z(\mathbf{x})$ can be expressed by

$$cov(Z(a), Z(b)) = \sigma^2 corr(a, b) \tag{19}$$

where the correlation matrix is given by

$$\mathcal{R}(\theta, w, x) = \prod_{j=1}^{n} \mathcal{R}_j(\theta, w_j, -x_j) \tag{20}$$

for a Gaussian process. Here $\mathcal{R}_j(\theta, d_j)$ are the correlation functions and $d_i = w_i - x_i$ is $\exp(-\theta_j d_j^2)$ [2]. Once the covariance for each pair of data points is calculated, the Kriging function predicts the response based on the covariances among data points involved in the interpolation process. Since the interpolation is not based on any specific form but rather is based on correlation between these data sets, thus ensuring that nonlinearity over design space is captured.

The correlation function must satisfy a number of conditions, but there is nonetheless a wide variety of possible choices. Furthermore, the Kriging model results in a different prediction based on the selection of correlation function. Since the DACE (Design and Analysis of Computer Experiments) tool box from MATLAB was used to construct the

Table 9: Correlation Functions of DACE [2]

	$\mathcal{R}_j(\theta, d_j)$	
EXP	$\exp(-\theta_j\|d_j\|)$	
EXPG	$\exp(-\theta_j\|d_j\|^{\theta_{n+1}})$,	$0 ¡ \theta_{n+1} \leq 2$
GAUSS	$\exp(-\theta_j d_j^2)$	
LIN	$max\{0, 1-\theta_j\|d_j\|\}$	
SPHERICAL	$1-1.5\xi_j+0.5\xi_j^3$,	$\xi_j = min\{1, \theta_j\|d_j\|\}$
CUBIC	$1-3\xi_j^2+2\xi_j^3$,	$\xi_j = min\{1, \theta_j\|d_j\|\}$
SPLINE	$1-15\xi_j^2+30\xi_j^3$ for $0 \leq \xi_j \leq 0.2$,	
	$1.25(1-\xi_j)^3$,	$\xi_j = \theta_j\|d_j\|$
	0 for $\xi_j \geq 1$	

$$where, R_i(d) = \exp -\theta_i d^2 \tag{21}$$

Kriging model, correlation functions that can be selected as options are provided in Table 9 with equations. For the Kriging model from here, a Gaussian process was used as a correlation function.

4.5.3 Comparison of RSM and Kriging Model

In this section, the simple equation with nonlinearity is chosen to examine how well each model capture the nonlinearity of design space with different of DOE. The test equation includes typical quadratic RSM and Cosine functions to add nonlinearity into the actual design space. The 2 design parameters were used to enable the visualization for comparison purpose. DOE tested here were Latin Hyper Cube, D-Optimal and Full Factorial with different levels. The exact equation is

$$y = \underbrace{\beta_0 + \beta_1 x_1 + \beta_2 x_2 + \beta_{12} x_1 x_2 + \beta_{11} x_1^2 + \beta_{22} x_2^2}_{Typical\ Quadratic\ Form\ of\ RSM} + \underbrace{100 \times \cos(x_1) + 100 \times \cos(x_2)}_{Ransom\ Nonlinear\ Function} \tag{22}$$

For the Full Factorial, three-, five- and seven-level DOE were tested that result in 9, 25 and 49 experiments; and 50 samples were used for Latin Hyper Cube DOE. The results are shown as 3D plots in Figs. 32 – 34. Fig. 32 shows the actual design space with sampling point and its predicted values. Fig. 33 represents the predicted function as surface plot, and Fig. 34 indicates errors between actual function values and predicted values as a surface plot.

The quadratic RSM predictions do not differ much from each other based on the type of DOE. However, Kriging showed significant differences among different selections of DOEs. The D-Optimal DOE did not capture the nonlinearity of the actual function with RSM or Kriging. The D-Optimal DOE shows rather poor prediction in both cases and predicted area was almost same for both. It is suspected that since the sampling cannot cover the whole design space due to the minimization of the sampling points, D-Optimal DOE can skip the points that are critical to capture the nonlinearity. As for Full Factorial DOE, it is shown that high resolution sampling is needed to have a more precise approximation. The three-level Full Factorial approximation gave the same prediction as RSM, which did not show any nonlinearity of actual function. As Full Factorial sampling is tested with increased resolution, e.g. in level such as five- and seven-level DOE, the precision of the predicted response is also increased. The Latin Hyper Cube generated satisfying results compare with RSM. It was also determined from the results that Kriging needs an orthogonal array of DOE. If the Full Factorial is to be used, at least a seven-level is recommended, which will increase number of experiments drastically as the number of design variables increases. However, for both Full Factorial and Latin Hyper Cube DOE, increasing number of experiments does not always guarantee more precise prediction. Therefore, it is necessary to set a limitation in increasing number of experiments.

The following table shows the characteristics of RSM and Kriging surrogate model along with Neural Networks and where each model can be best fit. As is it shown, the Neural Network is best used for large problems with even higher number of training data set which means, predicted model is more accurate when the model fitting procedure is repeated. Due to this characteristic of Neural Network, this surrogate model does not show much improvement from Kriging for this specific example and the implementation model that is used in next chapter. Therefore, Neural Network is not tested nor used as surrogate model.

Table 10: Recommendations for surrogate model choice and use [3]

Model Choice	Characteristics/Appropriate Uses
Response Surfaces	• well-established and easy to use
	• best suited for applications with random error
	• appropriate for applications with < 10 factors
Kriging	• extremely flexible but complex
	• well-suited for deterministic application
	• can handle applications with < 50 factors
	• limited support is currently available for implementation
Neural networks	• good for highly nonlinear or very large problems($10,000$ parameters)
	• best suited for deterministic applications
	• high computational expense (often $> 10,000$ training data point)
	• best for repeated application

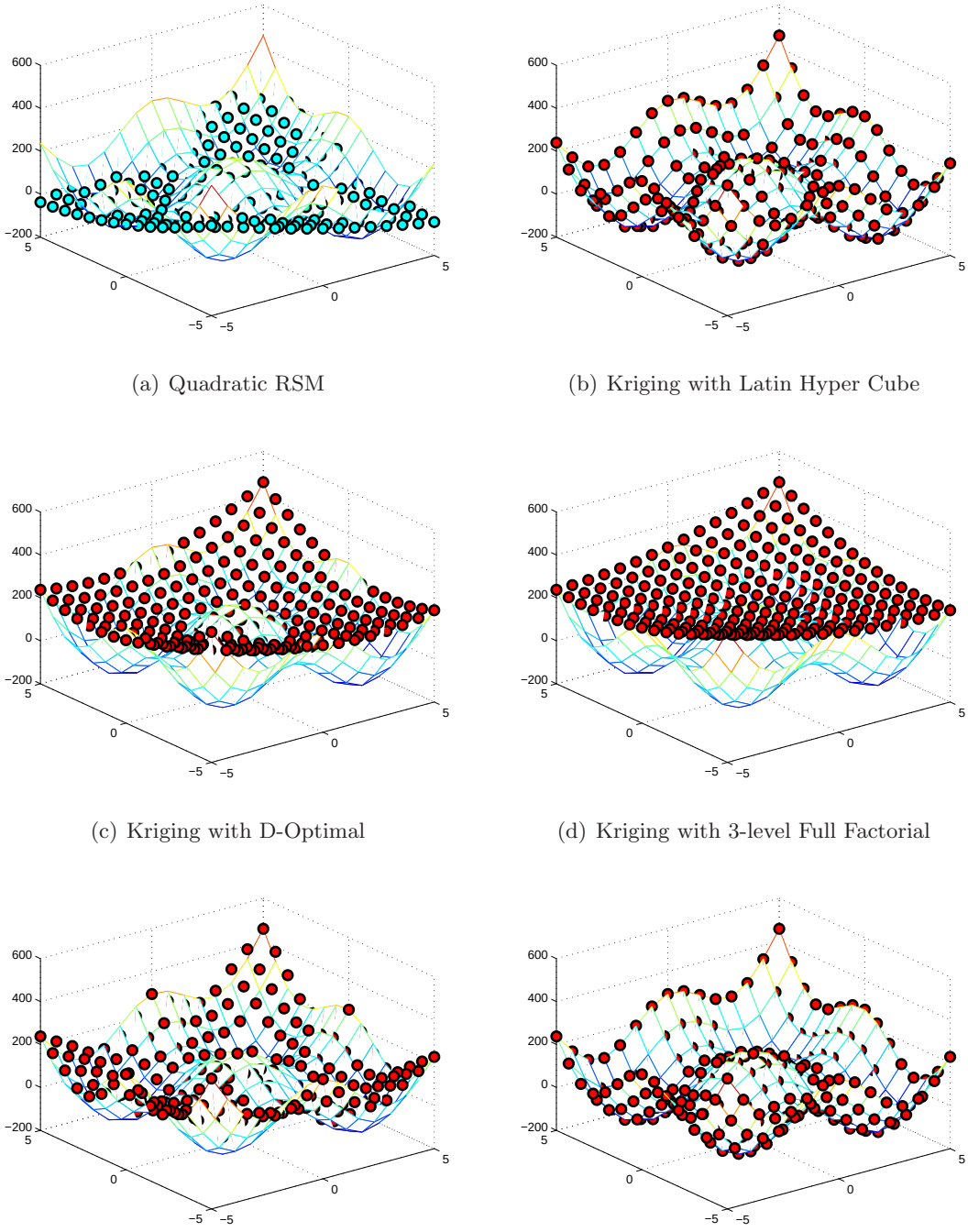

(a) Quadratic RSM

(b) Kriging with Latin Hyper Cube

(c) Kriging with D-Optimal

(d) Kriging with 3-level Full Factorial

(e) Kriging with 5-level Full Factorial

(f) Kriging with 7-level Full Factorial

Figure 32: Exact Function vs Predicted Samples

* Dot mark is the samples and mesh graph is exact function.

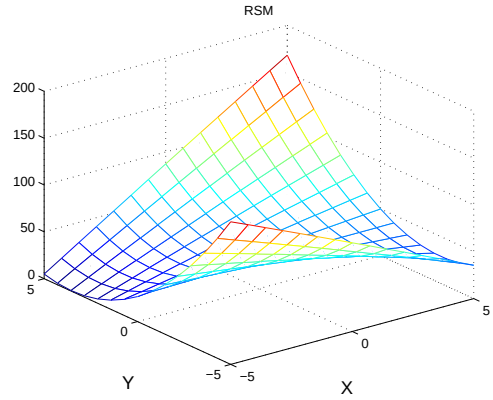

(a) Quadratic RSM

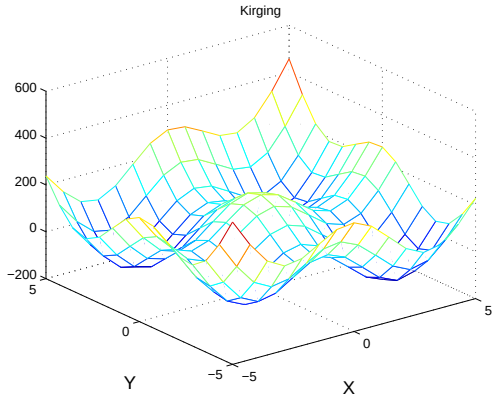

(b) Kriging with Latin Hyper Cube

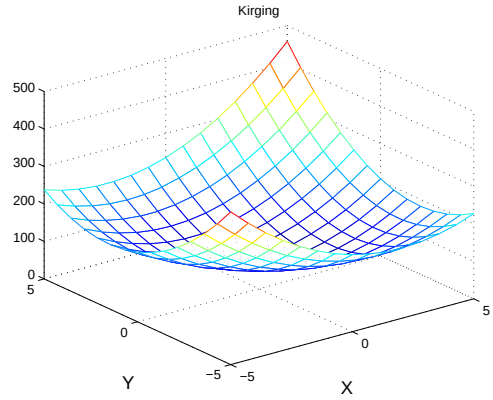

(c) Kriging with D-Optimal

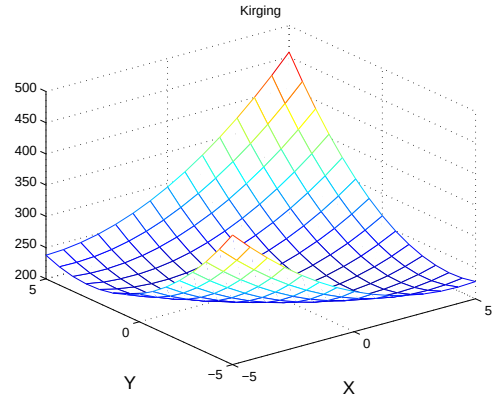

(d) Kriging with 3-level Full Factorial

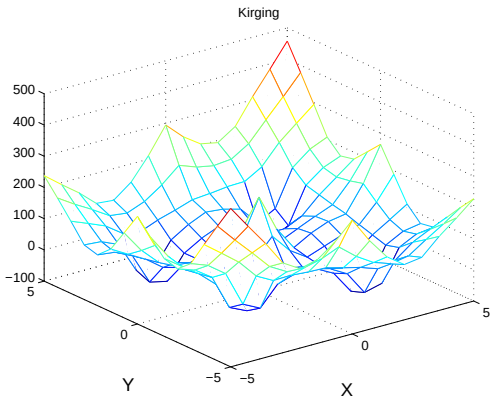

(e) Kriging with 5-level Full Factorial

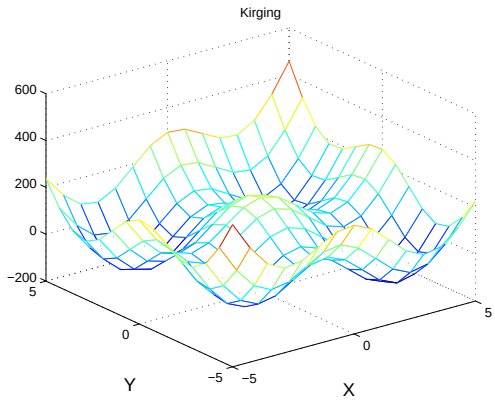

(f) Kriging with 7-level Full Factorial

Figure 33: Predicted Response

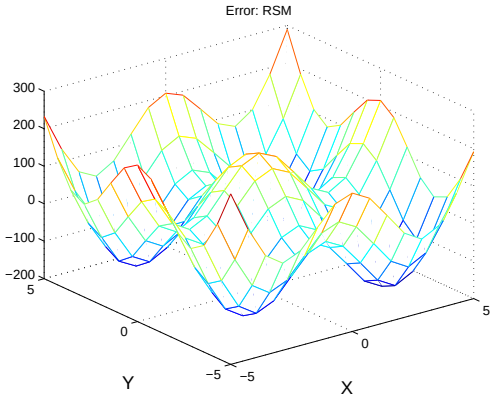

(a) Quadratic RSM

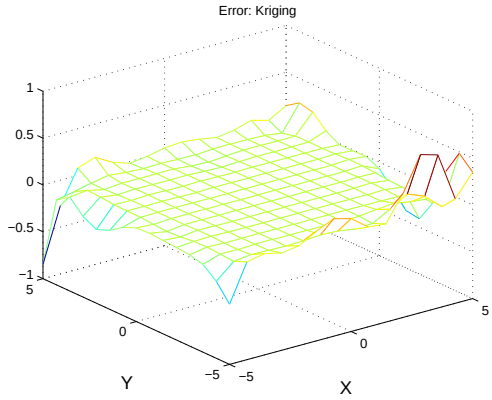

(b) Kriging with Latin Hyper Cube

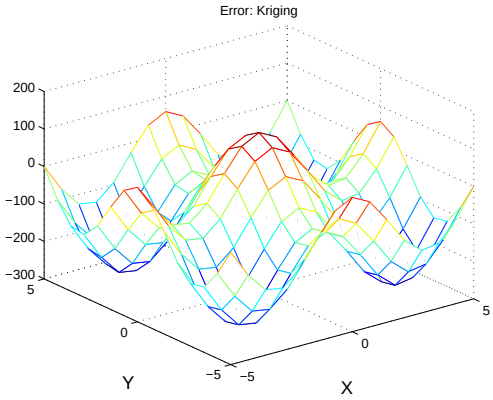

(c) Kriging with D-Optimal

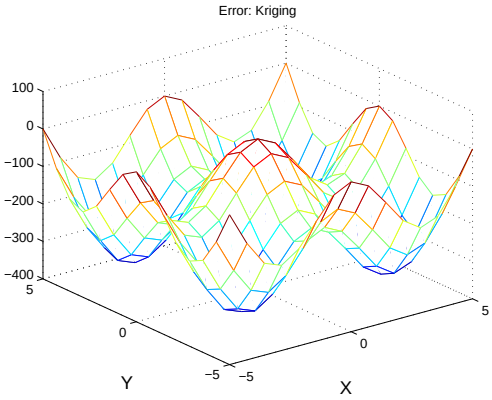

(d) Kriging with 3-level Full Factorial

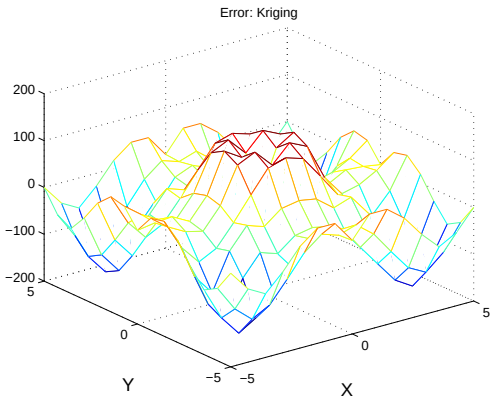

(e) Kriging with 5-level Full Factorial

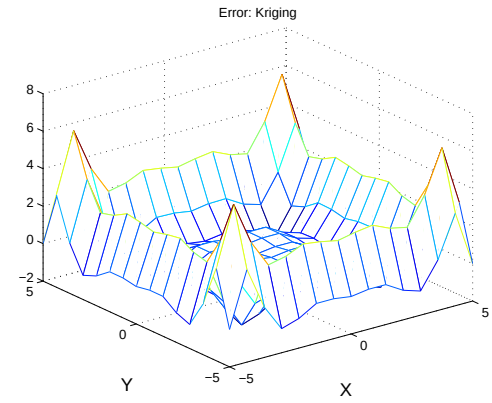

(f) Kriging with 6-level Full Factorial

Figure 34: Error of Predicted Function from Exact Function

CHAPTER V

IMPLEMENTATION – GGTH BLADE OPTIMIZATION

5.1 Overview

In this chapter, issues raised in previous chapters are further explored. The methodology introduced here is a multilevel, multiphase approach with a surrogate model. The original methodology suggested in Chapter 3 did not show a clear indication of the communication between global and local levels because both levels reached the optimal solution without iteration between levels. Also, the design variables used at the global level were treated as independent of each other even though three stiffness related design variables were highly dependent on each other. The surrogate models were embedded in the procedure to ensure the communication between global and local levels by enforcing the design variables at the global level to stay in the feasible design space of the local level optimization. The candidates for surrogate models include Kriging and linear and quadratic response surface regression (RSM), which were investigated in Ref. [79, 82].

5.2 Methodology

The methodology in Chapter 3 was modified with alternative approach. The methodology used here utilizes high-fidelity structural beam analysis tools in the same manner as previous methodology: DYMORE [10, 11] and VABS[6, 7]. However, instead the so-called "geometry generator" of the previous work, an alternative automated procedure was developed; and the surrogate model was incorporated into the present methodology. In previous studies [72, 73, 83], the geometry generator and other tools under development at the time of the work were used for the local-level optimization process. These tools all had limitations. In particular, if the geometry generator were required to be adapted for a different blade configuration, relatively complex programming would be needed. Also, for the configuration of the Generic Georgia Tech Helicopter (GGTH) blade, those tools were not at a sufficiently

mature stage of development to be applied. To overcome these limitations the VABS-ANSYS macro [84] was utilized and modified. The VABS-ANSYS macro was one of the early ways to generate VABS input files, making use of ANSYS. However, as it was originally developed, this method required human interaction for each area to assign a material and, for composite materials, to assign ply angles and lamina orientation angles; see Appendix A of Ref. [85]. This action would take a few seconds to a minute based on skill of a user, but the whole process of specifying these parameters can take up to a day based on the number of areas in the model. The original VABS-ANSYS macro was thus modified and wrapped using MATLAB with ANSYS to automate this process. As a result, the entire procedure could be done within 1.5 – 3.0 seconds, whereas it previously took up to an hour to only generate one VABS input file per function call. The schematic of this automated VABS-ANSYS macro procedure is provided in Fig. 35.

This automated VABS-ANSYS procedure starts from selection of an airfoil shape from the subfunction generated in MATLAB. Each subfunction was generated to play a role as a library of airfoil shapes. Under the airfoil shape subfunction, data points are provided [86], along with a function that can generate necessary data points using interpolation. Once, the outer points are generated, outer shapes are scaled down to generate skin layers as additional contours of the airfoil. The skin thickness can be different for each layer in this procedure. Once all the points are generated for skin layers of the airfoil, it generates the areas. The scheme that generates areas is based on a simple FEM scheme that is used to generate elements. This so called "connectivity vector" follows same sequence when elements are generated with nodes in FEM. Using same scheme yields the result all the areas to have same sequence of points and lines created; therefore, when ANSYS reads information about each area, the last line number is set to be the reference line for ply angle for composite material case. For this case, the fourth line numbers are stored to correspond with the area number to be used as a reference line later. Once these data sets are constructed MATLAB runs the program to generate the macro file used for constructing the geometry. Other information about the airfoil, such as whether each area uses an isotropic or composite material and which material the area is assigned to, are stored as separate data files. Once

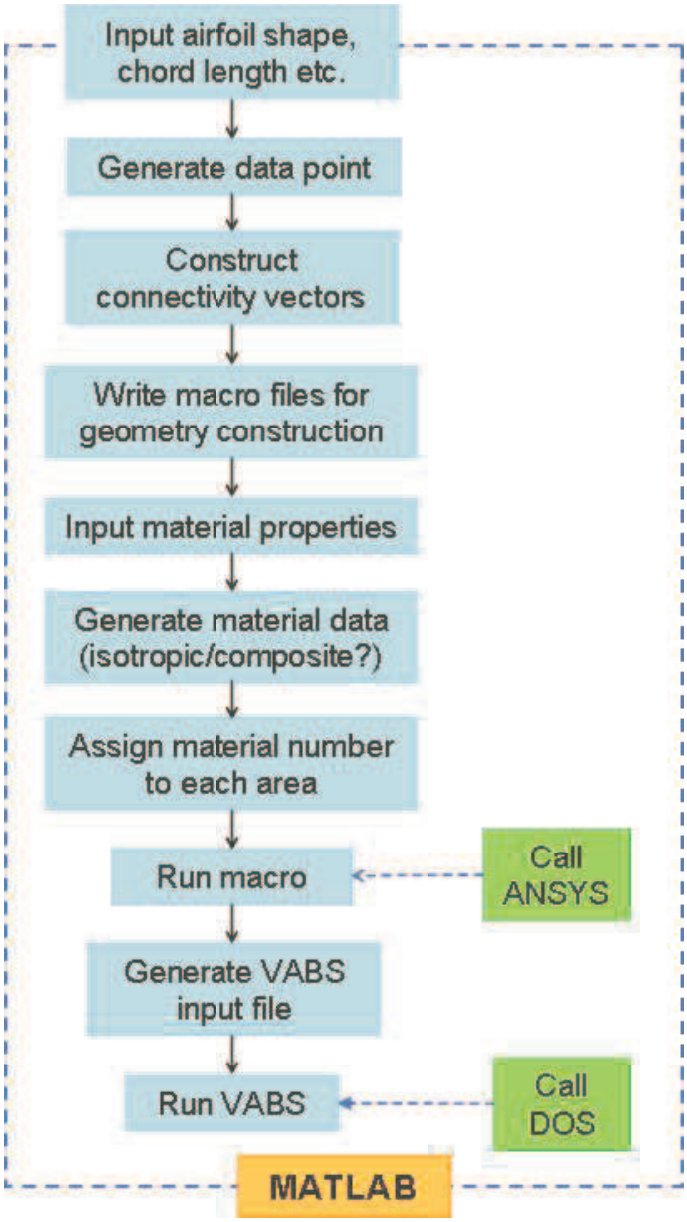

Figure 35: Automative procedure of VABS

the geometry generating macro is run, the modified VABS-ANSYS macro calls each data file to generate a VABS input file. While these macros are running, MATLAB uses a DOS command to start ANSYS. Also, the existing VABS program was modified to be run automatically also.

The methodology suggested in Chapter 3 was modified to make use of this new approach and surrogate models. The previous methodology, with global and local level optimization, ignored the high coupling between torsional, chordwise bending and flapwise bending stiffnesses therefore and instead treated them as dependent variables. However, these values are highly coupled to each other, and depend on local level design variables. This limitation resulted in producing an infeasible design to be achieved at the local level. Therefore, even the local level optimizer had two phase that are used in the design space exploration with GA to find the most promising candidates to be used as a starting point for the gradient-based method at the second phase. This could result in producing an infeasible design at each level and the levels passing information to each other in a sort of infinite loop. The current methodology was modified to overcome this limitation by incorporating the surrogate model constructed at the local level in order to enforce the global level design variables to stay in a feasible region of the local level design space. Also, this method can also yield the benefit of shorter convergence times since there a trend is established that design variables can follow. The surrogate model is imposed as a constraint at the global level with $\pm 15\%$ tolerance around predicted curve. The flow chart of new methodology is provided in Fig. 36.

This methodology will play a role as a branch of general rotorcraft preliminary design methodology which was suggested as IPPD originally and integrated in the "Model Center" environment later on [4]. The link between general rotorcraft preliminary design methodology and the methodology here in the "Model Center" environment has already been demonstrated in Ref. [4] and is illustrated in Fig. 37. With this procedure, DOE was performed to construct a surrogate model using the baseline model described in following section.

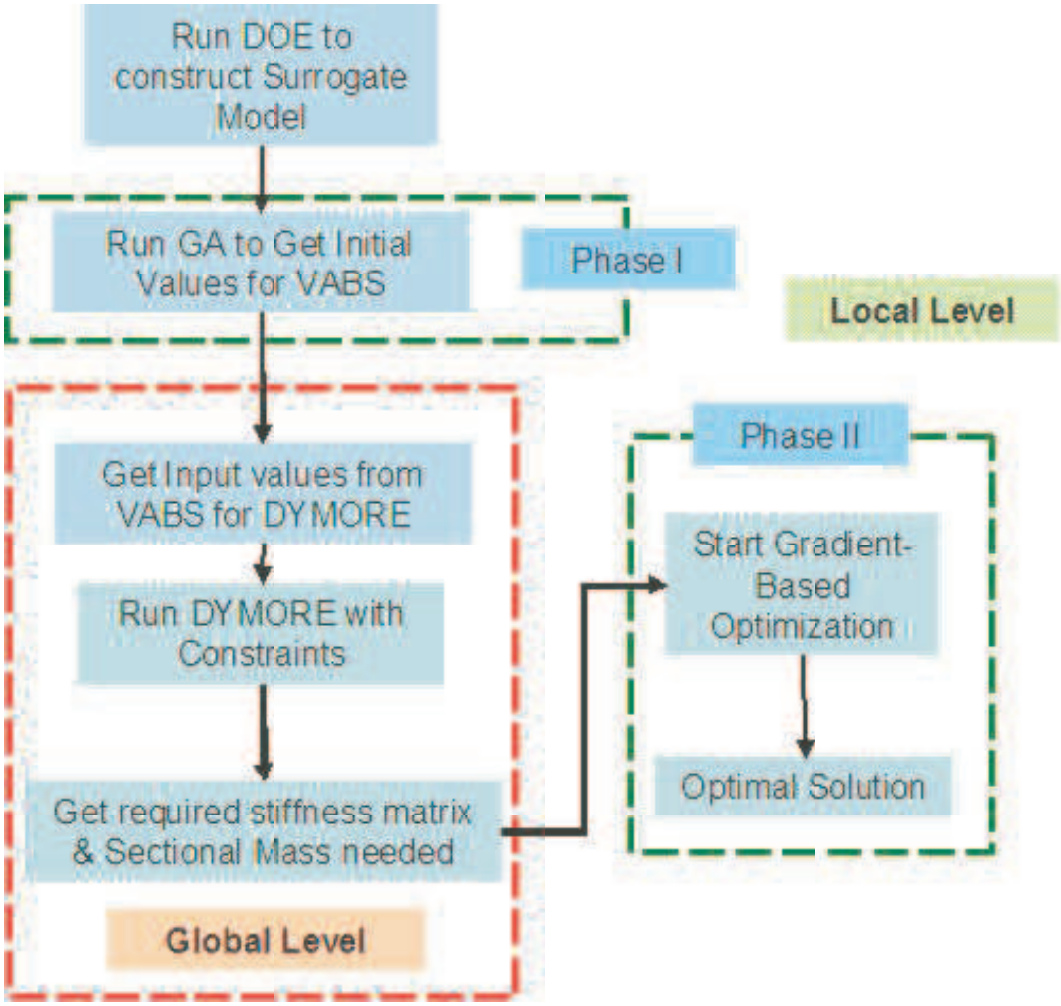

Figure 36: Final Methodology

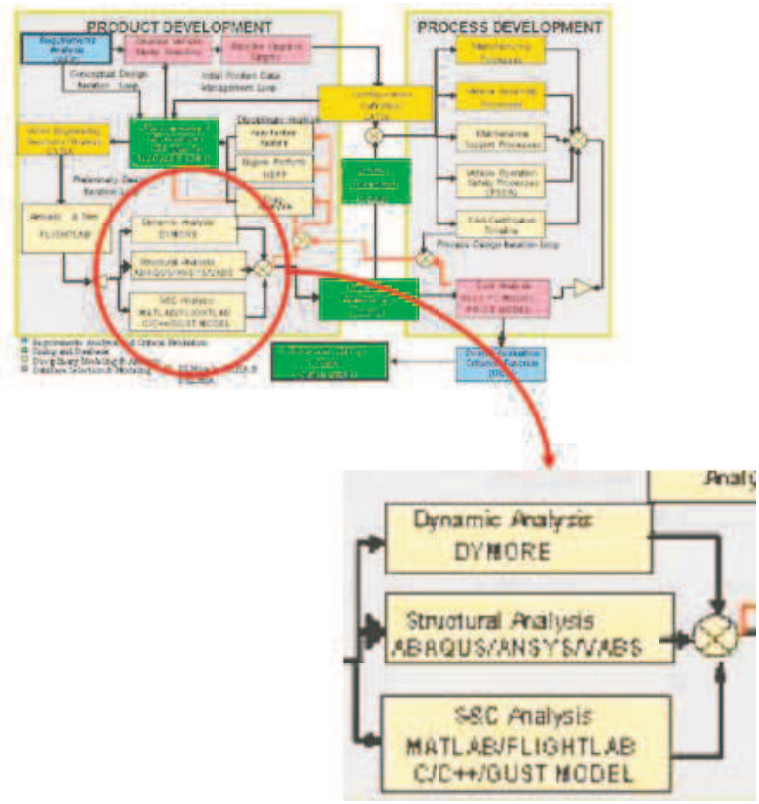

Figure 37: Structural Design and Optimization Process in IPPD

5.3 Baseline Model

The baseline model used here is the Elastic Articulation (EA) rotor system, the rotor system of the GGTH. The EA rotor is a soft-in-plane bearingless rotor with 10% effective flapping hinge offset and 2° forward sweep.

5.3.1 EA Rotor System

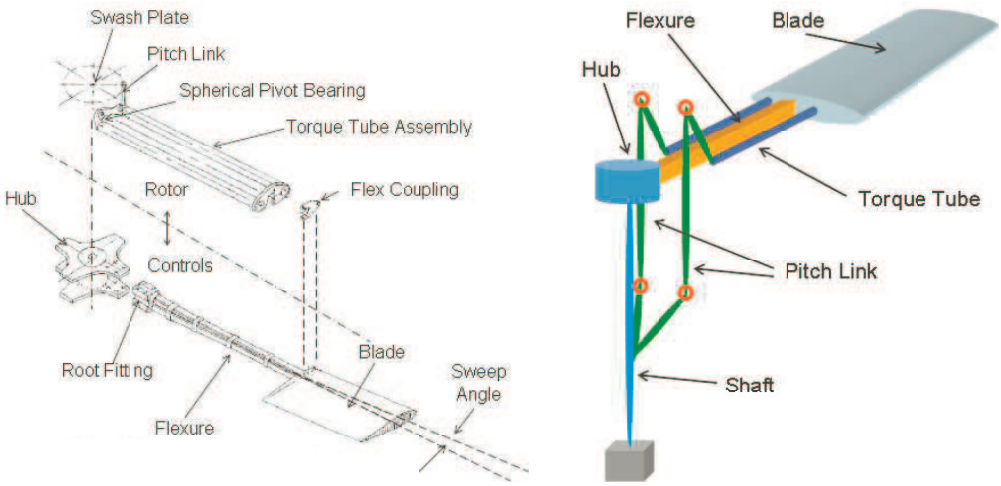

(a) Configuration of the EA Rotor System (b) Schematic of DYMORE Blade Model

Figure 38: Rotor System Analysis Model

The EA rotor system is mainly comprised of rotor blades, flexure beams, hub, torque-tube assembly, and pitch-link assembly (the configuration is depicted in Fig. 38). The flexure beams replace all hinges and bearings of an articulated rotor by allowing flapping, feathering, and lagging motions. Since the flexure is a cantilevered beam capable of supporting the static weight of the blade, no droop stops nor lag dampers are required. The torque tube assembly carries only feathering torque and is isolated from blade bending moments by the disc flexure coupling at the outboard attachment to the blade and by a spherical pitch pivot bearing at the inboard end.

5.3.2 Analysis Models

The optimization process relies on two complementary models: a flexible multi-body model used for rotor dynamic behavior analysis at the global level, and a blade cross-sectional

analysis that generates the cross-sectional stiffnesses at the local level. The description of each model is provided next.

Rotor System Model: The rotor systems are modeled to investigate the natural frequencies of the EA rotor by using the flexible multi-body analysis code, DYMORE. The blade is modeled by beam elements. The sectional properties of the blade are accurately computed using VABS and then inserted into the DYMORE model. The rigid body elements are used to model the shaft, hub, pitch links, and torque tubes. The torque tube assemblies are modeled with spherical, universal, and sliding joint elements to carry only feathering torque. The pitch links are connected to the torque tube assemblies by means of spherical joints that allow the connected components to be at an arbitrary orientation with respect to each other. Sliding joints with springs are attached to the pitch link to control and measure the pitch link displacement. The prescribed displacement of the sliding joint changes the pitch angle at the blade root. The flexures are rigidly connected to the hub and root of the blades at each end. Each flexure is modeled with two cubic beam elements. The sectional property of the flexure beam is computed in the flexure design section. The blades are rigidly attached to the flexure beams with two degrees of forward sweep angles. To change the pitch angle, torque tube assemblies are connected to the root of blades by universal joints. Each blade is modeled with four cubic beam elements that account for the elastic and inertial couplings arising from the use of composite materials and the forward sweep angle. The rotor system model has three-bladed assemblies.

Cross-Sectional Model: Due to the role of the flexure beams, the dynamic characteristics of the EA rotor are significantly affected by the sizing of flexure beams. Therefore, it can be said that the appropriate sizing of flexures is the key element for a successful rotor system. From the original design [87, 75], there are four flexure beams of square shape. To secure enough space inside of the blade for the flexure design, a NACA0015 was selected as baseline airfoil. Design parameters used here is provided in Table 11. As for the implemented cross-sectional model, three types of cross-sections were tested and compared. The first model starts with two layers of skin with thickness of 0.001 ft with varying ply

angles. The flexure is comprised of four thin structural members, which were assumed to have identical size and unidirectional ply angles. The choice of unidirectional ply angles for the flexures is suggested by original design. The second model has the same configuration as the first, except that each ply angle of the flexure is allowed to vary. The third model has 2 varying ply angles for skin layers, 2 sets of identical flexure beams that are horizontal and vertical, and two vertical beams can be located at different chordwise location. The ply angles of flexure beams are not used as design variables based on DOE results in following section. These results in four design variables for the first model and eight for the second and the third. The cross-section of the first blade is shown in Figs. 44, 45 for the second model and 46 for the third model. The surrogate models are constructed using the first model and optimization was conducted for first and third cases.

Table 11: Design Parameters

Design Parameters	Values	Units
Rotor Target Weight (W_t)	26.67	[lb]
Airfoil	NACA0015	
Chord Length (c)	0.64	[ft]
Skin Thickness (t_s)	0.001	[ft]

5.4 Surrogate Models

As discussed in Chapter 4, the Kriging model showed superior prediction capability over RSM when there is nonlinearity in the design space. Also, the Latin Hyper Cube DOE showed better performance compared to the Full Factorial for the Kriging model due to its orthogonality since the first assumption in DACE toolbox for sampling sets are orthogonality between samples. The Latin Hyper Cube DOE does not need the larger number of experiments as required by the Full Factorial as the number of parameters increases. Currently, ModelCenter has a maximum of 999 runs for performing the Latin Hyper Cube DOE. The cross-sectional model I with four parameters could perform a seven-level Full Factorial DOE only with 2,401 experiments. However, for the second cross-sectional model that includes two sizing parameters and six ply angle parameters, running the Full Factorial DOE with at least the five-level will be excessive, resulting in 390,625 runs with only

eight parameters. Therefore, the Latin Hyper Cube DOE was used for surrogate models. The cross-section of the flexure with lower and upper bound of values of flexure sizes are provided in Table 12.

Table 12: Design of Experiment(DOE) Parameters

Cross-sectional Model with 4 Design Variables		
Design Parameters	Lower Limit	Upper Limit
Width of Flexures (w_f)	0.005	0.04
Height of Flexure (h_f)	0.005	0.04
Ply Angle of Skin (θ_{outer}, θ_{inner})	$-90°$	$90°$
Cross-sectional Model with 8 Design Variables		
Design Parameters	Lower Limit	Upper Limit
Width of Flexures (w_f)	0.005	0.04
Height of Flexure (h_f)	0.005	0.04
Ply Angle of Skin (θ_{outer}, θ_{inner})	$-45°$	$45°$
Ply Angle of Flexures(θ_1, θ_2, θ_3, θ_4)	$-45°$	$45°$

*All the units are in ft. for size and deg. for angles

For the cross-sectional model II, since only a three-level full factorial was feasible, the upper and lower limits of the design parameters were set to be [-45°/45°] instead of [-90°/90°]. The main effect plots are provided in Fig. 39 for each response. From these results, the main effects come from the size of the flexure and from the two ply angles of the skin which results the cross-sectional model II same as cross-sectional model I. Based on DOE, the ply-angles of flexures are fixed as 0° and cross-sectional model III is used for optimization process and compared with model I. The main effects of cross-sectional model III is in Fig. 40.

As discussed earlier in this section, the Latin Hyper Cube DOE is used to construct surrogate models. Since a two-level Full Factorial DOE requires 256 experiments, the sampling number was chosen to be 256 experiments. It is expected for RSM models to produce poor predictions; however, these models were run only for comparison, and the main focus here is to use a Kriging model with a more economical DOE. The predicted versus actual sampling plot with RSM equations are as follows for each linear and quadratic model. The RSM surrogate model uses three stiffnesses that are torsional, chordwise bending and flapwise bending stiffness as design parameters and sectional mass as response. The linear equation

Table 13: Statistical Information of RSM Models

Linear					
Source	DF	SS	MS	F	Fsig(%)
Regression	3	0.1324900E-02	0.4416332E-03	0.3572654E+03	0.0000
Residual Error	252	0.3115095E-03	0.1236149E-05		
Total	255	0.1636409E-02			
S	0.1111822E-02				
Y_{avg}	0.8210761E-01				
CoV	1.35%				
R-Sq	80.96%				
R-Sq(adjusted)	80.74%				
Quadratic					
Source	DF	SS	MS	F	Fsig(%)
Regression	9	0.1406029E-02	0.1562254E-03	0.1668174E+03	0.0000
Residual Error	246	0.2303804E-03	0.9365055E-06		
Total	255	0.1636409E-02			
S	0.9677321E-03				
Y_{avg}	0.8210761E-01				
CoV	1.18%				
R-Sq	85.92%				
R-Sq(adjusted)	85.41%				

is

$$\widehat{m} = 0.6178372\times10^{-1}+0.9384285\times10^{-5}\times GJ+0.2595299\times10^{-5}\times EI_c-0.5348933\times10^{-7}\times EI_f \tag{23}$$

and the quadratic equation is

$$\begin{aligned}\widehat{m} \;=\; & 0.4133069\times10^{-1}+0.2711190\times10^{-04}\times GJ+0.8094299\times10^{-05}\times EI_c \\ & -.1726956\times10^{-06}\times EI_f-.3867131\times10^{-08}\times GJ^2-.3909645\times10^{-09}\times EI_c^2 \\ & +0.1475657c\times10^{-12}\times EI_f^2-.1666229\times10^{-08}\times GJ*EI_c \\ & +0.3878689\times10^{-10}\times GJ*EI_f+0.5600636\times10^{-12}\times EI_c*EI_f\end{aligned} \tag{24}$$

Statistical information for each model is provided in Table 13, and predictions are compared for the models in Figs. 41 and 42.

5.5 Optimization

The use of surrogate models significantly speeds up the optimization process. The main flow of the methodology remains unchanged. First, VABS runs with initial values in order to create input values for DYMORE. While DYMORE runs the optimization with frequency constraints, surrogate models were used to effectively impose constraints that force the design variables to stay in the feasible design space at the local level. This incorporation of constraints from the local level at the global level guarantees that the global optimizer achieves a solution that is feasible at the local level and without the need for an iterative process at the end of both optimizations (assuming that the surrogate models are of an adequate accuracy). The flow chart of the methodology is in Fig. 43. The described procedure was implemented within the MATLAB environment, which was used to connect several analysis tools. MATLAB utilizes the DOS command to run DYMORE, ANSYS and VABS. For constructing the Kriging model, the MATLAB toolbox DACE (Design and Analysis of Computer Experiments) was used.

5.5.1 Global level

At the global level, design variables are selected that significantly affect the dynamic behavior of the rotor blade: sectional mass (m), tip mass (m_t), torsional stiffness (GJ), lead-lag stiffness (EI_c) and flapping stiffness (EI_f). Design variables were non-dimensionalized, and the objective function was chosen to minimize the weight of blade. The objective function for minimization can be written as

$$F = W_b \tag{25}$$

where W_b is the weight of the blade.

Several constraints were imposed at the global level. The first constraint is related to safety considerations and stipulates that the auto-rotation index (I_A) must be greater than 60. This value is an accepted safe value for a single rotor system [70]. The equation of the constraint is

$$60 - I_A \leq 0 \tag{26}$$

Constraints were selected in order to appropriately place relevant blade frequencies in

ranges that do not lead to resonance. Since the baseline design has a three-bladed rotor system, the constraints were set to avoid coinciding with $N \times \Omega$/rev and $(N \pm 1) \times \Omega$/rev that are 2,3 and 4/rev for this example. Also, the first natural frequency is always to be avoided. As a result, the constraints related with resonance avoidance are

$$\begin{aligned} f_i - 0.95 \times \Omega &\leq 0 \\ 1.05 \times \Omega - f_i &\leq 0 \\ f_i - 0.95 \times 2 \times \Omega &\leq 0 \\ 1.05 \times 2 \times \Omega - f_i &\leq 0 \\ f_i - 0.95 \times 3 \times \Omega &\leq 0 \\ 1.05 \times 3 \times \Omega - f_i &\leq 0 \\ f_i - 0.95 \times 4 \times \Omega &\leq 0 \\ 1.05 \times 4 \times \Omega - f_i &\leq 0 \end{aligned} \tag{27}$$

Higher frequencies were not considered. Another constraint related to aeromechanical stability is imposed at the global level. From previous studies it is known that the potential for air resonance is virtually eliminated for soft-in-plane bearingless rotors when the lead-lag frequency is placed below 0.5/rev. However, if this frequency goes below than 0.4/rev, the likelihood of ground resonance is greatly increased [75]. To ensure aeromechanical stability at an early design phase, another constraint is imposed at the global level. Based on the assumption above, the first lead-lag frequency is to be placed between 0.4/rev and 0.5/rev so that

$$\begin{aligned} 0.4 \times \Omega - f_{L1} &\leq 0 \\ f_{L1} - 0.5 \times \Omega &\leq 0 \end{aligned} \tag{28}$$

Design parameters for the global level optimization are provided in Table 14.

Table 14: Design Parameters

Design Parameters	Values	Units
Hinge Offset (e)	10	$\%R$
Number of Blades (n)	3	
Angular Velocity (Ω)	41.14	[rad/sec]
Radius (R)	12.2	[ft]

5.5.2 Local level

For the local level optimization, two different types of cross-section models were tested. The first model assumed that the flexure has a single ply angle [0°] and the four flexural elements have identical dimensions. This leads to four design variables, two of which are ply angles of the skin, plus the height and width of each flexural element. The definitions of width and height of flexural elements are shown in Fig. 44. The second model has same outer shape and dimension as the first. However, each flexural element is now allowed to have different ply angles. These assumptions lead to a total of eight variables, resulting in making the running of the five-level Full Factorial and higher impossible. The cross section of second model is in Fig. 45. The upper and lower bounds of design variables are shown in Table 15 for model I – model III.

Table 15: Upper and Lower Bound of Design Variables

Cross-sectional Model I		
Design Variables	Lower Bound	Upper Bound
Height of Flexure (h_f)	0.001	0.04
Width of Flexure (w_f)	0.02	0.04
Inner and Outer Ply Angle of Skin (θ_{inner}, θ_{outer})	-90	90
Cross-sectional Model II		
Height of Flexure (h_f)	0.001	0.04
Width of Flexure (w_f)	0.02	0.04
Inner and Outer Ply Angle of Skin (θ_{inner}, θ_{outer})	-90	90
Ply Angle of Flexures(θ_{F_1}, θ_{F_2}, θ_{F_3}, θ_{F_4})	-90	90
Cross-sectional Model III		
Height of Horizontal and Vertical Flexure (h_{f_h},h_{f_v})	0.0025	0.02
Width of Horizontal and Vertical Flexure (w_{f_h},h_{w_v})	0.005	0.04
Location of Vertical Flexures (d_2, d_4)	0.005	0.04
Inner and Outer Ply Angle of Skin (θ_{inner}, θ_{outer})	-90	90

Two cases of objective functions were considered. The first minimizes the difference between required sectional mass (m_{req}) and calculated sectional mass (m_i) subject to upper and lower bound constraints on certain stiffnesses, i.e. minimize:

$$\mathrm{F} = \frac{|m_{req} - m_i|}{m_{req}} \tag{29}$$

subject to stiffness constraints of the form

$$\begin{aligned} 0.95 \leq \frac{|EIf_{req} - EIf_i|}{EIf_{req}} \leq 1.05 \\ 0.95 \leq \frac{|EIc_{req} - EIc_i|}{EIc_{req}} \leq 1.05 \\ 0.95 \leq \frac{|GJ_{req} - GJ_i|}{GJ_{req}} \leq 1.05 \end{aligned} \tag{30}$$

where EIf_{req}, EIc_{req} and GJ_{req} are flapping, lead-lag and torsional stiffnesses required to satisfy the global level constraints, and EIf_i, EIc_i and GJ_i are flapping, lead-lag and torsional stiffnesses calculated per iteration, respectively.

The second objective function minimizes differences between stiffnesses that are required for global level and those generated by ply angles of each lay-up with sectional mass. Uniform weighting factors were implied for the objective function, i.e. minimize

$$\begin{aligned} \mathrm{F} \quad = \quad & 0.25 \times \frac{|m_{req} - m_i|}{m_{req}} + 0.25 \times \frac{|EIc_{req} - EIc_i|}{EIc_{req}} \\ & + 0.25 \times \frac{|EIf_{req} - EIf_i|}{EIf_{req}} + 0.25 \times \frac{|GJ_{req} - GJ_i|}{GJ_{req}} \end{aligned} \tag{31}$$

5.6 Results

Results for the global and local level are provided separately in the following sections.

5.6.1 Global Level

For the global level optimization, two different initial values were used and each case were tested with three different surrogate models. Each surrogate model was imposed as a constraint with a bound of ±5%. The initial value and final values for each model are provided in Table 16 for each cases. The convergence history of each case is shown in Fig. 47 and 48 for cases I and II, respectively. As shown, linear and quadratic models required more iterations and resulted in values that were less likely to be minima. Furthermore, the number of iterations and the final minimized values demonstrate sensitivity with respect to the initial starting point. In contrast, the Kriging model showed relatively stable results. The Kriging model reached the same minimized value within the same number of iterations, so for this specific problem the Kriging model performed generally better than RSM models.

Table 16: Initial and Final Values of Gradient-Based Optimization for each Candidates from GA

Case I				
	Initial Value	Final Values		
		RSM (Linear)	RSM (Quadratic)	Kriging
Torsional Stiffness (K_{44})	2085.832741	1042.916371	1042.916371	2259.179066
Lead-Lag Stiffness (K_{55})	2310.507831	3003.771998	3003.771998	3283.686723
Flapping Stiffness (K_{66})	1449.569175	5721.561334	5721.561334	2425.928198
Tip Mass (m_t)	0.155280	0.192114	0.188452	0.201864
Sectional Mass (m)	0.084266	0.069656	0.067713	0.058127
Case II				
	Initial Value	Final Values		
		RSM (Linear)	RSM (Quadratic)	Kriging
Torsional Stiffness (K_{44})	1581.810560	0790.905280	0790.905280	1886.332409
Lead-Lag Stiffness (K_{55})	3776.426092	3498.747703	3449.921034	3936.324118
Flapping Stiffness (K_{66})	5530.207852	2187.980907	2187.980907	9254.246951
Tip Mass (m_t)	0.155280	0.097707	0.158303	0.201864
Sectional Mass (m)	0.081447	0.067618	0.062100	0.058127

Table 17: Final Values of Local Level Optimization

Case	Final Values of Design Variables				Number of Iterations
	θ_{inner}	θ_{outer}	h_f	w_f	
Case I with Eq. (29)	0.000062	-0.000062	0.04	0.04	56
Case II with Eq. (31)	0.005556	-0.005556	0.04	0.04	42

5.6.2 Local Level

Blade Model with Four Design Variables at Local Level Next, global-level optimization has been conducted with the Kriging surrogate model and two different objective functions used in the local-level optimizer. As shown in Table 17, both cases reached the same results. However, case II, the optimization with no constraint, showed a tendency to converge more quickly.

Blade Model with Eight Design Variable at Local Level The cross-sectional model III was used for local optimization here. The GA was used with results from both cases at global level. The number of population is 200 and 5 generations were used. The results are shown in Fig. 49 and 50.

From results, the GA produced lower objective function value when global level case II results were used as required values to be achieved at the local level. Therefore, only global level case II was proceed to phase 2 at the local level. The convergence history of the phase 2 is shown in Fig. 51.

The final configuration of the blade cross-section model is in Fig. 52.

5.6.3 Verification

Using the results from optimization, the fan plot for the rotor blade is shown in Figure 53. Therein, the frequencies are placed so that resonance can be avoided around operating rotor angular speed. Also f_2, the first lead-lag frequency is placed between 0.4/rev and 0.5/rev, the exact value being approximately 0.41/rev.

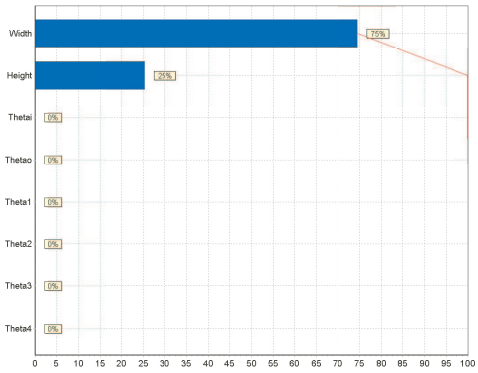

(a) Sectional Mass

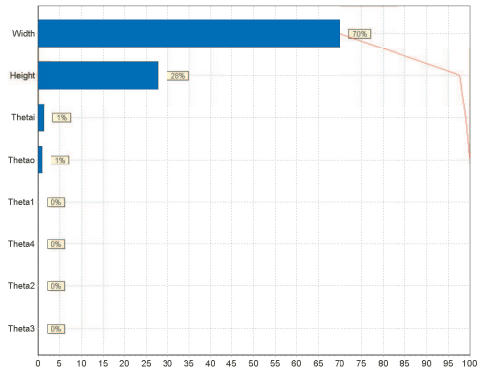

(b) Torsional Stiffness

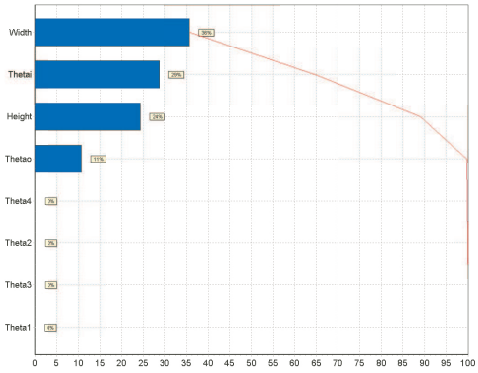

(c) Chordwise Bending Stiffness

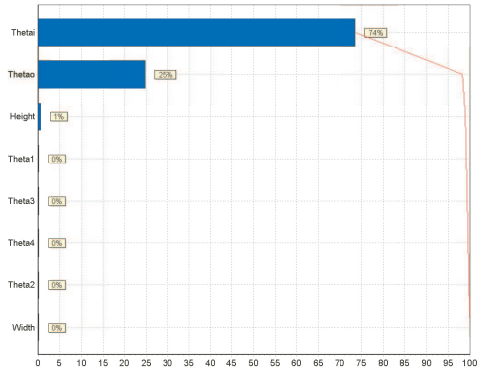

(d) Flapwise Bending Stiffness

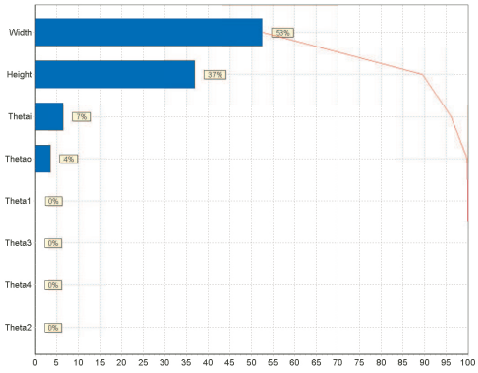

(e) Shear Center Location y-axis

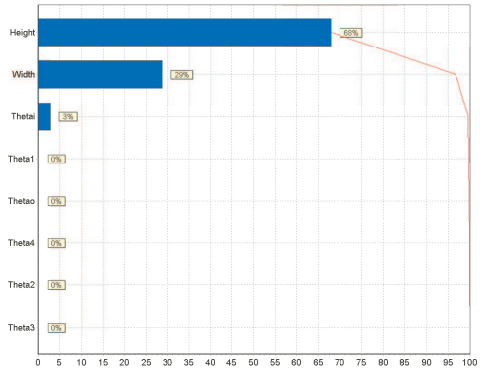

(f) Shear Center Location z-axis

Figure 39: Main Effects of Design Variables for Cross-sectional Model II

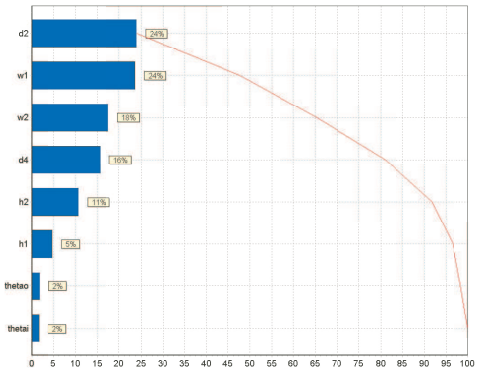

(a) Torsional Stiffness

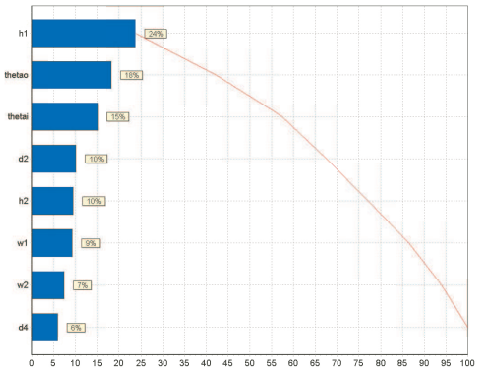

(b) Chordwise Bending Stiffness

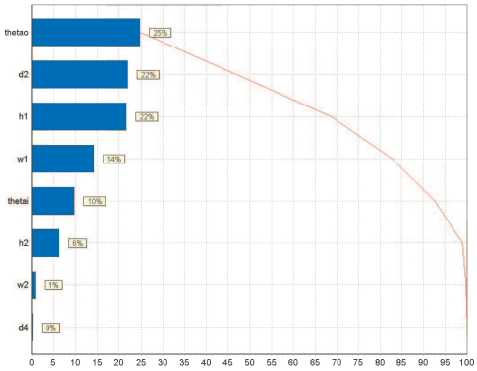

(c) Flapwise Bending Stiffness

Figure 40: Main Effects of Design Variables for Cross-sectional Model III

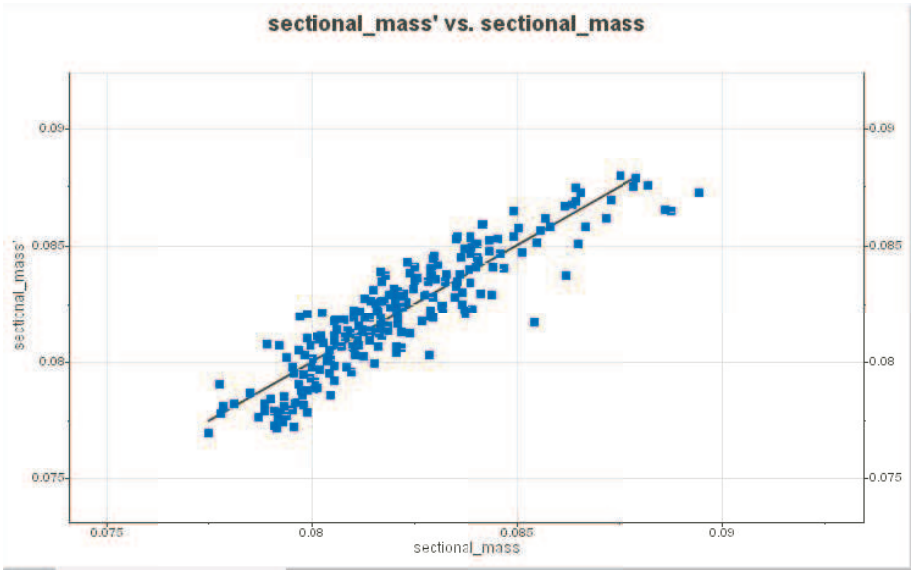

Figure 41: Predicted Linear RSM Model

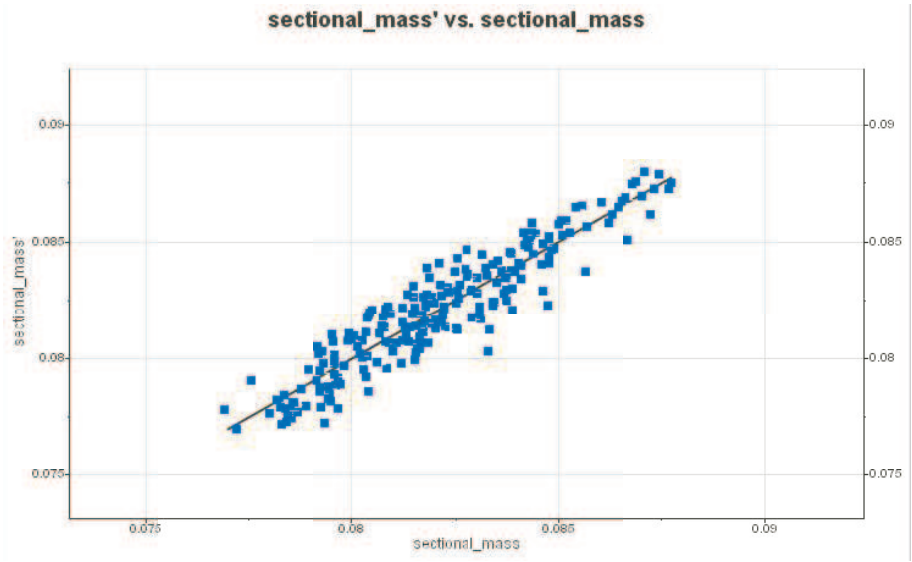

Figure 42: Predicted Quadratic RSM Model

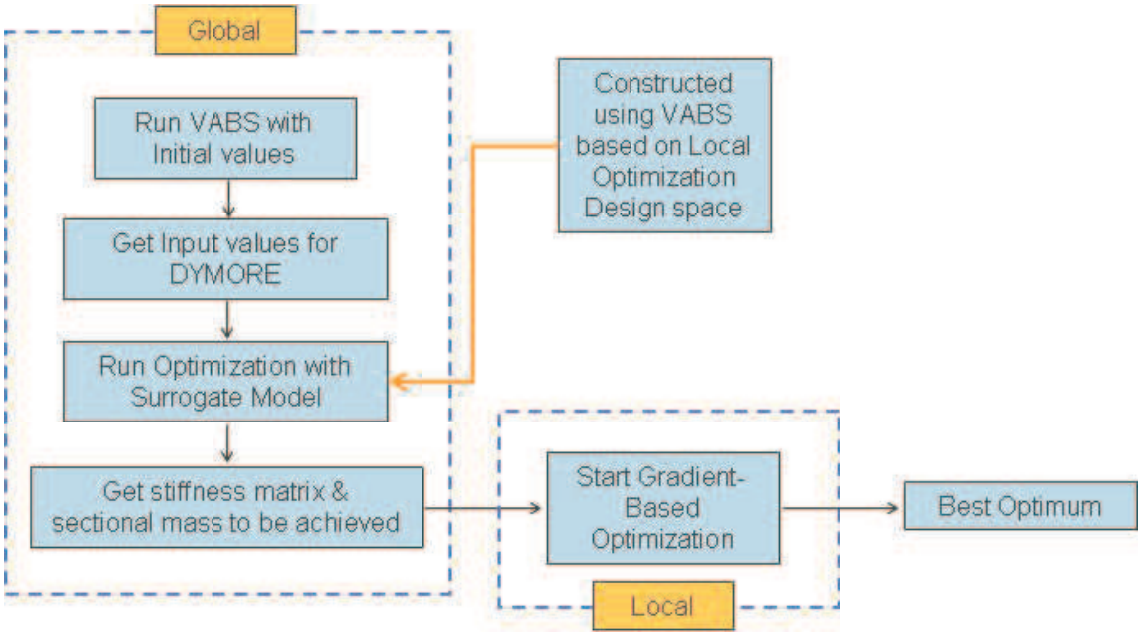

Figure 43: Flow chart of methodology

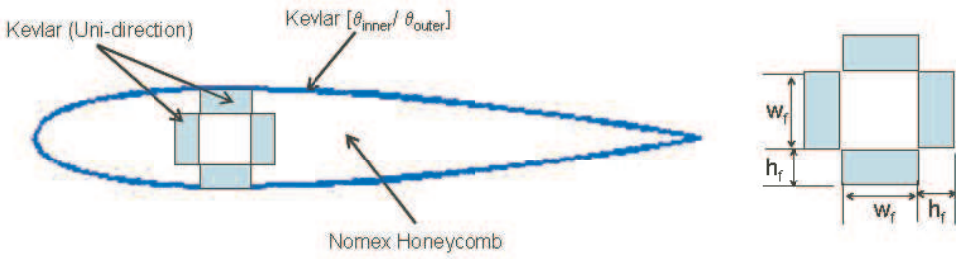

Figure 44: Cross-Section of the Blade

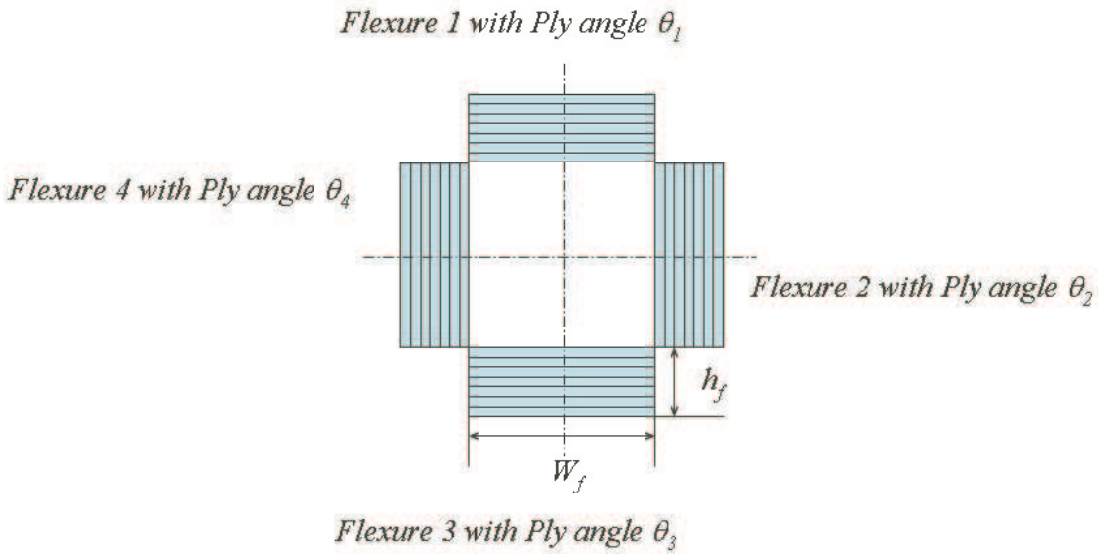

Figure 45: Cross-Section of the Blade

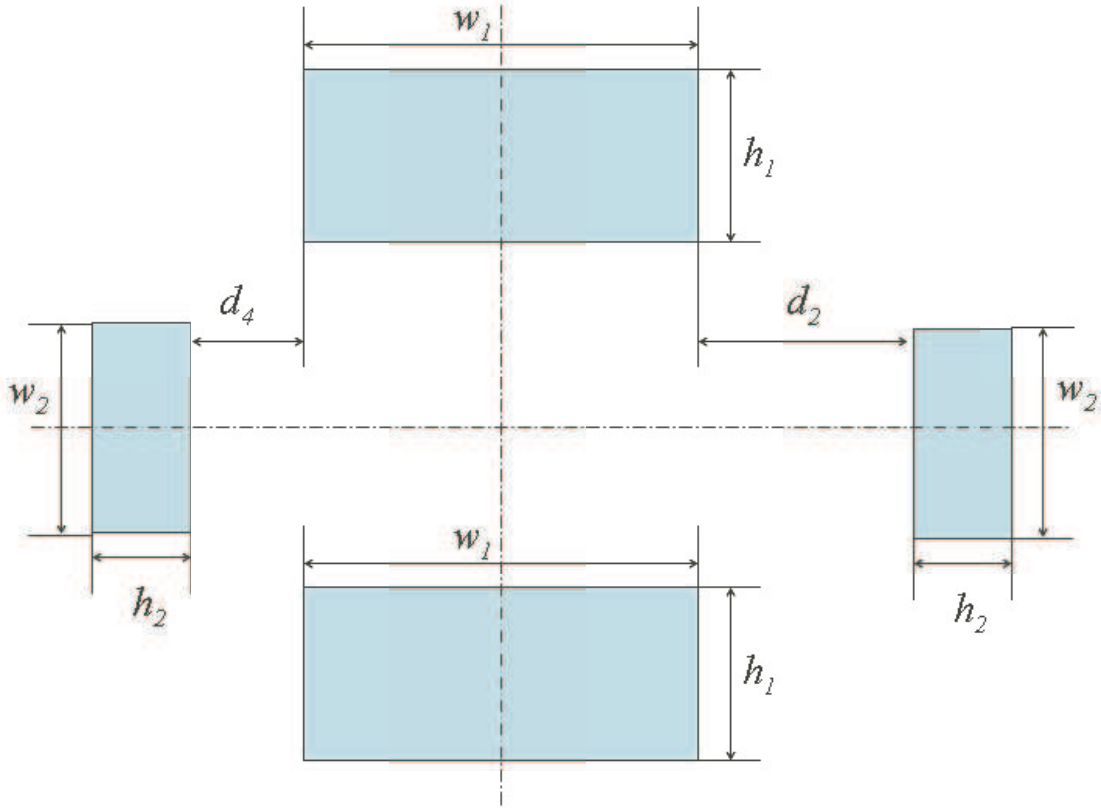

Figure 46: Cross-Section of the Blade

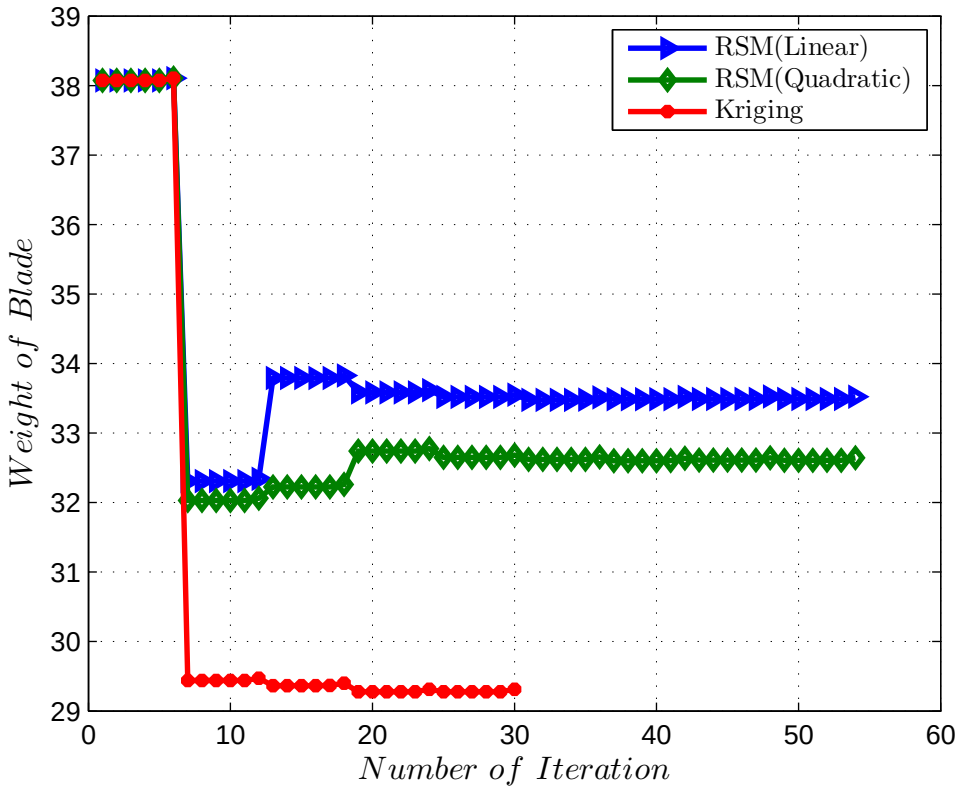

Figure 47: Convergence History of Global Level Optimization – Case I

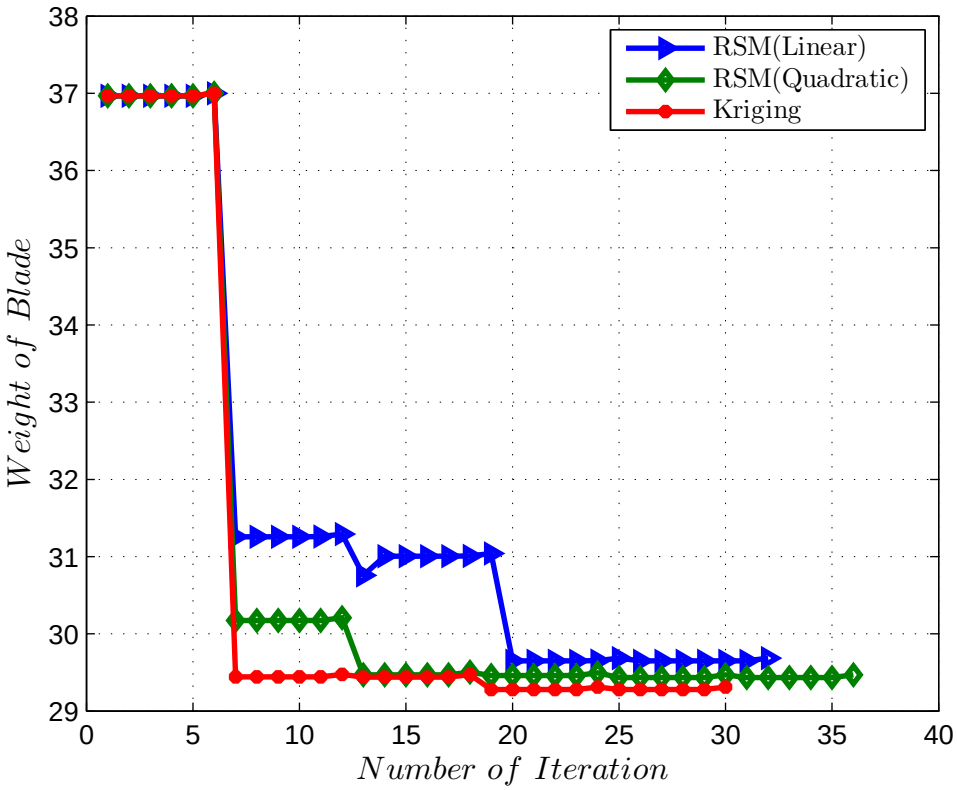

Figure 48: Convergence History of Global Level Optimization – Case II

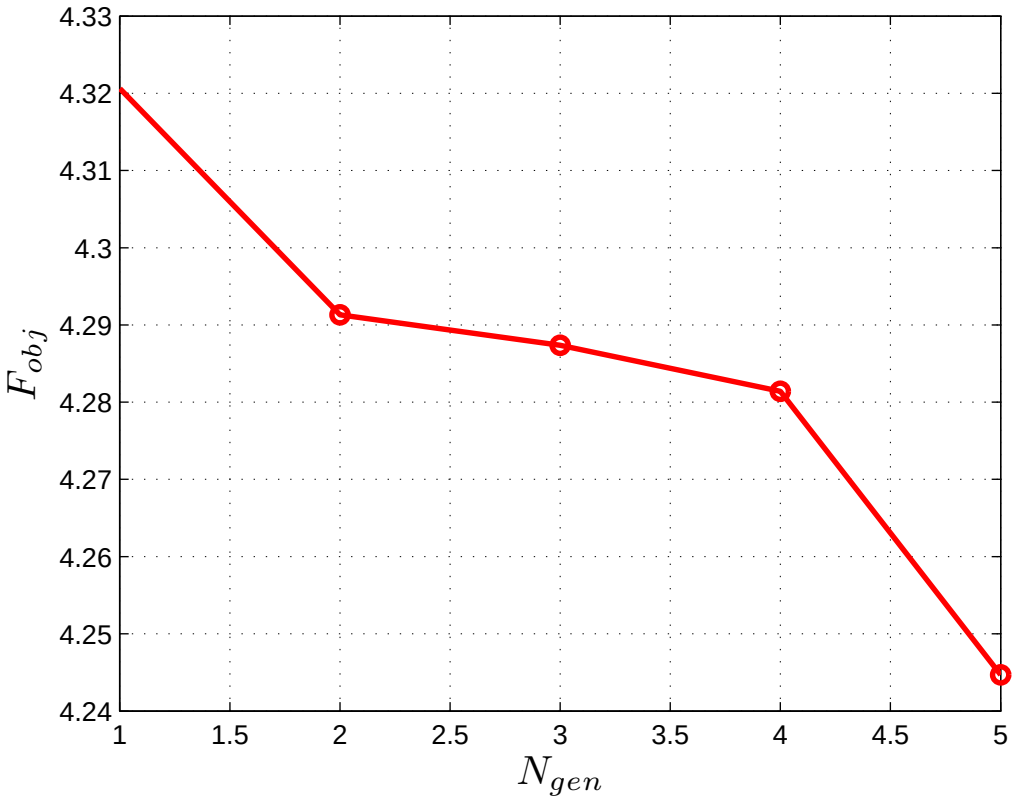

Figure 49: Local Level Phase 1 Optimization – Global Level Case I

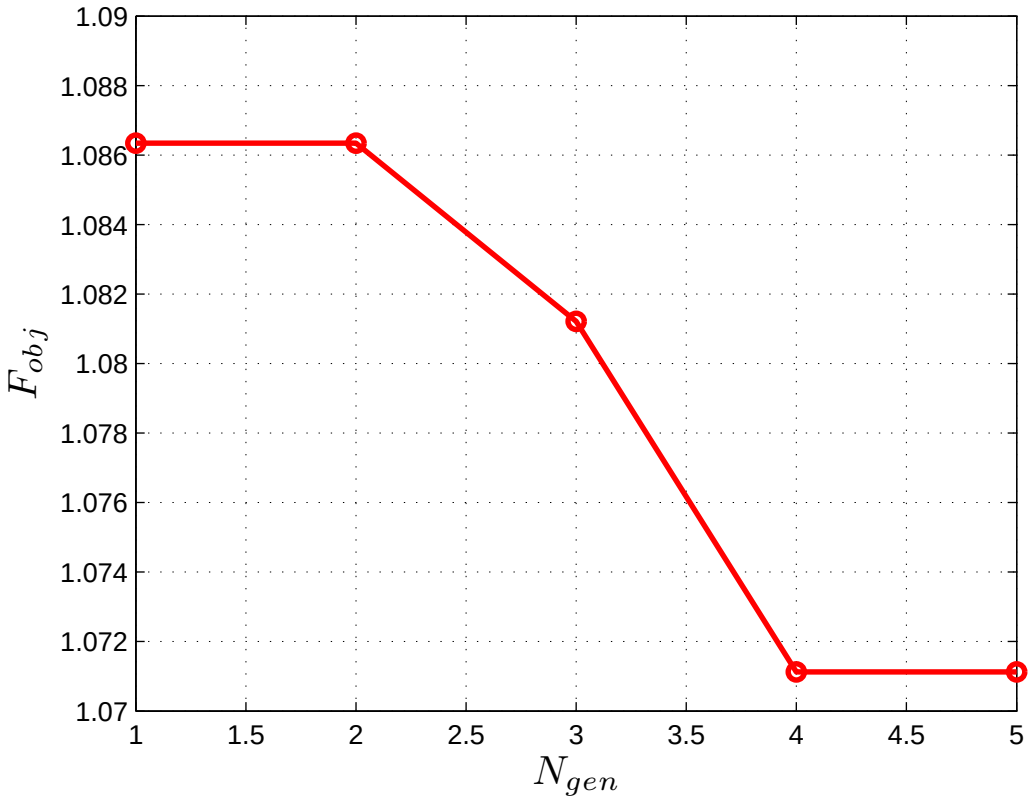

Figure 50: Local Level Phase 1 Optimization – Global Level Case II

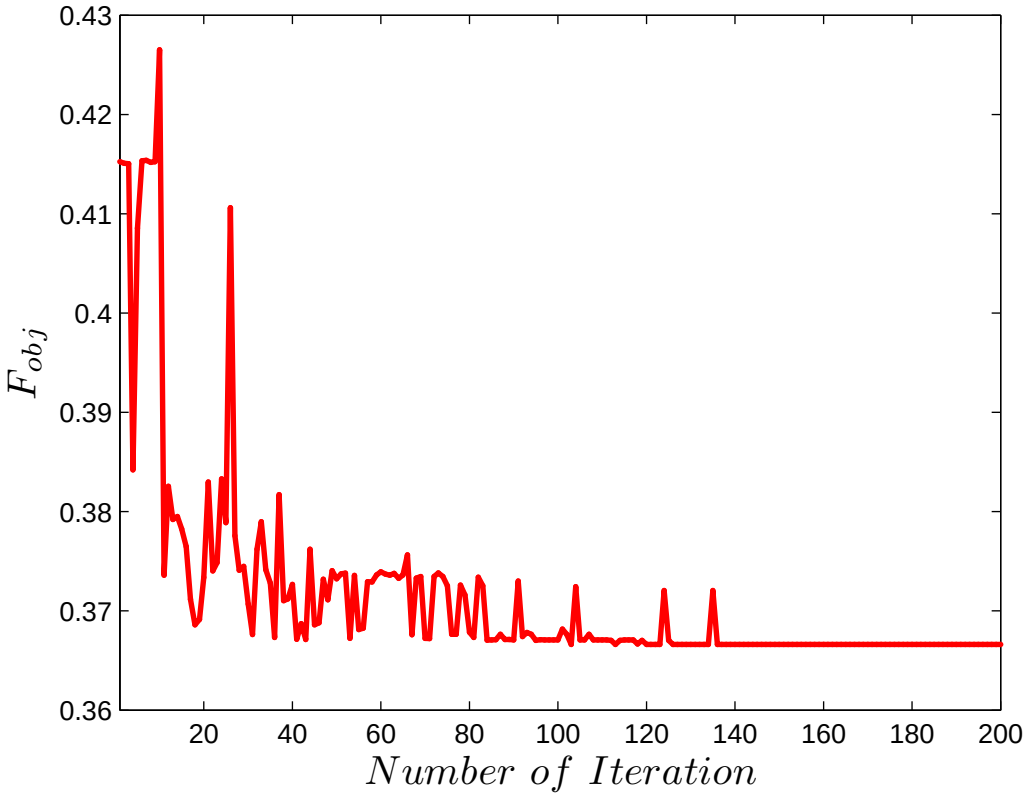

Figure 51: Local Level Phase 2 Optimization – Global Level Case II

Figure 52: Final Configuration of Cross-Section Model

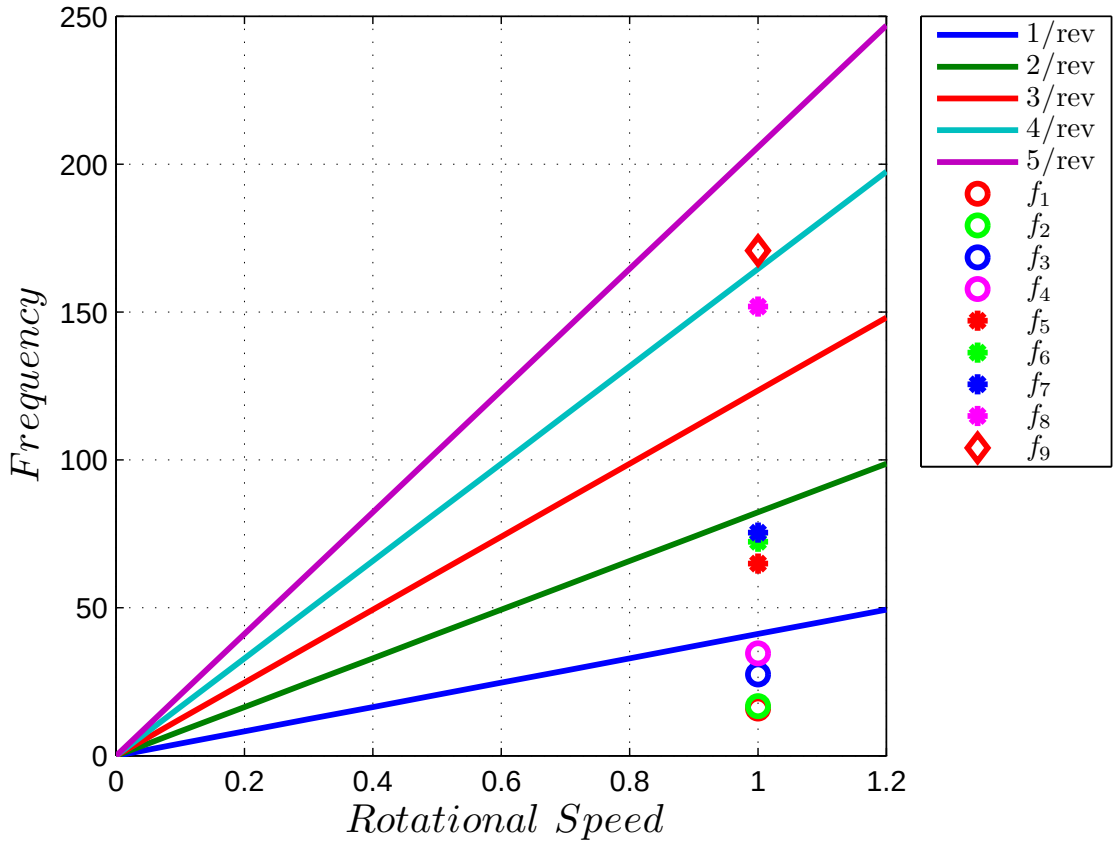

Figure 53: Fan Plot of Rotor Blade with Final Optimum Values

CHAPTER VI

CONCLUSIONS AND RECOMMENDATIONS

6.1 Conclusions

In the course of carrying out the research of this dissertation, the following conclusions were reached:

1. A multilevel optimization procedure was set up by establishing global level optimization and integrating a previous cross-sectional optimization scheme. Since the design space is multi-modal, exploration of the design space was needed in the local level optimizer. To find the most promising region that contains local minima and possibly the global minimum, a hybrid methodology was introduced that uses the genetic algorithm. The sensitivity of the genetic algorithm with respect to population size and generation number was investigated. The test problem was set to have the same number of function calls with different population size and generation number. The genetic algorithm tends to have better clustering with more populations and fewer generations. The results using this methodology showed improvement compared to previous methods based solely on gradient-based methods.

2. While the hybrid methodology shows improvement over previous methodologies that use only one optimization scheme, communication between the global and local optimizers was not clear due to its convergence to optimal solution on the first iteration. Several case studies were performed with changed objective functions and constraints. However, these test problems showed that global level introduces infeasible design requirements to the local level optimizer. The main problem was that the global level optimizer treats the design variables as independent, even though some of them are highly coupled to each other such as stiffnesses. To overcome this shortcoming, surrogate models at the global level, which are constructed based on the local level design

variables, are introduced into the methodology. The incorporation of surrogate models ensured that global level design variables stayed in feasible design space of local optimizer during the optimization process. Also, convergence rate of the optimization with surrogate models was improved. The results obtained indicate that the use of surrogate model to account for the local-level constraints at the global level optimization successfully facilitates compatibility with the constraints at the local level throughout the optimization process.

3. An automated procedure for generating geometry and VABS input files in ANSYS has been created that does not require an interaction with the user. The previously developed VABS-ANSYS macro was modified so that it now handles input files instead of inputs selected in a GUI environment. The procedure significantly improved the speed of model creation. For the baseline model under consideration, the new procedure takes 1.5 sec instead of the approximately two hours that was required previously.

4. The use of DACE from MATLAB toolbox showed a satisfactory fidelity of the Kriging model that relied on factorial Design of Experiments. However, it is important to point out that the larger number of design variables necessitates the use of a more economical Design of Experiments. Further investigation in determining the most economically efficient yet reasonably accurate DOE was performed. Based on the test problem result, the Latin Hyper Cube generated the least error between actual function and predicted function with 50 experiments for a two-design parameter problem, which showed better performance than a seven-level Full Factorial DOE based on 49 experiments. Based on this finding, the Latin Hyper Cube DOE was considered as the most efficient DOE for Kriging model for a higher number of design variable problems.

5. The multi-level optimization that utilizes the sophisticated yet computationally efficient tools, VABS and DYMORE and the overall optimization scheme, was improved by incorporating a surrogate model, the GA, and an automated version of the VABS-ANSYS macro into previously developed methodology. First, incorporation of the

surrogate model ensured that the global level optimizer would stay in the feasible design space of the local level analysis model. Therefore, each level communicates with an achievable design configuration. Second, using the GA in exploration of the design space ensured the selection only of promising candidates as starting points for gradient-based method instead of random starting points, which can lead the optimizer to unacceptable values. Finally, the elimination of human intervention between iterations by automating VABS-ANSYS macro process reduced computation time and effort immensely. The methodology suggested here exhibits appropriate flexibility for linkage with other design and/or optimization schemes.

6.2 Recommendations

The following recommendations for future work were reached:

1. The hybrid methodology uses a version of the genetic algorithm unaltered from the original concept. However, there are other types of genetic algorithm that can deal with high resolution with increased design variables in short time period. These so-called advanced genetic algorithms can be incorporated into the present methodology and can quite possibly improve it.

2. The surrogate models used and compared here are RSM and Kriging models. However, further investigation can be performed to incorporate the best method into the methodology. Other surrogate models that can be used here include Multivariate Adaptive Regression Splines (MARS), Radial Basis Functions (RBF), Adaptive Weighted Least Squares (AWLS), and Neural Network (NN). Studies showed that these surrogate models can be adapted for use in the current methodology. However, implementation will require computer coding since it is difficult to find general versions of these code that are publicly available.

3. The analysis models can be further updated. For the global level analysis model, only one blade from rotor system was used. Also, the local level analysis model uses only a NACA0015 airfoil shape. Further investigation is needed for treating a full rotor

system or a full vehicle system modeled in DYMORE, or for treating other airfoil shapes in VABS.

4. As discussed in Chapter 5, the methodology is an extension of integrated product/process (IPPD) methodology. Even the link between IPPD and the present methodology provided in previous studies is not yet fully integrated. Eventual integration with IPPD is required, and how the structural optimization affects the overall process needs to be investigated.

5. At this stage, the current methodology only has rotor dynamic and aeromechanical stability constraints. Also, DYMORE performs a static equilibrium analysis in a vacuum in order to generate the rotor system natural frequencies. In reality, a vehicle trim and stability analysis should be undertaken. Therefore, further investigation is needed in this area.

6. The methodology here deals with five and eight design variables at the global and local levels, respectively. However, in reality, the number of design variables can be increased significantly. To deal with an increase in the number of design variables, parallel computing can be used for constructing surrogate model and GA function calls. Parallel computation is based on appropriate decomposition of design variables into combinations suitable for calculation by one processor. Once these combinations are divided into small clusters of data sets, each cluster can be calculated on different computers and gathered into one later for construction of the surrogate model. Also, to reduce the computation time when GA is used for optimization, the idea of using values calculated at the surrogate model construction stage needs to be considered. This can be done by incorporating some relatively simple coding into the methodology that stores the results from the surrogate model construction, and filtering through these data so that only values of function that do not already exist in stored data are calculated.

APPENDIX A

DESCRIPTION OF TOOLS

A.1 VABS(Variational Asymptotic Beam Sectional Analysis)

VABS is a tool based on the variational asymptotic beam sectional analysis that is developed using a generalized Vlasov theory for composite beams with arbitrary geometric and material sectional properties. This tool rigorously split the geometrically-nonlinear, three-dimensional elasticity problem into a linear, two-dimensional, cross-sectional analysis and a nonlinear, one-dimensional, beam analysis. The developed theory is implemented into VABS, a general-purpose, finite-element based beam cross-sectional analysis code.

A.1.1 History of VABS

VABS(Variational Asymptotic Beam Sectional Analysis) is a 2-D finite element code that has its origin from an in-house engineering software since 1994 [88, 89]. After the original work, the new generation of VABS was developed by adding the features such as calculating the principal bending axes and the corresponding principal moments of inertia, calculating the neutral axes, eliminating the point constraints, solving the rank deficient linear system exactly and speed improvement [90, 6]. The study showed at least 20% speed improvement compare with original version of VABS. The program name VABS first appeared in [91].

A.1.2 Description of VABS

VABS is implements the various beam theories [6, 7, 8, 9] using the finite element method-based on the variational asymptotic method [92]. VABS can uses triangular or quadrilateral elements with 3, 4, 5, 6 nodes or 4, 5, 6, 7, 8, 9 nodes, however, if VABS-ANSYS macro is to be used, 3 or 4 noded triangular elements or 3 or 8 noded quadrilateral elements can be selected. VABS generates 6×6 cross-sectional mass matrix, 4×4 and 6×6 stiffness matrix based on classical model and Timoshenko model. These beam models can be prismatic or

initially twisted. Also, VABS results contains mass center and shear center. The element types used in VABS are shown in Fig. 54

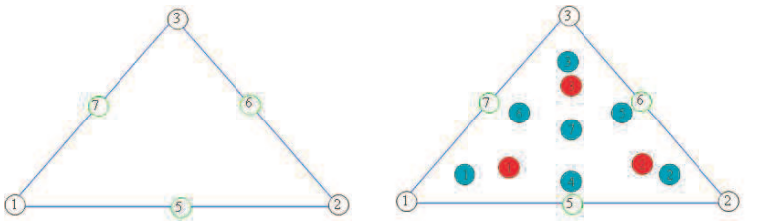

(a) Triangular Elements

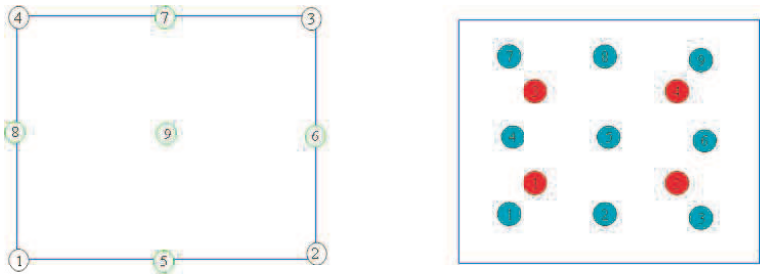

(b) Quadrilateral Elements

Figure 54: VABS elements and corresponding integration schemes[5]

To recover 3-D stresses and strains, VABS uses Gaussian integration schemes. The red numbers represents Gaussian points for linear elements and the green represents Gaussian points for quadratic elements.

VABS uses a right hand system. As in Figure 55, x1 is along the beam axis and x2 and x3 are the local Cartesian coordinates of the cross section.

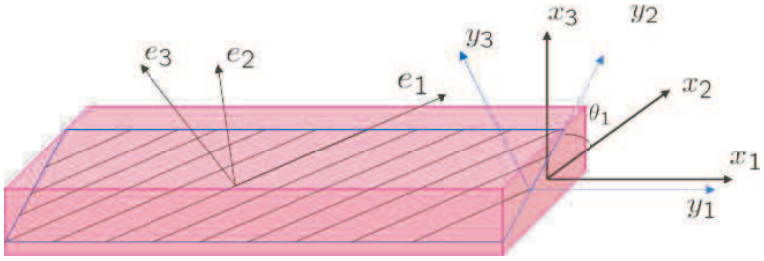

Figure 55: VABS Lay-up Convention[5]

The coordinate system (x1; x2; x3) is a global system used to define the geometry, (e1; e2; e3) used by to define the material properties, and (y1; y2; y3) is used to define the ply

plane.

REFERENCES

[1] "NIST/SEMATECH e-Handbook of Statistical Methods," `http://www.itl.nist.gov/div898/handbook/`, February 2003.

[2] Lophaven, S. N., Nielsen, H. B., and Sndergaard, J., *DACE - A MATLAB Kriging Toolbox*, 2002.

[3] Simpson, T. W., Peplinski, J. D., Koch, P. N., and Allen, J. K., "Metamodels for Computer-based Engineering Design: Survey and recommendations," *Engineering with Computers*, Vol. 17, 2001, pp. 129–150.

[4] Khalid, A. S., *Development and Implementation of Rotorcraft Preliminary Design Methodology using Multidisciplinary Design Optimization*, Ph.D. thesis, Georgia Institute of Technology,Daniel Guggenheim School of Aerospace Engineering, Atlanta,Georgia 30332, 2006.

[5] Yu, W., *An Tutorial of VABS*, 2005.

[6] Yu, W., Volovoi, V. V., Hodges, D. H., and Hong, X., "Validation of the Variational Asymptotic Beam Sectional Analysis (VABS)," *AIAA Journal*, Vol. 40, No. 10, 2002, pp. 21052112.

[7] Yu, W., Hodges, D. H., Volovoi, V. V., and Cesnik, C. E. S., "On Timoshenko-Like Modeling of Initially Curved and Twisted Composite Beams," *International Journal of Solids and Structures*, Vol. 39, No. 19, 2002, pp. 5101 5121.

[8] Yu, W. and Hodges, D. H., "Elasticity Solutions Versus Asymptotic Sectional Analysis of Homogeneous, Isotropic, Prismatic Beams," *Journal of Applied Mechanics*, Vol. 71, No. 1, 2004, pp. 15–23.

[9] Yu, W. and Hodges, D. H., "Generalized Timoshenko Theory of the Variational Asymptotic Beam Sectional Analysis," *Journal of the American Helicopter Society*, Vol. 50, No. 1, 2005, pp. 46–55.

[10] Bauchau, O., *DYMORE Users and Theory Manual*, 2003.

[11] Bauchau, O., "Computational Schemes for Flexible, Nonlinear Multi-Body Systems," *Multibody System Dynamics*, Vol. 2.

[12] Schmit, L. A., "Structural deisgn by systematic synthesis," *Proc. 2nd Conf. Electronic Computation, Am. Soc. Civil Engrs, New York*, 1960, pp. 105–122.

[13] Stepniewski, W. Z. and C. F. Kalmbac, J., "Multi-variable search and its applications to aircraft design optimization," *aeronaut. J. R. aeronaut. Soc.*, Vol. 74, 1970.

[14] Miura, H., "Applications of Numerical Optimization Methods to Helicopter Design ProblemsA Survey," *Vertica*, Vol. 9, No. 2, 1985, pp. 141–154.

[15] Blackwell, R. H., "Blade Design for Reduced Helicopter Vibration," *Journal of the American Helicopter Society*, Vol. 28, No. 3, 1983.

[16] Pritchard, J. I., Adelman, H. M., Walsh, J. L., and Wilbur, M. L., "Optimizing Tuning Masses for Helicopter Rotor Blade Vibration Reduction and Comparison with Test Data," *Journal of Aircraft*, Vol. 30, No. 6, 1993, pp. 906–910.

[17] Anusonti-Inthra, P. and Gandhi, F., "Optimal Control of Helicopter Vibration Through Cyclic Variations in Blade Root Stiffness," *Smart Materials and Structures*, Vol. 10, 2001, pp. 86–95.

[18] Peters, D. A., Ko, T., Korn, A., and Rossow, M. P., "Design of Helicopter Rotor Blades for Desired Placement of Natural Frequencies," *Proceedings of the 39th Annual Forum of the American Helicopter Society*, American Helicopter Society, Alexandria, VA, 1983, pp. 674–689.

[19] Vanderplaats, G. N., "CONMINA Fortran Program for Constrained Function Minimization, User's Guide," TM-X 62282, NASA, Aug 1973.

[20] Taylor, R. B., "Helicopter Vibration Reduction by Rotor Blade Modal Shaping," *American Helicopter Society 38th Annual Forum*, American Helicopter Society, Alexandria, VA, 1982, pp. 90–101.

[21] Yuan, K.-A. and Friedmann, P. P., "Aeroelasticity and Structural Optimization of Composite Helicopter Rotor Blades with Swept Tips," CR 4665, NASA, May 1995.

[22] Chattopadhyay, A. and Walsh, J. L., "Minimum Weight Design of Rotorcraft Blades with Multiple Frequency and Stress Constraints," Tm, NASA.

[23] Walsh, J. L., "Performance Optimization of Helicopter Rotor Blades," TM 104054, NASA, 1991.

[24] Smith, E. C. and Chopra, I., "Air and Ground Resonance of Helicopter with Elastically Tailored Composite Rotor Blades," *Journal of American Helicopter Society*, Vol. 38, No. 4, 1993, pp. 50–61.

[25] Chandra, R. and Chopra, I., "Analytical-Experimental Investgation of Free-Vibration Characteristics of Rotating Composite I-Beams," *Journal of Aircraft*, Vol. 30, No. 6, Nov.-Dec. 1993, pp. 927–934.

[26] Bir, G. S. and Chopra, I., "Aeromechanical Stability of Rotorcraft with Advanced Goemetry Blades," *Mathematical and Computer Modeling*, Vol. 19, No. 3/4, 1994, pp. 159–191.

[27] Ganguli, R. and Chopra, I., "Aeroelastic Optimization of a Helicopter Rotor with Two-Cell Composite Blades," *AIAA Journal*, Vol. 34, No. 4, 1996, pp. 835–854.

[28] Chopra, I., "Perspectives in Aeromechanical Stability of Helicopter Rotors," *Vertica*, Vol. 4, No. 1990, 14.

[29] Ormiston, R. A., "The Challenge of the Damperless Rotor," *Proceedings of the 22nd European Rotorcraft Forum*, Brighton, England, September 1996, pp. 17–19.

[30] Bousman, W. G., "The Effects of Structural Flap-Lag and Pitch-Lag Coupling on Soft Inplane Hingeless Rotor Stability in Hover," TP 3002, NASA, May 1990.

[31] Gandhi, F. and Hathaway, E., "Optimized Aeroelastic Couplings for Alleviation of Helicopter Ground Resonance," *Journal of Aircraft*, Vol. 35, No. 4, 1998, pp. 582–589.

[32] Hathaway, E. and Gandhi, F., "Concurrently Optimized Aeroelastic Couplings and Rotor Stiffness for Alleviation of Helicopter Aeromechanical Instability," *Journal of Aircraft*, Vol. 38, No. 1, 2001, pp. 69–80.

[33] Davis, M. W. and Weller, W. H., "Helicopter Rotor Dynamics Optimization with Experimental Verification," *Journal of Aircraft*, Vol. 28, No. 1, 1991, pp. 38–48.

[34] Nixon, M. W., "Preliminary Structural Design of Composite Main Rotor Blades for Minimum Weight," TP 2730, NASA, 1987.

[35] Barwey, D. and Peters, D. A., "Optimization of Composite Rotor Blades with Advanced Structural and Aerodynamic Modeling," *Mathematical and Computer Modelling, Special Issue on Rotorcraft Modelling: Part*, Vol. 19, No. 3.

[36] Chattopadhyay, A., Walsh, J. L., and Riley, M. F., "Integrated Aerodynamic Load/Dynamic Optimization of Helicopter Rotor Blades," *Journal of Aircraft*, Vol. 28, No. 1, 1991, pp. 58–65.

[37] Johnson, W., "A Comprehensive Analytical Model of Rotorcraft Aerodynamics and Dynamics, Part I: Analysis Development," TM 81182, NASA, 1980.

[38] Chattopadhyay, A. and Chiu, Y. D., "An Enhanced Integrated Aerodynamic/Dynamic Approach to Optimum Rotor Blade Design," *Structural Optimization*, Vol. 4, 1992, pp. 75–84.

[39] Walsh, J. L., LaMarsh, W. J., and Adelman, H. M., "Fully Integrated Aerodynamic/Dynamic Optimization of Helicopter Rotor Blades," *Mathematical and Computer Modelling, Special Issue on Rotorcraft Modelling: Part 1*, Vol. 18, No. 3.

[40] Walsh, J. L., Young, K. C., Pritchard, J. I., Adelman, H. M., and Mantay, W. R., "Multilevel Decomposition Approach to Integrated Aerodynamic/Dynamic/Structural Optimization of Helicopter Rotor Blades," TM 109084, NASA, May 1994.

[41] Walsh, J. L., Young, K. C., Pritchard, J. I., Adelman, H. M., and Mantay, W. R., "Integrated Aerodynamic/Dynamic/Structural Optimization of Helicopter Rotor Blades Using Multilevel Decomposition," TP 3465, NASA, Jan. 1995.

[42] Kim, J. E. and Sarigul-Klijn, N., "Structural Optimization For Light- Weight Articulated Rotor Blade," *Proceedings of the 41st AIAA/ASME/AHS SDM Conference, AIAA*.

[43] Kim, J. E. and Sarigul-Klijn, N., "Elastic-Dynamic Rotor Blade Design with Multiobjective Optimization," *AIAA Journal*, Vol. 39, No. 9.

[44] Crossley, W. A. and Laananen, D. H., "Conceptual Design of Helicopters Via Genetic Algorithm," *Journal of Aircraft*, Vol. 33, No. 6, 1996, pp. 1062–1070.

[45] Hajela, P., "Nongradient Methods in Multidisciplinary Design Optimization: Status and Potential," *Journal of Aircraft*, Vol. 36, No. 1, 1999, pp. 255–265.

[46] Hajela, P. and Lee, J., "Genetic Algorithms in Multidisciplinary Rotor Blade Design," *Proceedings of the AIAA 36th Structures, Structural Dynamics, and Materials Conference (New Orleans, LA)*, Washington, DC, 1995, pp. 2187–2197.

[47] Holland, J. H., *Adaptation in Natural and Artificial Systems*, Univ. of Michigan Press, Ann Arbor, MI, 1974.

[48] Goldberg, D. E., *Genetic Algorithms in Search, Optimization, and Machine Learning*, Addison Wesley, 1989.

[49] KrishnaKumar, K., Kumar, R., and Seywald, H., "Genetic Algorithms: Theory and Control Applications," AIAA Tutorial Session, August 1993.

[50] Anderson, M. B., Lawrence, W. R., and Gerbert, G. A., "Using an Elitist Pareto Genetic Algorithm for Aerodynamic Data Extraction," *AIAA-96-0514*, Jan 1996.

[51] LeRiche, R. and Haftka, R. T., "Optimization of Laminate Stacking Sequence for Buckling Load Maximization by Genetic Algorithms," *AIAA Journal*, Vol. 31, No. 5, 1993, pp. 951–956.

[52] Mitchell, M., *An Introduction to Genetic Algorithms*, MIT Press, third printing ed., 1997.

[53] Spears, W. M., "A study of crossover operators in genetic programming," *International Symposium on Methodologies for Intelligent System*, 1993, pp. 409–418.

[54] Syswerda, G., "Uniform crossover in genetic algorithms," *Third International Conference on Genetic Algorithms*, 1989, pp. 2–9.

[55] Tarzanin, F., Young, D. K., and Panda, B., "Advanced Aeroelastic Optimization Applied to an Improved Performance, Low Vibration Rotor," *Proceedings of the 55th American Helicopter Society Annual Forum*.

[56] Akula, V. R. and Ganguli, R., "Finite Element Model Updating of a Helicopter Rotor Blade Using Genetic Algorithm," *AIAA Journal*, Vol. 41, No. 3, 2003, pp. 554–556.

[57] Wrenn, G. A., "An Indirect Method for Numerical Optimization Using the Kreisselmeier-Steinhauser Function," CR 4220, NASA, 1989.

[58] Crossley, W. A., "A Genetic Algorithm with the Kreisselmeier- Steinhauser Function for Multiobjective Constrained Optimization of Rotor Systems," *Proceedings of the AIAA 35th Aerospace Sciences Meeting and Exhibit*, AIAA, Reston, VA, 1997.

[59] Crossley, W. A., Wells, V. L., and Laananen, D. H., "The Potential of Genetic Algorithms for Conceptual Design of Rotor Systems," *Engineering Optimization*, Vol. 24, No. 3, 1995, pp. 221–238.

[60] Crossley, W. A., "Genetic Algorithm Approaches for Multiobjective Design of Rotor Systems," *Proceedings of the AIAA/NASA/ISSMO 6th Symposium on Multidisciplinary Analysis and Optimization*, AIAA, Reston, VA, 1996, pp. 384–394.

[61] Hajela, P. and Lin, C.-Y., "Genetic Search Strategies in Multicriterion Optimal Design," *Structural Optimization*, Vol. 4, No. 2, 1992, pp. 99–107.

[62] Goldberg, D. E. and Richardson, J., "Genetic Algorithms with Sharing for Multimodal Function Optimization," *Genetic Algorithms and Their Applications: Proceedings of*

the 2nd International Conference on Genetic Algorithms, Lawrence Erlbaum Associates, Hillsdale, NJ, 1987, pp. 41–49.

[63] Yoo, J. and Hajela, P., "Immune Network Modeling in Multicriterion Design of Structural Systems," *AIAA Paper*, , No. 98-1911, 1998.

[64] Lin, C.-Y. and Hajela, P., "Genetic Search Strategies in Large Scale Optimization," *Proceedings of the AIAA/ASME/ASCE/AHS/ ASC 34th Structures, Structural Dynamics, and Materials Conference (La Jolla, CA)*, AIAA, Washington, DC, 1993, pp. 2437–2447.

[65] Schraudolph, N. N. and Belew, R. K., "Dynamic Parameter Encoding for Genetic Algorithms," *Machine Learning*, Vol. 9, No. 1, 1992, pp. 9–21.

[66] Manderick, B. and Spiessens, P., "Fine-Grained Parallel Genetic Algorithm," *Proceedings of the 3rd International Conference on Genetic Algorithms*, edited by M.-K. H. Schaffer, Palo Alto, CA, 1989, pp. 428–433.

[67] Muhlenbeim, H., Schomisch, M., and J. Born, J., "The Parallel Genetic Algorithm as a Function Optimizer," *Parallel Computing*, Vol. 17, No. 627, 1991, pp. 619–632.

[68] Lee, J. and Hajela, P., "GA's in Decomposition Based Design – Subsystem Interactions Through Immune Network Simulation," *Proceedings of the AIAA/NASA/USAF/ISSMO 6th Conference on Multidisciplinary Analysis and Optimization (Bellevue, WA)*, AIAA, Washington, DC, 1996, pp. 1717–1726.

[69] Lee, J. and Hajela, P., "Parallel Genetic Algorithm Implementation in Multidisciplinary Rotor Blade Design," *Journal of Aircraft*, Vol. 33, No. 5, 1996, pp. 962–969.

[70] Leishman, J. G., *Principles of Helicopter Aerodynamics*, Cambridge University Press, Cambridge, U.K., 2002.

[71] Paik, J., Volovoi, V. V., and Hodges, D. H., "Cross-Sectional Sizing and Optimization of Composite Blades," *AIAA paper*, , No. 2002.

[72] Volovoi, V. V., Yoon, S., Lee, C.-Y., and Hodges, D. H., "Cross-Sectional Sizing and Optimization of Composite Blades," *Proceedings of the 44th Structures, Structural Dynamics and Materials Conference*.

[73] Volovoi, V. V., Li, L., Ku, J., and Hodges, D. H., "Multi-Level Structural Optimization of Composite Rotor Blades," *Proceedings of the 44th Structures, Structural Dynamics and Materials Conference, Austin, Texas*.

[74] Alexander, H. R., Smith, K. E., McVeigh, M. A., Dixon, P. G., and McManus, B. L., "Preliminary Design Study of Ad- vanced Composite Blade and Hub and Nonmechanical Control System for the Tilt-Rotor Aircraft," CR 152336, NASA.

[75] Hanson, T. F., *A Designer Friendly Handbook of Helicopter Rotor Hubs*, www.ideasalacarte.com, 1998.

[76] Lockheed, "Wind Tunnel Tests of an Optimized Matched Stiffness Rigid Rotor," TR 64-56, U,S, Army TRECOM, 1964.

[77] McKay, M. D., Conover, W. J., and Beckman, R. J., "A Comparison of Three Methods for Selecting Values of Input Variables in the Analysis of Output from a Computer Code," *Technometrics*, Vol. 21, No. 2, 1979.

[78] Montgomery, D. C., *Design and Analysis of Experiments*, Wiley, New York, NY, 4th ed., 1997.

[79] Wang, L., Beeson, D., Wiggs, G., and Rayasam, M., "A Comparison Of Meta-modeling Methods Using Practical Industry Requirements," *47th AIAA/ASME/ASCE/AHS/ASC Structures, Structural Dynamics, and Materials Conferece*, AIAA, Newport, Rhode Islan, 2006.

[80] Matheron, G., "Principles of Geostatistics," *Economic Geology*, Vol. 58, 1963, pp. 12461266.

[81] Simpson, T. W., Korte, J. J., Maueryt, T. M., and Mistree, F., "Comparison of Response Surface and Kriging Models for Multidisciplinary Design Optimization," *AIAA*, 1998, pp. 381–391.

[82] Glaz, B., Friedmann, P. P., and Liu, L., "Surrogate Based Optimization of Helicopter Rotor Blades for Vibration Reduction in Forward Flight," *Proceedings of the 46th Structures, Structural Dynamics and Materials Conference, Newport, Rhode Island*, May 1–4 2006, AIAA Paper 2006-1821.

[83] Volovoi, V. V., Ku, J., and Hodges, D. H., "Coupling Global and Local Aspects of Cross-Sectional Optimization for Rotor Blades," *Proceedings of the 46th Structures, Structural Dynamics and Materials Conference, Newport, Rhode Island*, No. AIAA Paper 2006-1822, May 1–4 2006.

[84] Hodges, D. H., Bauchau, O. A., Craig, J. I., and Volovoi, V. V., "Comprehensive Aeromechanical Analysis Using Integrated Analysis Tools," Final report, Rotorcraft Industry Technology Association (RITA), Inc., 2002.

[85] Hodges, D. H., *Nonlinear Composite Beam Theory*, AIAA, Reston, Virginia, 2006.

[86] "UIUC Airfoil Coordinates Database - Version 2.0," `http://www.ae.uiuc.edu/m-selig/ads/coord_database.html`, November 2006.

[87] Hanson, T. F., "The Auto-Trim Rotor Stability System," *The American Helicopter Society 53rd Annual Form*, American Helicopter Society, Virginia Beach, Virginia, April 1997, pp. 1503–1514.

[88] Cesnik, C. E. S., *Cross-Sectional Analysis of Initially Twisted and Curved Composite Beams*, Ph.D. thesis, Georgia Institute of Technology, 1994.

[89] Cesnik, C. E. S. and Hodges, D. H., "VABS: A New Concept for Composite Rotor Blade Cross-Sectional Modeling," *Journal of the American Helicopter Society*, Vol. 42, No. 1, 1997, pp. 27–38.

[90] Yu, W., *Variational Asymptotic Modeling of Composite Dimensionally Reducible Structures*, Ph.D. thesis, Georgia Institute of Technology, 2002.

[91] Hodges, D. H., Atilgan, A. R., Cesnik, C. E. S., and Fulton, M. V., "On a Simplified Strain Energy Function for Geometrically Nonlinear Behaviour of Anisotropic Beams," *Composites Engineering*, Vol. 2, No. 5-7, 1992, pp. 513–526.

[92] Berdichevsky, V. L., "Variational-asymptotic Method of Constructing a Theory of Shells," *PMM*, Vol. 43, No. 4, 1979, pp. 664–687.